UiT
THE ARCTIC UNIVERSITY OF NORWAY

FACULTY OF HEALTH SCIENCES
DEPARTMENT OF MEDICAL BIOLOGY
MEDICAL PHARMACOLOGY AND TOXOCOLOGY RESEARCH GROUP

Modeling of glutamatergic and GABAergic drug targets in the CNS and their interactions with environmental toxicants

Maria Leiknes Ernstsen
Master thesis in Pharmacy (FAR-3911)
May 2016

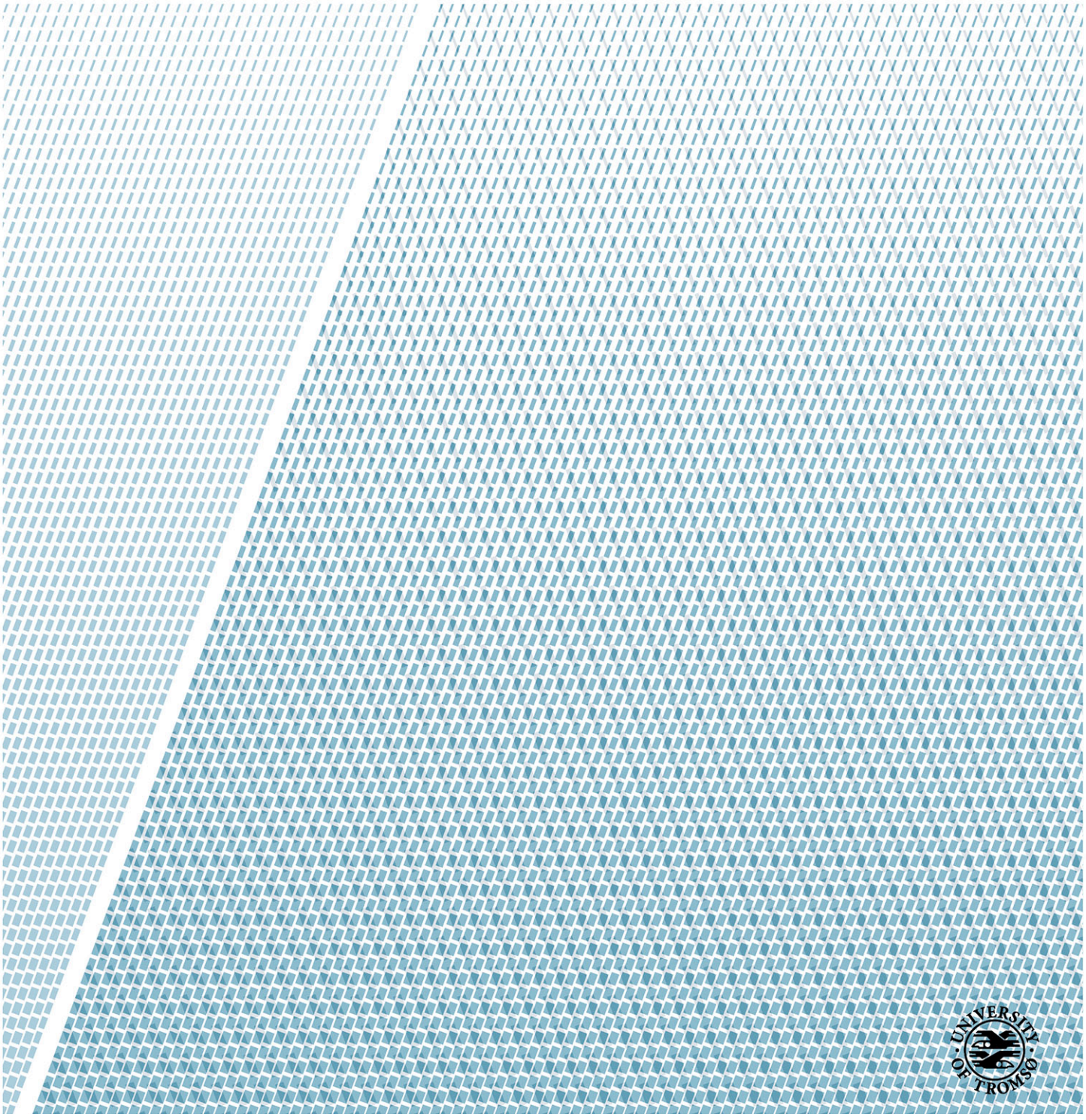

ACKNOWLEDGEMENT

This master thesis was written at The Medical Pharmacology and Toxicology research group in collaboration with The Department of Pharmacy (IFA) at UiT The Arctic University of Norway from August 2015 to May 2016.

I would like to thank everyone who has given me some of his or her time and helped me during this master thesis. My deepest gratitude goes to my main supervisor Assoc. Prof. Kurt Kristiansen and co-supervisor Prof. Ingebrigt Sylte. They were both very generous with their time and knowledge and assisted me during the work with my thesis.

I also wish to express my special gratitude to Isak Bøgwald for teaching me about molecular modeling, how to work with different molecular programs and for always finding time to help when it was needed. Furthermore I will say thank you to Richard Gravelsæter, who has spent time to read my master thesis and has given me constructive feedback.

Finally, I must show my appreciation to my parents and my sister for always supporting and encouraging me through my years of studying pharmacy and through the process of writing this thesis.

Maria Leiknes Ernstsen
Tromsø, May 2016

ABSTRACT

The exposure to pollutants is a serious and increasing health problem, which has been associated with increased morbidity and mortality among people. Many toxic compounds can accumulate in the environment and evidence suggests that most people have varying degrees of toxic compounds within their body. This can result in disruption of many physiological processes in the human body and the development of several central nervous system (CNS) diseases, including Alzheimer's disease (AD). Glutamate and γ-aminobutyric acid (GABA) are the major excitatory and inhibitory neurotransmitters in the human brain, which target both G protein-coupled receptors (GPCRs) and ionotropic receptors. They have important roles in physiological processes and play roles in different CNS diseases, and disruption of their neurotransmission may cause harmful effects in humans.

The aim of this study was to use constructed homology models and some resolved X-ray structures of glutamatergic GPCRs and homology models of the GABA transporter 1 (GAT1), in order to predict putative interactions and binding modes of several toxic compounds retrieved from the Toxicology in the 21st Century (Tox21) database.

Receptor and transporter models were able to bind several of the toxic compounds, including some drugs. Many of them showed better affinity to the models than their known binders. Toxicants with good affinity to a receptor or transporter can result in adverse effects in humans, where the toxicants can outperform several endogenous and exogenous binders. Further studies should involve *in vitro* assays to investigate the binding of toxicants, and especially those that have the ability to cross the blood brain barrier (BBB).

TABLE OF CONTENTS

INDEX OF FIGURES, TABLES AND APPENDIX

FIGURES

TABLES

APPENDIX

ABBREVIATIONS

2D	Two dimensional
3D	Three dimensional
AD	Alzheimer's disease
ALS	Amyptropic Lateral Sclerosis
AMPA	α-amino-3-hydroxy-5-methyl-4-isoxazolepropionic acid
ATP	Adenosine triphosphate
BBB	Blood-Brain Barrier
BEDROC	Boltzmann-Enhanced Discrimination of Receiver-Operation Characteristics
BMRB	Biological Magnetic Resonance Data Bank
BPS	The British Pharmacological Society
C-terminal	Carbone terminal
Cl^-	Chloride ion
Clog D	Calculated log D
Clog P	Calculated log P
CNS	Central nervous system
CNS MPO	Central nervous system Multiparameter Optimization
CRD	Cysteine-rich domain
DAT	Dopamine transporter
dDAT	*Drosophila* dopamine transporter
DDE	Dichlorodiphenyldichloroethylene
DUD.E	Database of Useful Decoys: Enhanced
E_{angle}	Angle bending energy
E_{bonded}	Bonded energy
E_{el}	Electrostatic interaction energy
$E_{non\text{-}bonded}$	Non-bonded energy
E_{str}	Bond stretching energy
E_{tot}	Total energy of a molecule
E_{tors}	Energy for rotation around a bond
E_{vdw}	Van der Waals interaction energy
EAAT	Excitatory amino acid transporters (Glutamate transporter)

EC_{50}	Half maximal effective constant
ECD	Extracellular domain
ECL	Extracellular loop
EF	Enrichment factor
EPA	United States Environmental Protection Agency
FITM	4-fluoro-N-(4-(6-(isopropylamino)pyrimidin-4-yl)thiazol-2-yl)-N-methylbenzamide
GABA	γ-aminobutyric acid
GAD	Glutamic acid dehydrogenase
GAT1	GABA transporter 1
GDP	Guanosine diphosphate
GERD	Gastro esophageal reflux disease
GPCR	G protein-coupled receptor
GTP	Guanosine triphosphate
H-bonds	Hydrogen bonds
HBD	Hydrogen bond donor
HBA	Hydrogen bond acceptor
HIV	Human immunodeficiency virus
hSERT	*Human* serotonin transporter
IC_{50}	Half maximal inhibitory concentration
ICL	Intracellular loop
ICM	Molsoft internal coordinate mechanics software
IFD	Induced fit docking
IUPHAR	The International Union of Basic and Clinical Pharmacology
K_i	Binding affinity constant
LeuT	Leucine transporter
LigPrep	Ligand preparation
Mavoglurant	methyl(3aR,4S,7aR)-4-hydroxy-4-[(3-methylphenyl)ethynyl]octahydro-1H-indole-1- carboxylate
mGlu receptor	Metabotropic glutamate receptor

MM	Molecular mechanics
ModFOLD	Model Quality Assessment Server
MS	Multiple Sclerosis
Mw	Molecular weight
N-terminal	Nitrogen terminal
Na+/K+ ATPase	Sodium-potassium adenosine triphosphatase (Na^+-K^+ pump)
NAM	Negative allosteric modulator
NIH	The National Institutes of Health
NMDA	N-methyl-D-aspartate
PAM	Positive allosteric modulator
PDB	Protein data bank
PDBe	Protein Data Bank in Europe
PDBj	Protein Data Bank Japan
PDB ID	Protein Data Bank Identification
PERC	Perchloroethylene
pEC_{50}	Logarithmic half maximal effective concentration
pIC_{50}	Logarithmic half maximal inhibitory concentration
pKa	Logarithmic acid dissociation constant
pK_i	Logarithmic binding affinity constant
PubChem	Open chemistry databank
QM	Quantum mechanics
R	Indicates the configuration of a stereocenter in a molecule
RCSM	The Reseach Collaboratory for Structural Bioinformatics
S	Indicates the configuration of a stereocenter in a molecule
SAVES	Structural Analysis and Verification Server
SLC6	Solute carrier 6
SMILES	Simplified molecular-input line-entry system
SP	Standard precition
TMH	Transmembrane α-helical
Tox21	Toxicology in the 21st Century

TPSA	Topological polar surface area
UniProtKB	Universal Protein Resource Knowledgebase
vdW	Van der Waals
VFT	Venus Flytrap
vGluT	Ventricular glutamate transporter
VSW	Virtual screening workflow
wwPDB	Woldwide PDB
Å	Angstrom

1. INTRODUCTION

1.1 Environmental pollutants/toxicants

Exposure to pollutants is a serious and increasing public health problem. Pollutants, such as air pollution have been associated with a more frequent morbidity and increased mortality among humans and wild life. Diseases affecting the human CNS, including stroke, AD, Parkinson's disease, and neurodevelopmental disorders have also been associated with exposure to pollution (1). Many toxicants have a half live that can take many years, and evidence suggests that most people have varying degree of assorted toxic pollutants within their body. Exposure of toxicants is usually not a single event, and most often humans are repeatedly exposed for chemical toxicants on a daily basis, and some of them can accumulate in human tissues for decades (2).

The human CNS comprises of many neurotransmitters and their corresponding receptors. Neurotransmitters are chemical substances that act as signaling molecules and transmit impulses between nerve cells, or between nerve cells and effector cells (glands and muscles). Neurotransmission consists of the following steps: [1] synthesis of neurotransmitters, [2] package of neurotransmitters in storage vesicles, [3] action potential reaching nerve terminals, [4] release of neurotransmitters into the synaptic cleft by exocytosis, [5] activation of pre- and postsynaptic receptors, [6] removal of neurotransmitters from the synaptic cleft by transporters and enzymes. Toxicants that enter the CNS may interfere with the neurotransmitter systems, which can result in a wide range of adverse effects in humans including neurodegenerative diseases. In fact, if one neurotransmitter system is affected it can result in a secondary effect on other systems. Pollutants may also give indirect effects on neurotransmitter systems by causing mitochondrial damage, oxidative stress, cell death, or endocrine disruption. Toxicant induced mitochondrial damage and oxidative stress seem to contribute to neurodegenerative diseases such as dementia (2,3).

Depending on the type of toxicant and dose, a single exposure may not be harmful for humans but repeatedly exposure and accumulation of toxicants in the body may interfere with physiological functions in humans. Many people are aware of the harmful effects of smoking cigarettes, but there is not enough knowledge about how low levels of exposure to other

toxicants can cause disruption of physiological function in the human body, and in the CNS. Acute high dose poisoning can easily be recognized, but the chronic accumulative low-dose exposure of toxicants is harder to identity. A consequence of this can be that underlying cause of some diseases such as neurodegenerative diseases can go unnoticed because clinicians only focus on symptomatic treatments (2).

Long term exposure to toxicants and the bioaccumulation in humans over time may induce neuroinflammation resulting in the development of dementia. The progression of AD can occur over several decades, making it difficult to point out the major factors triggering the disease. Even though epidemiological association between environmental pollutants and dementia are still limited, there are emerging evidences that there may be a link between development of AD and the exposure of different environmental factors. Environmental factors such as, various inorganic and organic toxicants, including toxic metals, pesticides, industrial chemicals, solvents, air pollution, plasticizers (table 1) (2,4). In addition to AD, there is ongoing research on the relationship of exposure to environmental toxicants and the development of other CNS diseases such as Parkinson´s disease, Multiple Sclerosis (MS) and Amyptropic Lateral Sclerosis (ALS) (2).

Acute or chronic toxicity of different metals does not always result in degenerative diseases, and some of them are essential to maintain the human health. But there has been evidence that metals, such at lead, can disrupt cell-to-cell communication and the release of glutamate and GABA in the CNS. In addition, lead may also make the brain extra vulnerable to compounds by increasing the permeability of the BBB, which seems to have an impact on CNS diseases including Parkinson´s disease, ALS and AD (2,4).

Exposure to pesticides has shown to result in cognitive and psychomotor impairment which can result in the development of AD and Parkinson´s disease. Plasticizers can cross the fetoplacental barrier and cause growth retardation and neurological damage to the fetus (4).

The increasing prevalence of neurodegenerative diseases in humans is often thought of as a result of old age, but it can also occur due to long exposure and accumulation of toxicants in the body and the increase of pollutants in the environment. Specific toxic agents and levels of exposure that can cause different neurodegenerative diseases remain unknown, but this is an important field of continuous research (2,4). Tox21 is an initiative by the United States Environmental Protection Agency (EPA) and The National Institutes of Health (NIH). Tox21

consists of collaborative research teams that try to develop better methods to be able to quickly and efficiently test and evaluate whether certain chemical compounds have the possibility to be harmful for different physiologic processes in the human body. The aim is to develop tools that can be used in the risk assessments process and reduce the need for animal testing. The Tox21 initiative is also maintaining a database of potentially harmful environmental chemicals and drugs (5).

Table 1: **Overview of some toxicants that have been associated with neurodegenerative diseases (2,4).**

Environmental factors	**Compounds**
Toxic metals	Aluminum, copper, lead
Pesticides	DDE, Organophosphates insecticides, Organochlorine
Industrial chemicals	Flame retardants
Solvents	Carbon disulfide, toluene, PERC
Air pollution	Particulate matter, ozone, nitrogen oxide, second hand smoke, carbon monoxide
Plasticizers	Phthalate esters, Bisphenol A

1.2 Blood brain barrier

To be able to enter the CNS, toxic compounds have to cross the BBB. BBB consists of a thick layer of endothelial cells that selectively control transfer of compounds in and out of the brain. The compounds can penetrate the BBB by mainly two processes: passive and active transport. Active transfer of compounds is often carrier mediated and is an energy dependent process. This applies often for polar compounds, which is not able to penetrate the BBB by passive transport (6).

There are certain physical properties that have to be met to be able to penetrate into the brain by passive transport. General rules were developed of Lipinski et al., which aimed to provide an overview of physicochemical properties for compounds regarding solubility and membrane penetration. This was primarily aimed at CNS drugs but other compounds, such as toxicants, must also satisfy the requirements for being able to cross the BBB. Lipinski's "rule of five" summarizes the essential physical parameters for good absorption and permeability (molecular weight (Mw) $\leq$ 500; Log P $\leq$ 5; number of hydrogen bond donor (HBD) $\leq$ 5; number of hydrogen bond acceptor (HBA) $\leq$ 10; number rotatable bonds $\leq$ 10). In general, if two or more of this "rules" are not fulfilled, the compounds are not likely to be soluble and able to penetrate the BBB (6). Such hard cutoffs can result in a disregard of compounds that can actually cross the BBB.

Central Nervous System Multiparameter Optimization (CNS MPO) is a tool that has been developed in order to predict if a molecule has physicochemical properties similar to known CNS drugs and most probably can pass the BBB. CNS MPO balances different variables without a hard cutoff, because there are many ways for compounds to get a similar score value (7). CNS MPO algorithm is build on the basis of six parameters (table 2). All physicochemical properties have a desirable score ranging from less desirable (0.0) to more desirable (1.0). The summation of each scoring range yields in the final CNS MPO desirable score, which ranges from 0 to 6 were the most desirable score is $\geq$ 4 (7).

Table 2: **Overview of the CNS MPO properties.** The range values are from less desirable to more desirable (0.0-1.0) for each property. The summation of the properties score results in the final CNS MPO score.

Physicochemical properties	Less desirable range (Score = 0.0)	More desirable range (Score = 1.0)
Clog P	> 5	≤ 3
Clog D	> 4	≤ 2
Mw	> 500	≤ 360
TPSA	20 ≤ TPSA ≤ 120	40 < TPSA ≤ 90
HBD	> 3.5	≤ 0.5
p*K*a	> 10	≤ 8

Clog P: calculated log P, Clog D: calculated log D, TPSA: Topological polar surface area, p*K*a: the most basic center.

By using this tool it is possible to predict the ability of toxicants to cross the BBB. In order to know which toxicants that can harm the human brain, it is of importance to sort out only those that can reach the CNS. To be able to understand how the toxicants can affect the CNS it is also important to have knowledge about the CNS systems and its major neurotransmitters.

1.3 Glutamate and GABA as neurotransmitters

1.3.1 Glutamatergic neurotransmission

Glutamate is the major excitatory neurotransmitter in the human CNS and has important roles in sensing, motor coordination, emotion and cognition. Approximately 80-90 % of the neurons in the CNS use glutamate as their neurotransmitter and up to 90 % of the synapses are glutamatergic (8). Glutamate is packed into vesicles in the presynaptic neuron. When such a neuron fires, glutamate-containing vesicles fuse with the presynaptic membrane and release their contents into the synaptic cleft by exocytosis. Glutamate then enters the synaptic cleft and induce fast excitatory responses trough activation of three ionotropic glutamate receptors (NMDA, AMPA and kainate) and slower responses through activation of eight metabotropic glutamate receptors (mGlu1 to mGlu8 receptors) in the brain. Glutamate can also diffuse away from the synaptic cleft and bind to extrasynaptic receptors or be taken up by EAAT

glutamate transporters 1 and 2 (EAAT1, EAAT2) in gliacells. EAAT 3, which is estimated to be expressed postsynaptic, plays a minor role in the reuptake of synaptic glutamate (figure 1) (9–11).

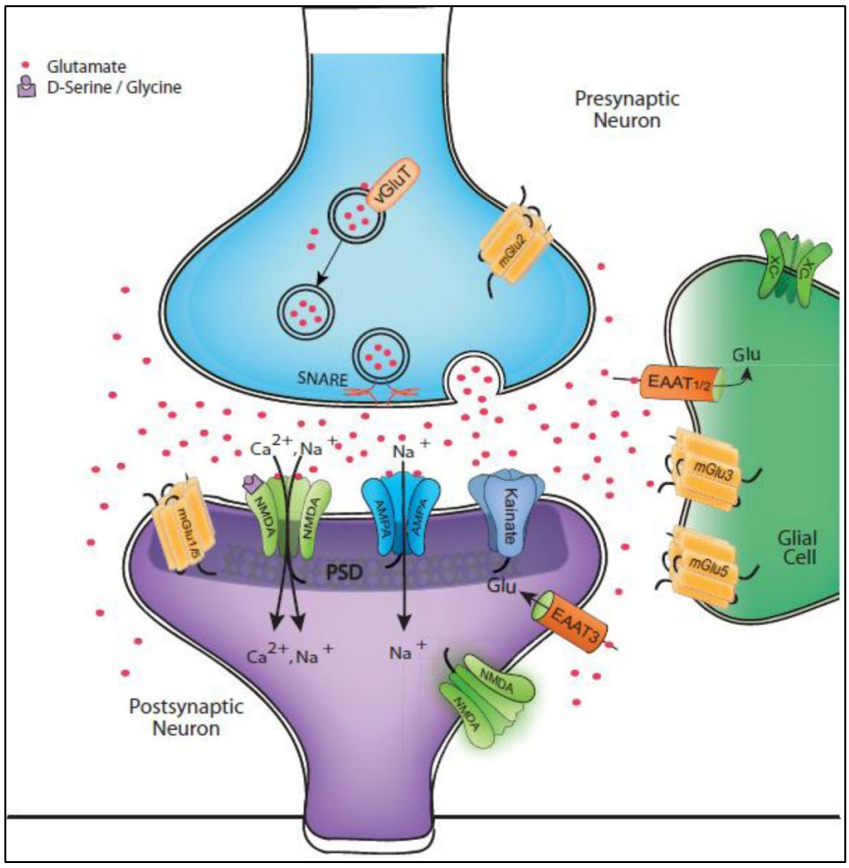

Figure 1: **The main components of the glutamate synapsis**. Glutamate is packed into vesicles by the ventricular glutamate transporter (vGluT). Glutamate can bind to its receptors presynaptic, postsynaptic and extrasynaptic. Glia cells play a major role in glutamate reuptake through the EAAT1 and EAAT2 transporters, terminating the glutamate signal. Adopted from (11).

NMDA, AMPA and kainate are tetrameric receptors and comprise of different subunits. When an agonist binds to an ionotropic glutamate receptor, a conformation change occurs in the receptor and it increases the probability of the channel to open which leads to influx of sodium and calcium ions into the cell (8).

Excessive activation of glutamate neurons can promote degeneration and cell death. The toxic effect of glutamate is primarily related to its excitatory properties, and this type of toxicity is called excitotoxicity. Excessive activation of e.g NMDA can kill the neuron by flooding the cell with too much calcium ions. In addition, activation of extrasynaptic NMDA receptors can lead to apoptosis and cell death. Glutamate concentration is therefore carefully controlled and regulated through high affinity glutamate transporters (8).

1.3.2 GABAergic neurotransmission

Glutamate is the precursor for GABA, which is the major inhibitory neurotransmitter in the human CNS. Glutamate is converted to GABA by glutamic acid dehydrogenase (GAD) in GABAergic cells. GABA is then packed into vesicles and fuses through the cell membrane by depolarization of the presynaptic neuron, and enters the synaptic cleft where it primarily targets receptors in the postsynaptic surface. It is removed from the synaptic cleft by the GABA transporters by reuptake into presynaptic neurons and glia cells (11,12).

GABA is present in high concentration in several regions in the human brain. In fact, the concentration of GABA is approximately 1000 times higher than the concentrations of the monoamine neurotransmitters in many brain regions. Studies of the GABA receptors have led to the discovery of at least three distinct GABA receptors: the GABA-A, the GABA-B and the GABA-C receptor. The GABA-A receptor is a ligand-gated ion channel. The receptor consists of five subunits (main ones are α, β and γ subunits). GABA can bind to the receptor on two binding sites, located between the α and β subunits. The receptor is primarily located postsynaptic and activation results in opening of the channel and influx of Cl^- ions into the postsynaptic neuron. (12). The GABA-B receptor is a GPCR and has structural similarities to the mGlu receptors and mediates slow signals in the CNS in response to agonist binding, while the GABA-C receptor is also a ligand gated ion channel (13).

GABA plays a part in several diseases and GABA dysfunction has been implicated in neurological and psychiatric disorders including development malfunctions, mental retardation and epilepsy, sleep disorders, drug dependence, sensorimotor processing and motor coordination (12).

The GABA-A receptor is a target for several CNS acting drugs, including benzodiazepines and barbiturates. Benzodiazepines bind selectively to an allosteric binding site in GABA-A with high affinity, in which enhances GABAergic transmission by increasing the frequency of channel opening of GABA-A receptors in response to GABA. This can result in sedative, anxiolytic and anticonvulsant effects. Long term use of benzodiazepines has shown to induce tolerance and dependence, where the patient has to increase the dose in order to produce the required effect. Sudden cessation of the drug intake can cause physical and psychological withdrawal symptoms. Barbiturates have been used since 1921 to treat epilepsy, and are now

also used as anesthesia. The most commonly used barbiturates are phenobarbital and pentobarbital. At pharmacological concentrations barbiturates increase the binding of GABA to its binding site through allosteric binding. In addition, high concentrations of barbiturates can activate the GABA-A receptor directly. The GABA analog Baclofen ((β-(4-chloro-phenyl)-γ-aminobutyric acid)) has shown to be a potent and selective GABA-B receptor agonist and is primarily used in the treatment of muscle spasticity especially in MS patients (12,13).

Glutamate and GABA both target GPCRs in the human CNS. GPCRs are in a complex network and have the ability to interact with each other. Toxicants can modulate the neurotransmission of glutamate and GABA by interacting with specific receptors or by interacting with specific transporters.

1.4 G protein-coupled receptors

GPCRs comprise of approximately 800 members and represent the largest protein superfamily of cell surface signaling receptors in the human genome (14,15). They are expressed in nearly all tissues and have diverse role in many physiological processes, ranging from vision, smell, and taste, to endocrine system, and neurological and cardiovascular functions. Many GPCRs are also involved in diseases, including cardiovascular, neurodegenerative, psychiatric, cancer and infectious diseases (15–17). Because of their diverse physiological roles, these receptors are attractive drug targets. In fact, more than 30 % of drugs on the market target GPCRs for the treatment of heart failure and hypertension (e.g β-adrenoceptors, adrenergic and angiotensin receptors), peptic ulcer (histamine receptors), pain (opioid receptors) and bronchial asthma (β_2-adrenoceptors) (16). Many endogenous compounds bind to GPCRs, including neurotransmitters, hormones, lipids, ions and enzymes (15,17). Since this type of receptors mediates such diverse physiological effects, agonist/antagonist binding can have great impact on the physiological processes (14,15).

All GPCRs share a 7 transmembrane α-helical (TMH) topology with three intra- and extracellular loops (ICL and ECL) and an extracellular N-terminal and an intracellular C-terminal (figure 2).

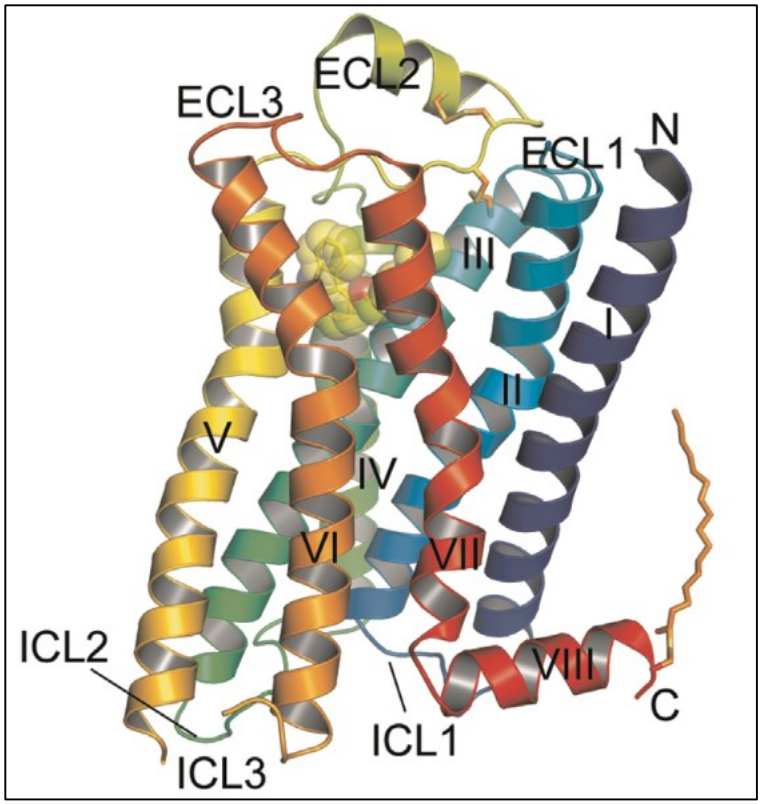

Figure 2: **Structure representation of a GPCR.** The figure shows the backbone of the β2-adrenergic receptor that has a 7 TMH topology with three ICL and ECL. The GPCRs also have an extracellular N-terminal and an intracellular C-terminal. Adopted from (14).

Agonists bind to the receptors on the extracellular side resulting in conformational changes in the 7 TMH domain, and activation of a heterotrimeric G protein that interacts with the intracellular regions of the receptor. The G protein comprises of three subunits: Gα, Gβ and Gγ. When the protein is in the inactive resting state, the Gα subunit contains guanosine diphosphate (GDP). When an agonist binds to the receptor and the G protein is activated, the subunits split into Gα and Gβγ complex and GDP dissociates from the Gα subunit and is replaced by guanosine triphosphate (GTP) (active state). The Gβγ complex has the ability to activate or inhibit specific target effectors (enzymes and ion channels) leading to cellular effects. The Gα-GTP complex dissociates from the receptor and activates target effectors leading to cellular effects. Finally, GTP hydrolyzes to GDP and the α-unit reunites with the Gβγ complex. The GPCR goes back to its resting state (figure 3) (16,18).

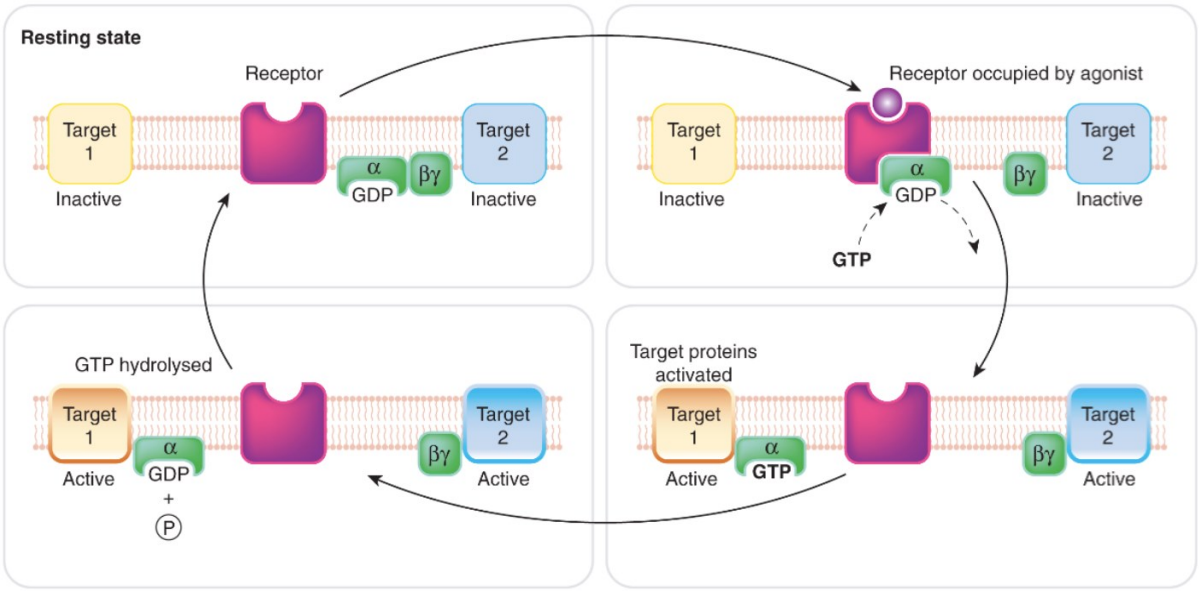

Figure 3: **Schematic representation of the function of a GPCR.** Adapted from (18).

Several different G proteins have been identified in the human genome, which contributes to the specificity of GPCR signaling and effects (16). Which signaling pathway a receptor activates, depends on the type of G protein the receptor recognizes and binds (19).

GPCRs in humans are classified into four main classes (or five families): A (*Rhodopsin*), B (*Secretin* and *Adhesion*), C (*Glutamate*) and F (*Frizzled/TAS2*) depending on the basis of sequence similarity. Class B, C and F are relatively small receptor classes, while the class A is the largest class and comprises of hundreds of receptors, which can be divided into subgroups: α, β, γ and δ. (14).

There are mainly two numbering systems for amino acid residues in the 7 TMH domain. The residues can either be identified by its sequence number or by a generic numbering system proposed by Ballesteros and Weinstein. In the latter numbering system, the amino acid residues are assigned two numbers termed X.YY, which is superscripted. The first number (X) refers to the TMH domain number (1 to 7) and the second number (YY) indicates the amino acids position relative to the highest conserved residue within one helix, which is given the number 50 (20,21). For instance, amino acid $Arg^{3.32}$ exists for both the mGlu2 and the mGlu7 receptors, located 18 amino acids upstream of the most conserved amino acid in TMH3. For the mGlu2 receptor, this Arginine is amino acid number 635 in the sequence, while for the mGlu7 receptor it is number 658.

1.4.1 Class C of G protein-coupled receptors

The class C of GPCRs are mainly activated by small molecules and comprises fifteen receptors, including eight mGlu receptors, the GABA-B receptor, and the calcium sensing receptor, taste 1 receptors and some orphan receptors (19). As for all the other GPCRs, class C receptors contain a 7 TMH domain. In addition, most class C receptors also have a large extracellular domain, which contains the orthosteric binding site. The mGlu and the calcium sensing receptors are homodimers, whereas the GABA-B and taste receptors are heterodimers.

1.4.1.1 Metabotropic glutamate receptors

mGlu receptors were first discovered in the late 1980s and belong to the class C of GPCRs (22)**.** MGlu receptors are mainly expressed in the CNS and eight receptor subtypes have been identified: mGlu1 to mGlu8 receptors. The receptors are divided into three groups based on their sequence homology, pharmacology, and signal transduction mechanism (G-protein coupling preferences) (table 3) (20). The receptors activate intracellular heterotrimeric G protein, which further activates signaling cascades inside the cell (14,19).

Table 3: **An overview of the mGlu receptor subtypes.** Their primarily G protein-coupling pathways and their location in the synapsis are indicated.

Group	Receptors	G protein pathway	Location
I	mGlu1 mGlu5	G_q – Increases intracellular calcium	Post-synaptic
II	mGlu2 mGlu3	$G_{i/o}$ - Decreases cAMP synthesis	Pre-synaptic (Often located far from the synaptic cleft along the axon)
III	mGlu4 mGlu6 mGlu7 mGlu8	$G_{i/o}$ – Decreases cAMP synthesis	Pre-synaptic (Expressed near the site of fusion with synaptic vesicles)

Group I mGlu receptors are mainly expressed postsynaptic in excitatory glutamatergic synapses in the CNS. The mGlu5 receptor is found in brain areas involved in emotion, motivation and cognition, which makes this receptor an important drug target (22,23).

Group II and III mGlu receptors are primarily found presynaptically in glutamateric synapses of the brain. They serve as autoreceptors and the activation of these receptors has shown to decrease glutamate release. Their mechanism contributes to the regulation of glutamate concentration in the synapsis and thereby regulating the synaptic transmission (22).

MGlu receptors exist as homodimers that are cross-linked through an intermolecular disulfide bond. Each monomer consists of the GPCR signature motif of 7 TMH with three ICL and three ECL that connect the helices, as well as an intracellular C-terminal and an extracellular N-terminal. In addition, mGlu receptors also contain a large extracellular domain (ECD) composed of a Venus Flytrap (VFT) domain linked to the 7 TMH via a cysteine-rich domain (CRD) (figure 4) (19,24).

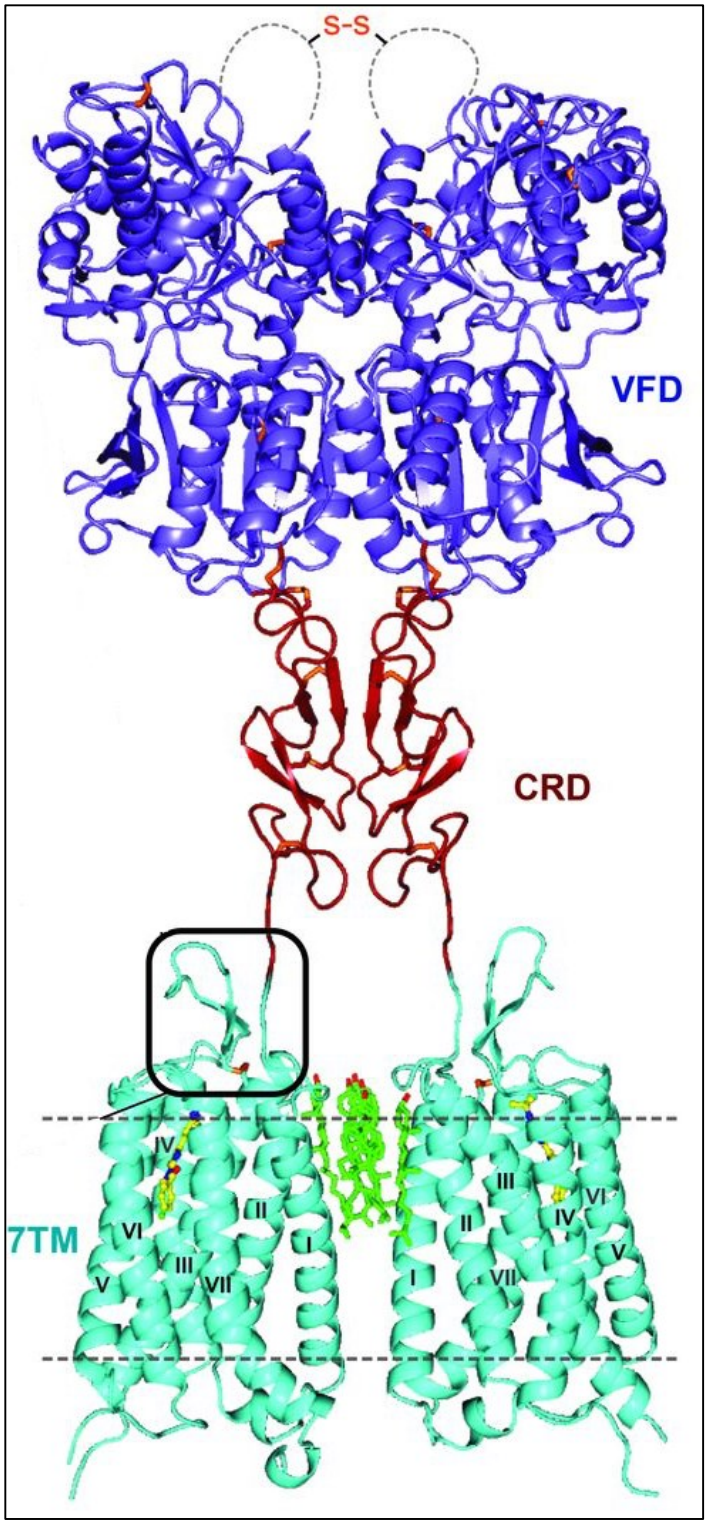

Figure 4: **Full length mGlu1 receptor.** The figure is modified from Wu et al. (24) and is showing the backbone of a full length mGlu1 receptor homodimer with the VFT, CRD and 7 TMH domains colored in purple, red and green. Disulfide bonds link the ECD together, and a cluster of cholesterol molecules (shown as green molecules) makes interactions between the two TMH1 in each dimer (24).

The mGlu receptors can be activated in two different ways: [1] By binding to the orthosteric binding site in VFT [2] By activation through allosteric binding, referred as the allosteric binding site (22).

The VFT forms a bi-lobed structure, where each lobe (I and II) is separated by a cleft in which the ligand can bind and interact. It is now clear that this region serves as the orthosteric binding site and is responsible for agonist activity (figure 5). VFT domain is in a constant dynamic equilibrium between an open and a closed conformational state. The exogenous ligands that bind to the orthosteric binding site are competing with the endogenous neurotransmitter, glutamate. When the receptor is bound to an agonist, the VFT is generally stabilized in a closed conformational state, whereas in the absent of a ligand or bound to an antagonist, the VFT is more frequently in an open conformational state. In the same way as glutamate, the exogenous agonists induce a conformational change in the receptor, which activates the second messenger system inside the cell (14,19,22).

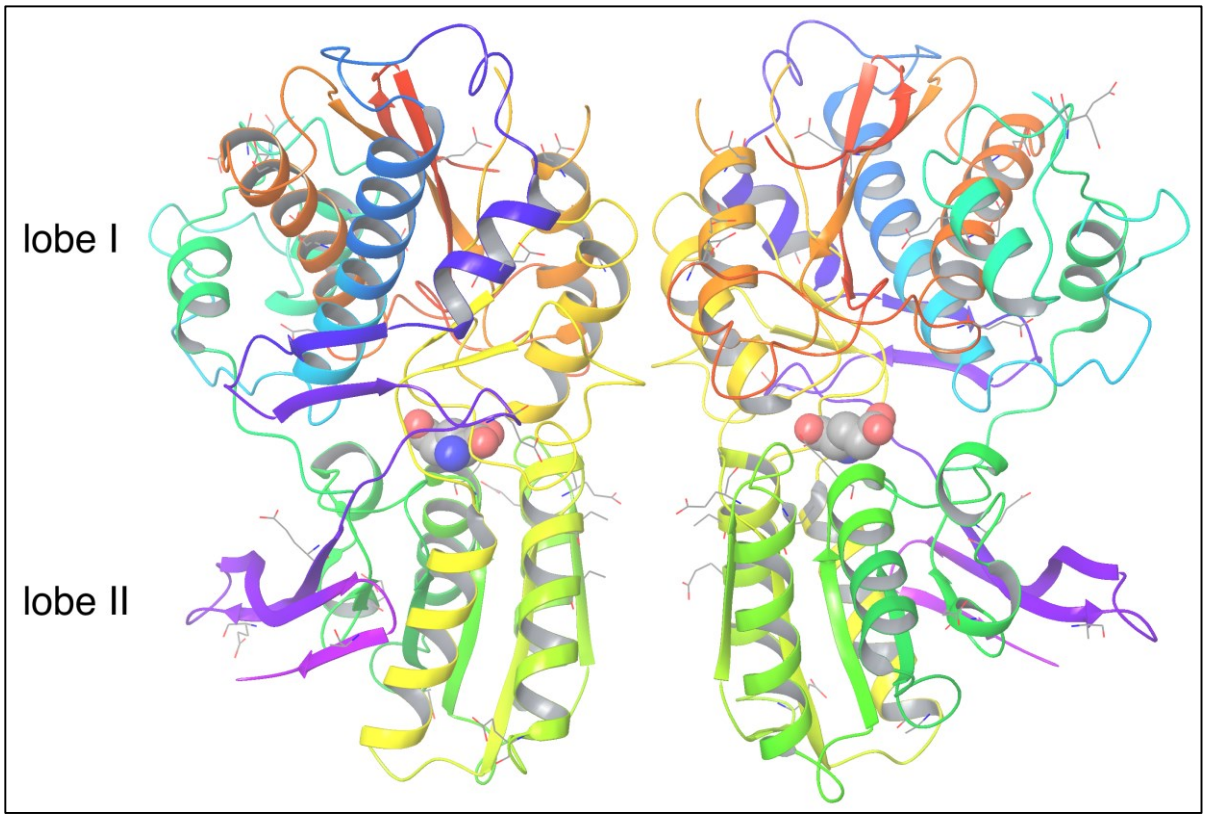

Figure 5: **The crystallized three dimensional (3D) structure of the homodimer VFT of mGlu5 receptor (PDB ID: 3lmk) in complex with the neurotransmitter glutamate (shown in bulked cartoon).** The figure shows the backbone of the VFT of mGlu5 receptor in a closed conformational state. Lobe I and II are indicated. Both ligands placed in the binding pockets are glutamate, but one is orientated so that the nitrogen is not visible. The carbons in glutamate are shown in gray color, oxygens are shown in red color and nitrogens are shown in blue color.

The allosteric binding pocket is located within the 7 TMH domain of mGlu receptors (figure 6). Allosteric activation adjusts the intensity of the receptor response and is only functional if the orthosteric ligand is present. Compounds that bind to the allosteric binding site are referred to as allosteric modulators and are classified on the basis of their pharmacology. They act primarily by inducing conformation changes in the receptor without activating the G protein pathway on its own and modulate affinity or efficacy of orthosteric agonists in a positive or negative way. Allosteric modulators that enhance an agonist-mediated receptor response are referred to as "positive allosteric modulators" or PAMs, while allosteric modulators that reduce receptor activity are known as "negative allosteric modulators" or NAMs. In addition, a special type of agonist PAMs also exists, which are able to activate the receptor as an allosteric agonist without the need of an agonist that binds to the orthosteric site (22,25,26). With some variety among the mGlu receptors, the main TMH and ECL that participate in the binding of allosteric modulators are TM2, TM3, TM5, TM6 and TM7 and ECL2 (23,24,27).

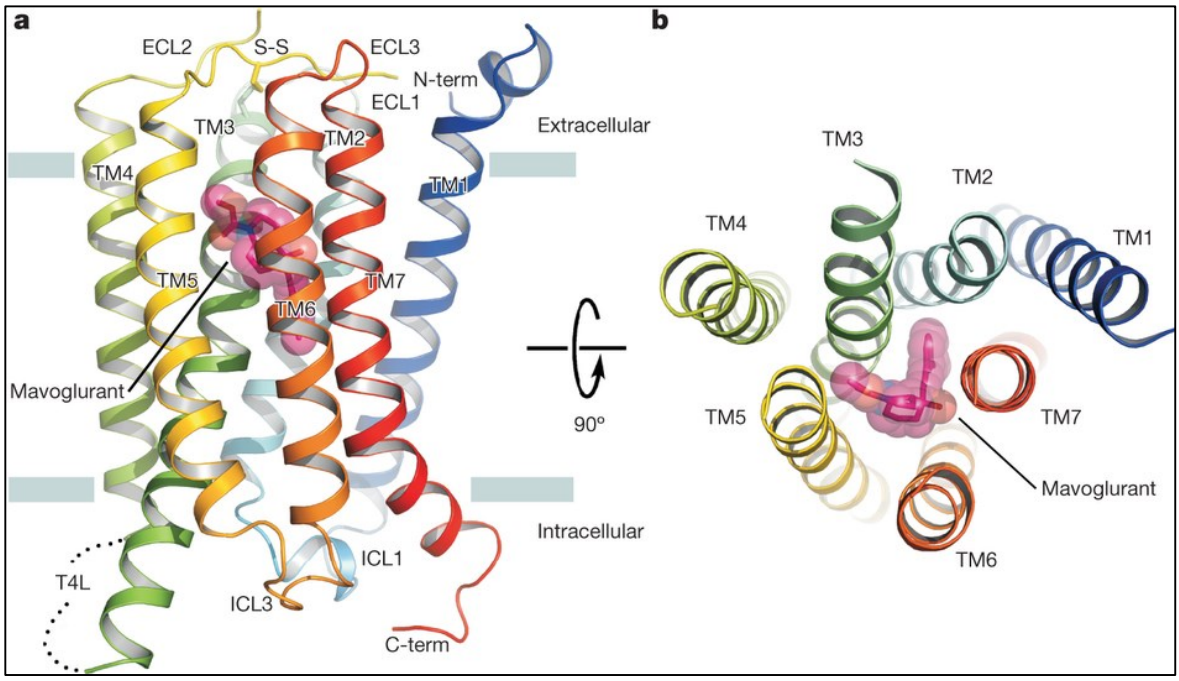

Figure 6: **A ribbon representation of the backbone of the 3D structure of mGlu5 receptor 7 TMH domain bound to the NAM mavoglurant (shown in translucent stick representation).** a) View of the receptor domain from the side parallel to the cell membrane. b) View down into the 7 TMH domain from the extracellular side. Adapted from (23).

1.4.1.2 GABA-B receptor

GABA-B receptor is also a member of class C of GPCRs and has a structural topology similar to that of the mGlu receptors. GABA-B receptor is the target for the major inhibitory neurotransmitter GABA, and mediates slow and prolonged synaptic inhibition effects in the CNS. The receptor is localized both pre- and postsynaptic, in which the presynaptic GABA-B receptor suppresses neurotransmitter release and the postsynaptic GABA-B receptor hyperpolarizes neurons (12,13).

GABA-B and mGlu receptors are similar in structure, but unlike mGlu receptors that are homodimers, GABA-B receptor is a heterodimer that comprises of two subunits: GABA-B1 and GABA-B2 subunits. In addition, GABA-B receptor does not comprise of a CRD, and the VFT and the 7 TMH domain are therefore directly linked to each other (figure 7). The GABA-B1 subunit contains the orthosteric binding site and is responsible for ligand binding on the extracellular site. The GABA-B2 subunit contains the allosteric binding site within the 7 TMH, and interacts and activates the G protein inside the cell ($G_{i/o}$). GABA-B2 VFT domain does not have any known binder, but it contributes to enhancement of the agonist affinity of the receptor by interacting with the VFT of the GABA-B1 subunit. Both subunits for the GABA-B receptor must be present for the receptor to function (8,13,22,28).

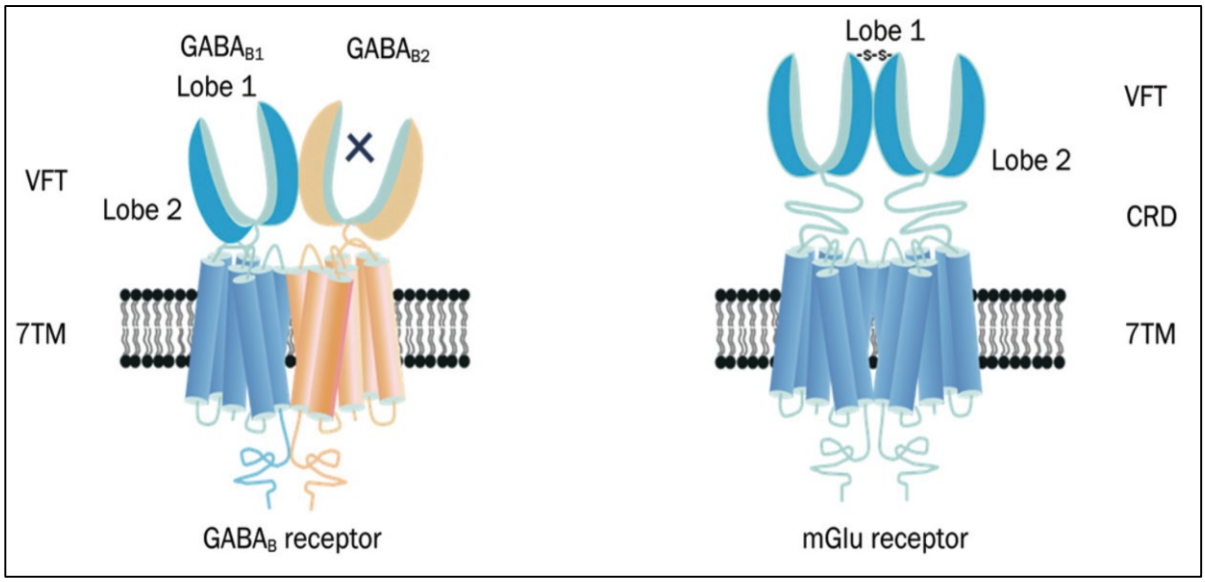

Figure 7: **Schematic representation of GABA-B receptor and mGlu receptor as hetero- and homodimers**. The cysteine rich domain in mGlu receptors is not present in GABA-B receptors. The X in GABA-B2 VFT indicates that it is not the orthosteric binding site. Adopted from (28).

1.4.2 X-ray structures of G protein-coupled receptors

Knowledge about the structures and the dynamics of proteins are important for understanding many biological processes as well as for getting a better understanding of molecular physiological processes (16,29). Resolved high-resolution X-ray structures of GPCRs and the knowledge of 3D structure of a receptor have a great impact on drug discovery. It opens up for more reliable structure-based drug design, and the ability of designing drugs with better selectivity and pharmacokinetic properties (30).

The recent years breakthrough in crystallography and protein engineering have expanded the understanding of GPCRs 3D structures. Crystal structures of GPCRs can provide better templates in homology modeling and provide detailed information about ligand binding to GPCRs. Nearly all of the receptor crystal structures are in complex with a ligand, which helps stabilizing the protein structure. Most of the ligands are high-affinity antagonists, and some are agonists (30).

The first GPCR to be crystallized was rhodopsin in 2000. Later on, more and more GPCRs have been crystallized. In fact, more than 60 ligands and 20 receptor X-ray structures, for all classes of GPCRs (A, B, C and F) have been reported. Most of the structures solved for mGlu receptors have been of the VFT domain only, containing the orthosteric binding site. In 2014, the first X-ray structures of 7 TMH of mGlu1 and mGlu5 receptor in complex with a NAM were reported. MGlu1 receptor in complex with FITM (4-fluoro-N-(4-(6-(isopropylamino)pyrimidin-4-yl)thiazol-2-yl)-N- methylbenzamide) and mGlu5 receptor in complex with mavoglurant (methyl (3aR,4S,7aR)-4-hydroxyl-4-[(3-methylphenyl) ethynyl] octahydro-1H-indole-1- carboxylate) (30).

1.5 GABA transporters

GABA is not enzymatically removed from the synaptic cleft and its clearance depends on GABA transporter reuptake (31). GABA transporters are widely expressed in the human brain and they belong to a large family referred to as the solute carrier 6 (SLC6), which also includes transporters for dopamine, serotonin, norepinephrine, tryptophan, tyrosine, leucine and glycine. Approximately 117 eukaryotic and 167 prokaryotic transporters have been

classified, and the first X-ray crystal structure of a prokaryotic SLC6 member was published in 2005, the *Aquifex aeolicus* leucine transporter (LeuT) (31,32). Since then, several crystal structures of these transporters have been resolved and in April 2016 six X-ray structures of the *human* serotonin transporter (hSERT) were published (PDB ID: 5I6X, 5I6Z, 5I71, 5I73, 5I74 and 5I75), which must be considered as breakthrough. The SLC6 family is membrane proteins comprised of 12 TMH expanding through the membrane with cytoplasmic N- and C-terminal domain (31). The 3D structure of the *drosophilia* dopamine transporter (dDAT) or the hSERT structures can be used as representative members of the SLC6 family (figure 8).

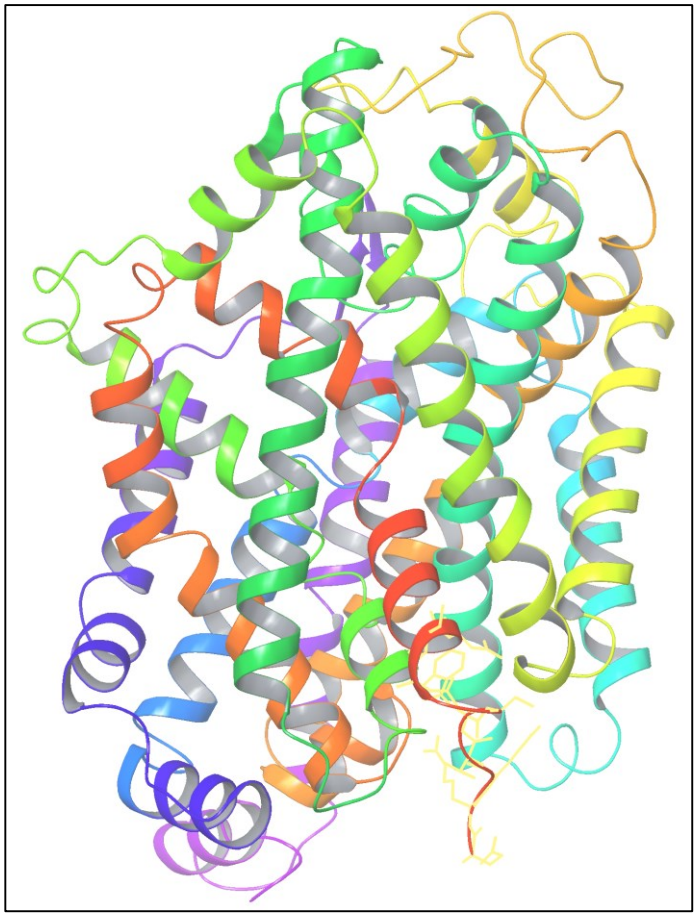

Figure 8: **The crystal structure of *drosophila* dopamine transporter (dDAT) (PDB ID: 4XP4) retrieved from www.pdb.org.** The dopamine transporter structure comprises of 12 TMH and is a structural representative for the SLC6 family. The extracellular site of the transporter is located at the top of the figure.

The GABA transporters are secondary transporters that are classified into six groups, where GAT1, GAT2 and GAT3 are the most characterized. GAT1 are located both pre- and postsynaptic. The function of postsynaptic GAT1 is not completely understood. Presynaptic GAT1 is primarily responsible for reuptake of extracellular GABA but it also translocates GABA from the intracellular cytoplasm to the extracellular space. The transport of GABA across the membrane is an active process and requires Na^+ electrochemical gradient, which is mainly created by the membrane Na^+/K^+ ATPase that actively pumps Na^+ out and K^+ into the cell by using the energy from adenosine triphosphate (ATP) (31,32).

1.6 New approaches in treatment of CNS disorders

The widespread location of mGlu receptors throughout the CNS makes them attractive targets for drug treatment of generalized anxiety disorder, Parkinson's disease, Fragile X syndrome, schizophrenia, acute migraine, gastro esophageal reflux disease (GERD), drug addiction, chronic pain and certain types of cancers (20,33).

It was assumed that the orthosteric binding site in the VFT among the mGlu receptors were well conserved compared with the 7 TMH domain, making it an unattractive drug binding site because of difficulties with selectivity. But recently it was shown that there is in fact greater sequence conservation among the 7 TMH than the VFT. However, the main focus in drug development for mGlu receptors are allosteric modulators (14,33).

There has been an increase in the discovery and understanding of allosteric modulators of GPCRs over the years, and there are now some allosteric modulators marketed as drugs, including treatment of HIV infections (interacting with class A receptors) and hyperparathyroidism (interacting with a class B receptors). However, no allosteric modulators for the mGlu receptors have been approved as drugs for threatening psychiatric and neurological disorders but some have entered clinical studies (17).

NAMs for the mGlu5 receptor have or are being tested in clinical trials for the treatment of Fragile X syndrome, Parkinson's disease, levodopa-induced dyskinesia, anxiety, GERD, neuropathic pain, obsessive-compulsive disorder, migraine, chorea in Huntington's disease and depression. The NAM mavoglurant were tested for the treatment of Fragile X syndrome

but the study failed to show efficacy. Reports from phase II in clinical trial by Roche with the use of the NAM basimglurant as an adjunctive drug in major depressive disorder has shown encouraging results, which can strengthen the approach of developing novel antidepressant for glutamateric systems in the CNS. In addition, the Addex Therapautic's NAM dipraglurant is in clinical development for rare dystonia and Novartis have evaluated mavoglurant in the phase II in the treatment of obsessive-compulsive disorder (34).

Some drug candidates that target mGlu receptors have been tested in both preclinical and clinical studies. Preclinical studies have shown that these drug candidates have putative antidepressant, anxiolytic, antipsychotic, anti-parkinsonian, anti-addictive, analgesic and anti-fragile X syndrome activities in animal models (22).

Designing allosteric modulators for mGlu receptors offers great possibilities for subtype selectivity, but there are some challenges. It exists some possibility for cross activity among the receptors, where for example mGlu4 receptor PAMs act as NAMs for mGlu1 and mGlu5 receptors. It is important to design drugs that are selective for a subtype receptor and does not act on other receptors, to avoid side effects and toxic effect in humans (10,20).

1.7 Molecular modeling

Molecular modeling is a collective term of different computational techniques where scientists are allowed to visualize 3D molecules, to simulate, analyze and predict properties and behaviors of molecules on an atomic level. It is also used in the discovery of new lead compounds for drug development and to refine existing drugs *in silico*. Molecular modeling includes molecular mechanics (MM) and quantum mechanics (QM) methods (35).

MM is a relative fast computational method and is based on the assumption that the energy of a whole system is the sum of inter- and intra molecular interactions. MM calculates the total energy of a molecule (E_{tot}) as the sum of bonded and non-bonded interactions, including bond stretching energy (E_{str}), angle bending energy (E_{angle}), energy for rotation around a bond (E_{tors}), van der Waals interaction energy (E_{vdW}) and electrostatic interaction energy (E_{el}) (35,36). The total energy function is given by the following equation:

$E_{tot} = E_{bonded} + E_{non\text{-}bonded}$; or

$E_{tot} = (E_{str} + E_{angle} + E_{tors}) + (E_{vdW} + E_{el})$

The collections of these individual interaction values are referred to as force field (36).

QM methods can calculate molecular geometry and relative conformational energy and offers the most detailed description of molecules chemical behavior. It has disadvantages relative to MM that it has high computational costs and it is limited to only small molecules (35,36).

1.7.1 Homology modeling

Computational methods in protein modeling for constructing 3D structural models are widely used in research within academia and pharmaceutical industry. Several 3D structures of proteins have been crystallized and the structures have been solved at high resolution. However, there are still several proteins with unknown 3D structure, and there are still quite few membrane proteins of known 3D structure (37). To be able to study their structure and function, homology modeling is an important approach for constructing 3D models of GPCRs and other membrane proteins (38).

Homology modeling is considered to be the most accurate available computational method for studying proteins with unknown structure and has been commonly applied in drug discovery. It is based on the fundamental observations that evolutionally related proteins can adopt similar 3D structures. The homology modeling approach is primarily based on the different steps included in figure 9, which can be repeated until the satisfactory model quality is achieved or until it cannot be further improved (37–39).

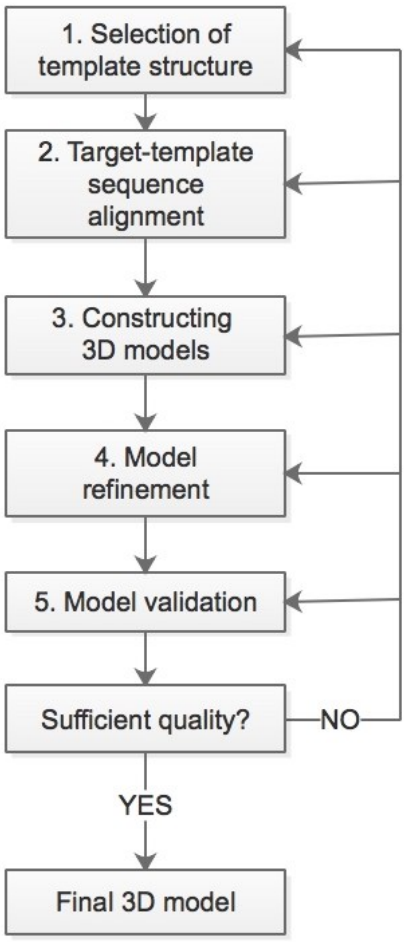

Figure 9: **Main steps in homology modeling**.

Selection of the most suitable experimental template structure

Selection of a suitable crystallized 3D structure ("template") for the modeling is the first step in homology modeling. Since only the amino acid sequence of the receptor structure of interest ("target") is known, it is important to select a template that has as high sequence and functional similarity to the target as possible. Template structures can be obtained by comparing its amino acid sequence to the target sequence. If the target and the template share sequence similarity, it can be said that they share a common evolutionary structure and their 3D structures can be expected to be similar (39). For modeling of receptor structures in an active or an inactive state, it is desired to select templates bound to an agonist or an antagonist to examine interaction with the appropriate active or inactive conformational state of the receptor. The most suitable template is the one that is in the appropriate conformation state and has the highest sequence homology to the target (21).

Target-template sequence alignment

After the template has been selected, the target sequence is aligned with the amino acid sequence of the template. Target-template sequence alignment is a major determinant for the final resulting quality of the constructed model. The more accurate the alignment is, the more accurate are the models and less work is to be done with the final model refinements (29,39).

When generating a target-template sequence alignment it is important to locate the regions in the alignment that may need adjustments, for instance removing gaps from regions in the alignment representing structurally conserved regions (e.g. conserved helices and beta-strands). There may be regions in the alignment displaying significant structural differences between the target and the template. This becomes common for proteins that are not so structurally related. Often it is desired to align the target with a number of available templates to get an accurate alignment. Different regions in the target sequence can be aligned with different templates to improve the alignment and the model. It is possible that only some regions of the receptor template are available as 3D structures or that the alignment is not accurate over the entire sequence length of the target. Multiple template alignment can contribute to an improvement of the modeling procedure (39).

A correct target-template sequence alignment should include all the similar structural and evolutionary residue pairs, but at the same time leave out structurally divergent regions between the target and the template (39).

Homology model building

When the sequence alignment has been obtained, a 3D structure of the target can be constructed by homology modeling. The 3D structure is built on the basis of the target-template sequence alignment.

In general, the amino acids in the 7 TMH domains are often conserved in different GPCRs. This makes the modeling quite straight forward concerning the helices. Modeling of ICL and ECL is a challenge because they can differ between the GPCRs in shape and in number of

amino acids (21). However, it has been demonstrated that “loop-less” models can be used in structure based virtual screening, where the binding pocket is of main interest (37).

Model refinement

Model refinement is an important step in homology modeling. It is used to eliminate the structural errors that may have occurred in the building of the 3D models. Energy functions in homology modeling can give the models correct covalent geometry and it can also help avoiding errors, like steric clashes and atomic overlap of residues (40).

Homology modeling is based on Anfinsen’s thermodynamic hypothesis, where a proteins native structure is determined by its amino acid sequence and that its favorable conformation is the one with the lowest free energy. This assumption gives an approach in protein structure modeling to construct a structure with as low free energy as possible. Model refinement with energy functions can help selecting the near-native structures based on the Anfinsen’s thermodynamic hypothesis. Overall, it helps to refine the models and give a final model with high quality (40).

Model quality validation

Making a series of virtual screening experiments is an optimal approach to validate the correctness and predictivety of the constructed models. This applies especially if the purpose of the homology models is to investigate receptor-ligand interactions. A set of active compounds (known binders) for the receptor and a large number of inactive compounds (decoys) are docked with molecular docking to the binding site in the receptor model (41). Decoys are compounds with similar Mw and physiochemical properties as the known binders, but their affinity for the receptor is much lower. The result from the docking calculations is then evaluated by calculations of enrichment factors (EF) and Boltzmann-enhanced discrimination of receiver-operating characteristic (BEDROC) parameters and enrichment plots for each receptor model are also constructed. The models are ranked by their ability to discriminate between decoys and actives (41–43).

1.7.2 Docking and scoring

A major challenge many molecular modeling programs have today is to be able to mimic the flexibility of a protein target. A native protein target will always be in equilibrium between different conformations, and the ligand bound conformation is not necessarily the conformation obtained by X-ray crystallography or homology modeling.

Molecular programs use docking and scoring to be able to identify the best ligand binding pose and protein structure conformation. A binding pose is the preferred orientation and conformation a ligand gets in a protein binding site during docking [37]. Many molecular modeling programs uses semi-flexible docking, with a flexible ligand docked into a rigid receptor (44). An ideal situation would be for both the ligand and the receptor to be flexible, and one approach to enhance the docking procedure is by including some flexibility into the receptor. This includes induced fit docking (IFD) protocol where the receptor side chains in the binding pocket are refined after docking a ligand to the binding pocket. In addition, docking one ligand into an ensemble of several receptor conformations can also incorporate receptor flexibility (45).

Scoring assess the quality of a binding pose where each predicted pose is given a score and is ranked from lowest to highest score (44). The free energy of binding (ΔG) is given by the Gibbs-Helmholtz equation:

$$\Delta G = \Delta H - T\Delta S = -RT\ln K_i$$

ΔH is the enthalpy, T is the temperature in kelvin, ΔS is the entropy, R is the gas constant and K_i is the binding constant. It exists several techniques for predicting the binding free energy and the scoring function can be classified into four main categories: the empirical, the force-field-based, the knowledge-based and the consensus function. The functions differ in accuracy and speed, where one with the highest accuracy is generally the one that is the most time consuming. The ideal scoring function would rank highest the binding mode that is most similar to the experimental one. The empirical energy function calculates binding scores fast based on simple energy terms known to be important in ligand binding such as vdW, electrostatics, hydrogen bond (H-bond), desolvation, entropy and hydrophobicity energy terms. Force-field-based scoring function is based on terms of MM force field, including bond

stretching/bending/torsional forces and vdW interactions and electrostatic interactions. The knowledge-based scoring function uses energy potentials derived from structural information gathered from experimentally determined atomic structures. Consensus scoring function combines the empirical, the force-field-based and the knowledge-base scoring function (36,46).

Docking and scoring can be used for different purposes, including identifying the binding mode of a known ligand in a binding site or screening a set of ligands to the binding site. In addition, docking and scoring can be used for searching large virtual databases for identification of potential drug hit/lead compounds for a particular protein and for prediction of binding affinity of a ligand to a protein structure or homology model (44,46).

2. AIM

The aim of this study is to predict putative interactions and binding modes of 8194 exogenous toxicants from the Tox21 database (version spring 2012) with mGlu receptors and the GAT1 using molecular docking. Constructed homology models of mGlu receptors and the GAT1 and known X-ray structures of mGlu receptors retrieved from Protein Data Bank were used for the docking.

Interactions of exogenous toxicants with these receptors and transporters could possibly result in harmful CNS effects and diseases. These proteins are also very interesting targets for new drug development and exogenous toxicants may interfere with the effects of drugs functioning by binding to these receptors. The study will provide information concerning which of the toxicants that may interact with the mGlu receptors and the GAT1. Docking calculations is done for 3D structures/models of mGlu receptors (mGlu2, mGlu5 and mGlu7 receptors) and the GAT1 models with known agonists, antagonists, allosteric modulators and decoys in order to test the predictivety of the models. Therefore, the study also gives detailed information into how known agonists, antagonists, NAMs and PAMs interact with the binding sites in mGlu2, mGlu5 and mGlu7 receptor and the GAT1. The information of different binding interactions in these proteins is of pharmacological importance for development of future drugs.

3. METHODS

3.1 Software

Molsoft Internal Coordinate Mechanics software (ICM) (version 3.8.4)

ICM is an approach, which gives a general modeling and structure prediction framework for many different tasks of structural biology and rational drug design. In this thesis, ICM was used to convert ligands and decoys from SMILES to two dimensional (2D) structures and construction of multiple sequence alignments of mGlu receptors.

Schrödinger (version 2015.3)

Maestro is a software that gives a molecular environment with a wide selection of analysis tools. It is an interface for all Schrödinger software (http://www.schrodinger.com/Maestro/). Modules used for docking in this thesis were glide docking. Protocols used were one-step protein preparation, ligand preparation (Ligprep), virtual screening workflow (VSW) and induced fit docking (IFD).

MODELLER (version 9.13)

MODELLER is a computer program for protein structure modeling that is frequently used in homology modeling. It is a non-graphical program that is used with a scripted language. Based on aligned protein sequences, MODELLER will automatically calculate and construct 3D structure models of proteins that include all non-hydrogen atoms (47). In this thesis, MODELLER was utilized for homology model building of mGlu2 and mGlu7 receptors and the GAT1.

CNS MPO

Putative BBB penetration of the compounds of the Tox21 database was performed with the CNS MPO software. CNS MPO is normally used to predict BBB penetration of CNS drug candidates. The CNS MPO algorithm is built on the basis of six parameters: [1] Clog P; [2]

Clog D; [3] Mw; [4] TPSA; [5] number of HBD; [6] p*K*a. All of these physicochemical properties have a desirable score ranging from less desirable (0.0) to more desirable (1.0). Summarized scoring range yields in the final CNS MPO desirable score, which ranges from 0 to 6 were the most desirable score is ≥ 4 (7).

3.2 Databases

Protein Data Bank (PDB)

The Research Collaboratory for Structural Bioinformatics (RCSM) is responsible for the management of the PDB, which is available at no cost for users. PDB consists of different databases to form a single uniform worldwide PDB (wwPDB) for all users, in collaboration with PDBe (UK), PDBj (Japan) and BMRB (USA). PDB contains information about 3D structures of large biological molecules of proteins and nucleic acids found in all organisms, including bacteria, flies, human and other animals (48). Most of the structures in PDB have been solved using X-ray crystallography. The template crystal structures used in homology modeling are downloaded from this database. (www.pdb.org).

Universal Protein Resource Knowledgebase (UniProtKB)

The UniProtKB provide users with scientific collection of functional information about proteins and protein sequences. The database comprises of two sections; Swiss-Prot and TrEMBL. The targets sequences used for the construction of multiple sequence alignment and in homology modeling are retrieved from Swiss-Prot section of UniProtKB. The database was also used to align sequences to identify their homology. (www.uniprot.org)

Database of Useful Decoys: Enhanced (DUD.E)

DUD.E is a database with useful decoys. These are molecules that have similar physical properties as the binders, but different topology. DUD.E were used to generate and download decoys of active compounds that were further used in docking calculations. (www.dude.docking.org)

IUPHAR/BSP Guide to Pharmacology

The database provides quantitative information about drug targets and compounds that act on them, including some medicines and experimental drugs. The British Pharmacological Society (BPS) and the International Union of Basic and Clinical Pharmacology (IUPHAR), in collaboration create this database. It exists detailed introductory chapters for each target receptor with information about pharmacological, physiological, structural, genetic and pathophysiological properties (49). Known binders (agonists, antagonists, NAMs and PAMs) for each receptor subtype were retrieved as SMILES from this database and used in docking calculations. (http://www.guidetopharmacology.org)

PubChem

Pubchem contains information of the biological activities of small molecules. It is organized into three sections: PubChem Substance, PubChem Compound, and Pubchem BioAssay. In this thesis, PubChem Compound section was used to download SMILES of compounds that were not to be found in the IUPHAR/BSP Guide to Pharmacology database.
(https://pubchem.ncbi.nlm.nih.gov)

Toxicology in the 21st Century (version spring 2012)

Tox21 is a collaboration between research teams including United States Environmental Protection Agency (EPA), NIH, including National Center for Advancing Translational Sciences and the National Toxicology Program at the National Institute of Environmental Health Sciences, and the Food and Drug Administration (5). The initiative is also to maintain a database of approximately 8000 environmental toxicants. In this thesis, the Tox21 database was used to retrieve 8194 exogenous toxic compounds for docking into constructed homology models and X-ray structures.

3.3 Homology modeling

The crystal structures of 7 TMH of mGlu2 and mGlu7 receptors have not yet been resolved. In order to calculate interactions between exogenous toxicants and the allosteric binding sites of these receptors, it was necessary to build theoretical 3D models by using the homology modeling approach. In addition, 3D structure models of GAT1 were constructed with homology modeling based on the related dDAT as template.

Selection of the most suitable experimental template structure

The template was chosen based on the following criteria 1) the template should have as high as possible homology to the target, 2) contain the binding site of interest in complex with a ligand 3) have as high resolution as possible.

There are only few structures of the 7 TMH for mGlu receptors that have been crystallized, so the selection was limited to crystal structures of the mGlu1 receptor and the mGlu5 receptor. The crystallized 7 TMH of mGlu5 receptor (PDB ID: 4OO9) had a higher resolution than of the crystal structure of mGlu1 receptor (PDB ID: 4OR2) and was therefore selected as template for the homology modeling of the allosteric site of mGlu2 and mGlu7 receptor (table 4). Selection of template for GAT1 was based on the homology identity between GAT1 and DAT. The sequences of the transporters were aligned in Uniprot databased to identify their homology. The overall sequence identity between GAT1 and DAT was approximately 41 %. In addition, the template dDAT (PDB ID: 4XP4) had the highest resolution out of the available DAT X-ray structures and was therefor selected as template for the homology modeling of GAT1.

Table 4: **Information about the crystal structures of the templates used in homology modeling.** 7 TMH of mGlu5 receptor was used for the modeling of 7 TMH of mGlu2 and mGlu7 receptor, and dDAT was used for the modeling of GAT1.

PDB ID	Receptor	Area of the receptor	Ligand	Resolution (Å)	Binding site
4OO9	mGlu5	7 TMH	Mavoglurant (NAM)	2.6	Allosteric
4XP4	dDAT	Entire transporter	Cocaine (inhibitor)	2.8	Orthosteric

Target-template sequence alignment

The protein sequences of the mGlu receptor targets were retrieved from UniProt (www.uniprot.org) with the codes Q14416 for the mGlu2 receptor and Q14831 for the mGlu7 receptor. Crystal structure of 7 TMH mGlu5 receptor bound to mavoglurant (PDB IDs: 4OO9) was downloaded from the PDB (www.pdb.org) and used as template. The amino acid sequence of GAT1 was retrieved from UniProt (code: P30531) and the crystal structure of the selected template dDAT (PDB ID: 4XP4) was downloaded from the PDB.

The sequences of the target and template were aligned in the multiple sequence viewer of maestro (version 2015.3), and inspected and adjusted for gaps. A lysozyme domain in the crystal structure of 7 TMH mGlu5 receptor and an antibody fragment in the crystal structure of dDAT were removed before modeling.

Homology model building

Based on the constructed alignments, MODELLER automatically calculated and constructed 3D models of the targets. Different restraints were extracted from the target-template sequence alignment, such as Cα-Cα distances, main chain and side chain dihedral angles and H-bonds. The final 3D models comprised of the main chain and side chains without hydrogen atoms. One hundred homology models of each target (GAT1 and 7 TMH of mGlu2 and mGlu7 receptors) were constructed with MODELLER (version 9.13). All the 100 models varied slightly in the initial structure and increased the possibility of getting one or several high quality models.

The constructed 3D homology models were imported to maestro (version 2015.3) and renumbered such that the residue numbers in the models could match the target sequence numbering. The models were prepared with one-step protein preparation in maestro (version 2015.3) with default settings. Disulfide bonds were created and H-bonds were added in proper distances and angles, and the models were energy minimized and prepared for docking.

3.4 Molecular docking

Different docking calculations with known binders and decoys were performed in order to validate the models. This approach aimed to test if the constructed homology models and retrieved X-ray structures were reliable for docking of toxicants and if they were as near the native favorable state as possible. Docking calculations with known binders and decoys were performed for the allosteric site of the 7 TMH homology models of mGlu2 and mGlu7 receptor, and the homology models of GAT1. In addition, docking calculation were also performed for the allosteric binding site of 7 TMH crystal structure of the mGlu5 receptor (PDB ID: 4OO9), the orthosteric binding site of the crystal structure of the VFT of the mGlu2 receptor (PDB ID: 5CNJ) and the mGlu7 receptor (PDB ID: 3MQ4). The molecular docking steps varied slightly for the homology models and the retrieved X-ray structures. The main steps are included in figure 10, which were repeated until the models had sufficient quality or until they could not be further improved.

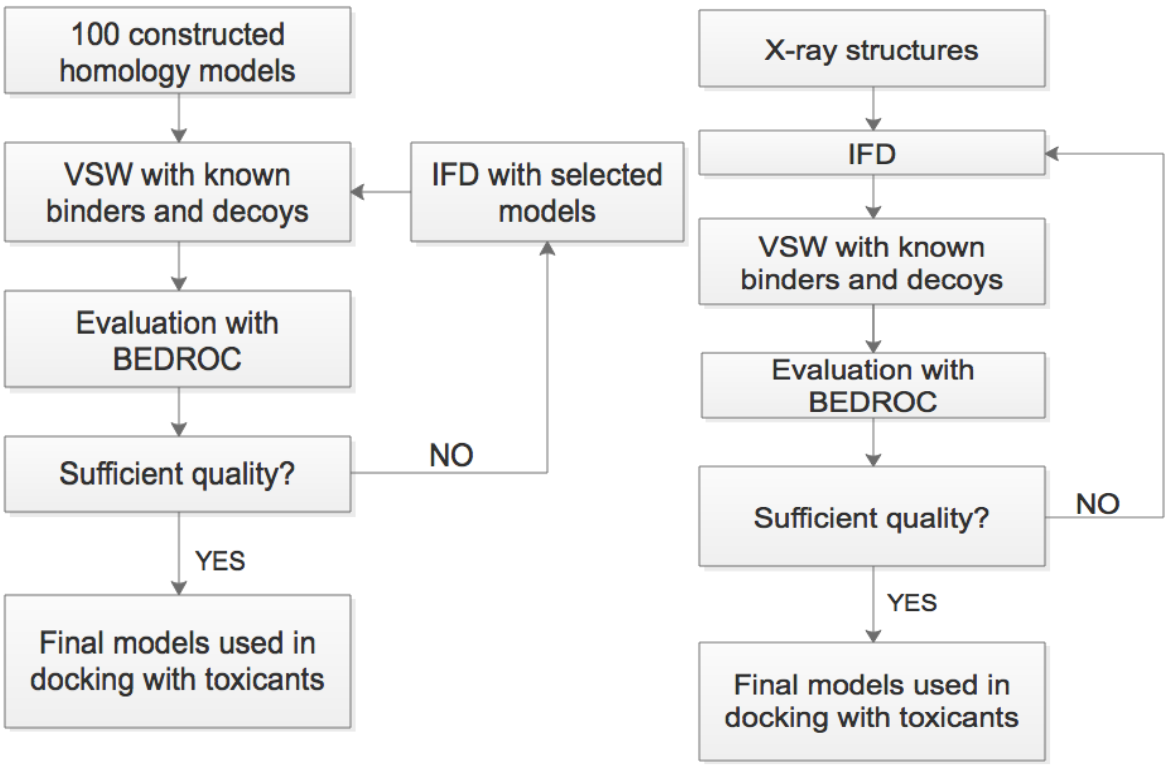

Figure 10: **The main steps of the molecular docking approach for the constructed homology models and the retrieved X-ray structures.**

3.4.1 Generation of binders and decoys

Known binders for GAT1, mGlu2 and mGlu7 receptors were retrieved from IUPHAR (www.guidetopharmacology.org) as SMILES and converted to 2D structures in ICM (version 3.8.4). To simulate the physiological pH of blood circulation system in human body, the pH was set to 7.4 to protonate the molecules (ICM Chemistry: assign formal charge).

Decoys for each binder were downloaded from DUD.E (www.dude.docking.org) in the relationship 200:1 (200 decoys per 1 ligand). The decoys were imported into ICM and prepared and adjusted with the same settings as for the binders.

To find the individual energy minimum state for each compound, all binders and decoys were imported to maestro (version 2015.3) and prepared for docking with ligand preparation (Schrodinger: LigPrep). There was some deviation from the default settings: no changes in ionization, no desalt, no generation of tautomers and generate at most 2 conformations per ligand.

3.4.2 Virtual screening workflow

VSW module was used to dock sets of ligands and decoys into the receptor and transporter models. A python-script (grider), developed by collaborators in Krakow, Poland, (Krzysztof Rataj), was used to generate receptor grids from the constructed homology models and the retrieved X-ray structures. The ligands to be docked were confined to an enclosing box (inner- and outer box) where they could bind (binding pocket). The outer box was set to 30 Å, and the inner box was set to 10 Å. The binding pocket for each constructed homology model of the mGlu2 and mGlu7 receptors was defined by selecting residues that have been identified to be important for binding of NAMs (table 5). This was retrieved from a previous study by Harpsøe et al. (36) where they compared binding modes of different mGlu receptors in complex with ligands with available mutagenesis data. The allosteric binding pocket of the 7 TMH mGlu5 receptor was defined on the basis of its interactions with the NAM mavoglurant. It was decided that the selected residues were used for both the active (PAM) and the inactive (NAM) state, since most of the same residues are anticipating in binding of NAMs and PAMs.

Table 5: **Overview of residues that were selected to define the allosteric binding site in the 7 TMH.** Residues that were defined as the key residues for the allosteric binding site during docking into mGlu2 and mGlu7 receptor models are highlighted in red. They were not necessarily in direct contact with the ligands after docking. Corresponding amino acids in mGlu5 receptor are also shown. The corresponding residues between mGlu2, mGlu7 and mGlu5 7 TMH are shown in black. "Residues in 7 TMH" are shown with Ballesteros and Weinstein numbering system.

Residues in 7 TMH	mGlu2	mGlu7	mGlu5
3.32	R635	R658	Q647
3.33	R636	R659	R661
3.44	Y647	Y670	Y659
5.40	M728	I756	V740
5.43	S731	S759	P743
5.47	N735	S763	N747
6.50	W773	W801	W785
6.53	F776	F804	F788
7.36	S797	S828	S805

The crystal structure of VFT mGlu2 receptor (PDB ID: 5CNJ) is in complex with the glutamate analog LY2812223 and the crystal structure of VFT mGlu7 receptor (PDB ID: 3MQ4) is in complex with the antagonist LY-341495. The orthosteric binding pocket of mGlu2 and mGlu7 receptor was defined on the basis of residues that were within an approximate 3.5 Å sphere radius of the bound ligand (table 6).

It was decided to use the same residues for both agonist and antagonist state of the selected residues for mGlu2 and mGlu7 receptor orthosteric binding site.

Table 6: **Overview of residues that were selected to define the orthosteric binding site in the VFT**. Residues that were defined as the key residues of the orthosteric binding site during docking into mGlu2 and mGlu7 receptor models are highlighted in red. They were not necessarily in contact with the ligands after docking. Corresponding amino acids in mGlu5 receptor are also shown. The corresponding residues between mGlu2, mGlu7 and mGlu5 VFT are shown in black. Docking calculations for the mGlu5 receptor VFT domain were not performed.

mGlu2	mGlu7	mGlu5
Arg 57	Asn74	Ala 59
Tyr 144	Gly 158	Val 146
Ser 145	Ser 159	Ile147
Ala 166	Ala 180	Ala 166
Ser167	Ser 181	Ser 167
Thr 168	Thr 182	Ile 170
Tyr 216	Tyr 230	His 218
Asp 295	Asp 314	Leu 302
Lys377	Lys 407	Lys 377

The binding site of GAT1 was defined on the basis of dDAT in complex with cocaine. By selecting residues 3.5 Å in distance from cocaine, it was possible to detect the corresponding residues in GAT1 by comparing both transporters amino acid sequences in the constructed alignment (table 7).

Table 7: **Overview of residues that were selected to define the orthosteric binding site in GAT1**. Residues 3.5 Å from the inhibitor cocaine bound to dDAT crystal structure are shown. The corresponding amino acid residues in GAT1 are shown, and were selected to define the binding pocket of GAT1 during docking. These residues were not necessarily in direct contact with the ligands after docking.

dDAT	GAT1
Phe43	Tyr60
Asp46	Gly63
Ala117	Phe134
Asp121	Ile138
Tyr123	Tyr140
Phe319	Ser295
Phe325	Gly301
Ser421	Gln397

All the generated binders and decoys for each receptor and transporter were docked with VSW protocol in the prepared grid models.

3.4.3 Induced fit docking

Selected receptor-ligand complexes were further optimized with IFD protocol in maestro (version 2015.3). The outputs from the IFD are different ligand-receptor complexes with slightly different structure of the ligand and the receptor. The IFD protocol is based on the Glide module and the Refinement of Prime module. Receptor flexibility is incorporated by Prime and the ligands are docked into their respective receptors with Glide. The receptors and ligands were prepared in the same manners as for the VSW module. The binding sites were defined with the same residues as before (see section 3.4.2). Default settings were used and the docking score and the IFD score were estimated for each output pose.

Compounds that have been reported as high affinity binders at target receptors were selected for IFD. After IFD, grids were constructed for each output pose (different receptor conformations) and the ligand sets (known binders and decoys) were docked with VSW protocol and BEDROC was calculated.

3.4.4 Evaluation of homology models, BEDROC

To evaluate the models, enrichment factors and BEDROC parameters were calculated for each VSW result and enrichment plots were generated. Those models that performed best in discriminating active compounds (known binders) from inactive compounds (decoys) were considered as the most reliable models. Models with the best BEDROC score were selected for docking with toxicants, and models that did not have satisfaction BEDROC scores were improved further with IFD protocol in maestro (version 2015.3).

3.4.5 Docking calculations with exogenous toxicants

The ligand set of toxicants retrieved from Tox21 database (spring 2012) were imported to ICM (version 3.8.4), prepared by removing ions from the ligands and protonated at pH = 7.4, to mimic the native pH in the human body (ICM Chemistry: assign formal charge). The toxicants were then imported to maestro (version 2015.3) and prepared with ligand preparation (Schrödinger: LigPrep). Ligand preparation separates ligands according to their chirality and conformations, which resulted in that the number of molecules for docking was increased from 8194 to 9757.

The models with satisfactory BEDROC scores for each target were used for docking with toxicants. A total of 9757 putative toxic molecules were docked with Glide into the constructed homology models and crystal structures, and scored. Default settings were used for all glide docking calculations.

4. RESULTS

4.1 Homology models

4.1.1 Alignments

A multiple sequence alignment of mGlu1-mGlu8 receptors was generated in ICM (version 3.8.4) and used to investigate the conservation of amino acids between the subtypes (figure 11). The amino acid sequences were retrieved from UniProt with the codes GRM1_HUMAN to GRM8_HUMAN, which represents human mGlu1-mGlu8 receptors. The amino acid sequence of the crystal structure of VFT and 7 TMH of the mGlu5 receptor (PDB ID: 3lmk and 4OO9) were also included in the alignment and are in addition illustrated as secondary structures beneath the amino acid sequences.

The amino acid residues are highly conserved between the subtypes of mGlu receptors, and the conservation are indicated with different colors in the alignment.

An alignment of GAT1 and DAT were also constructed in order to find the suitable template for GAT1 (figure 12). This was done in www.uniprot.org with the UniProt codes P30531 for GAT1 and Q01959 for DAT. Figure 12 shows the alignment of the DAT and the GAT1.

Figure 11: **Alignment of human mGlu receptors (mGlu1 to mGlu8).** Each TMH is indicated with a red square and is given the name TMH1-7. The degree of conservation in the alignment is shown in colors. The most conserved residues are shown in dark green color, then follows lighter green, yellow, pink, lighter pink and the least conserved residues are shown in white color. Red and purple cylinders represent α-helices and π-helices, and the green arrows represent β-sheets for the secondary structure.

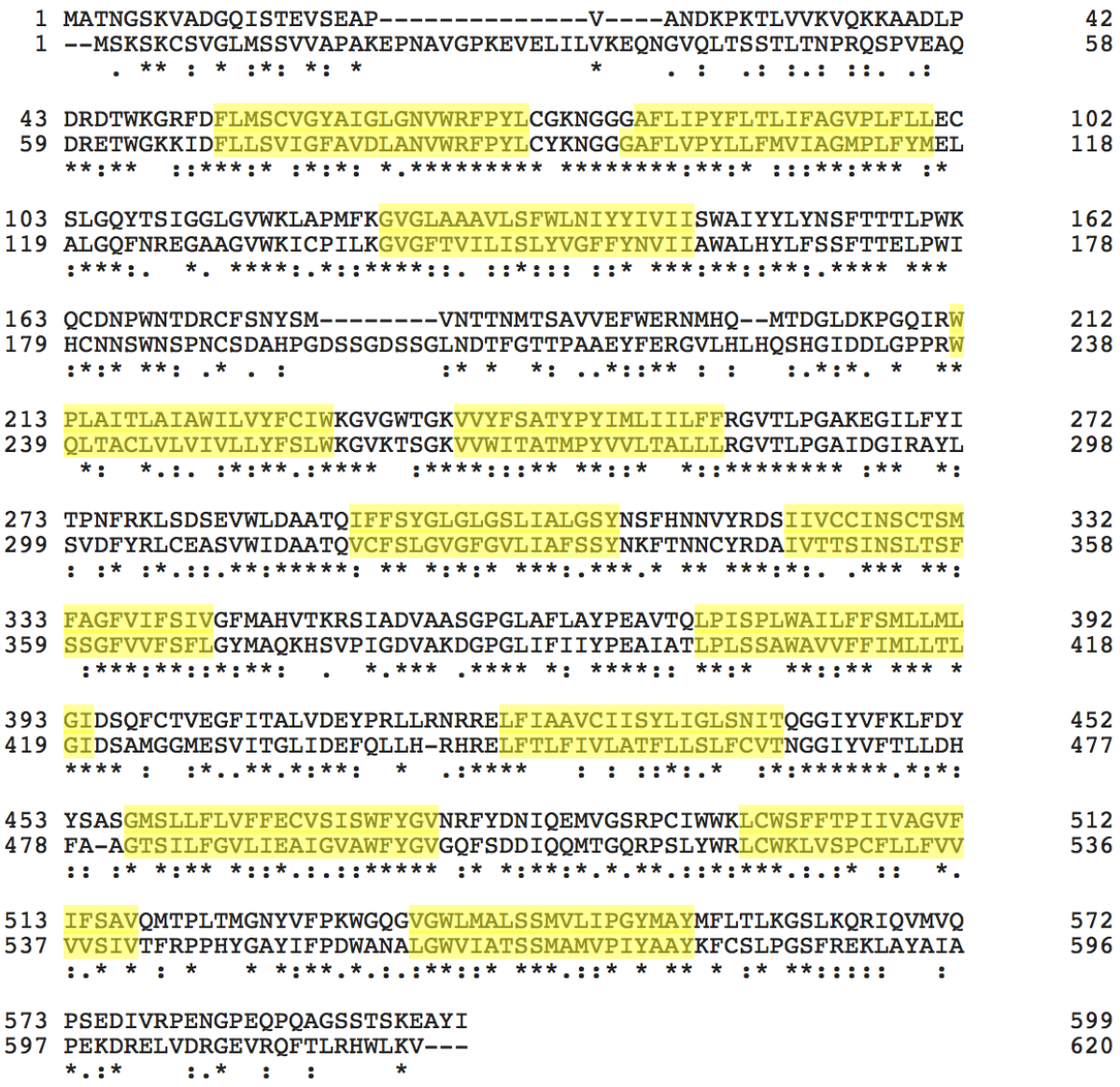

Figure 12: **Alignment of GAT1 and DAT constructed in www.uniprot.org.** The upper amino sequence is GAT1 and the lower is DAT. The 12 TMHs are indicated in yellow color. * represents identical amino acids. **:** and **.** represents similar amino acids. The overall identity between GAT1 and DAT were 41 %.

4.1.2 Models constructed by MODELLER

One hundred homology models of the 7 TMH of the mGlu2 and mGlu7 receptors and of GAT1 were constructed with MODELLER. The models of the mGlu2 and mGlu7 receptors were constructed based on the target-template sequence alignment of the mGlu receptor (target) and the crystal structure of the 7 TMH of mGlu5 receptor (PDB ID: 4OO9) as template. The models of GAT1 were based on an alignment between GAT1 and the dDAT, which also was used as the template (PDB ID: 4XP4). MODELLER automatically constructed non-hydrogen 3D models of the targets by extracting different restrains from the target-template alignment, including Cα-Cα distances, main chain and side chain dihedral angles and H-bonds.

Superposition of the constructed models showed that the 100 models differ slightly from each other in structure conformation (figure 13-15). The most variable regions are in the loops where both backbone and side chain conformations differs, while in the TMH, the main difference between the models were seen in the side chain conformations. Loop modeling is quite challenging due to limited amino acid conservation and structural flexibility, and this enables larger variation in loop regions.

The TMH1-7 for the mGlu2 and the mGlu7 receptor are shown in different colors (figure 13-14). The TMH1 is in red color, then follows orange, yellow, green, turquoise, blue and TMH7 which is shown in dark purple color. The allosteric binding pockets for the mGlu receptors are mainly situated between TM2, TM3, TM5, TM6 and TM7 and ECL2 (corresponding to orange, yellow, turquoise, blue and dark purple color. The ECL2 are shown in dark green color).

Figure 13: **Superposition of the backbone of one hundred homology models of the 7 TMH of mGlu2 receptor.** The extracellular site of the receptor is located at the top of the figure. The crystal structure of 7 TMH mGlu5 receptor (PDB ID: 4OO9) was used as template.

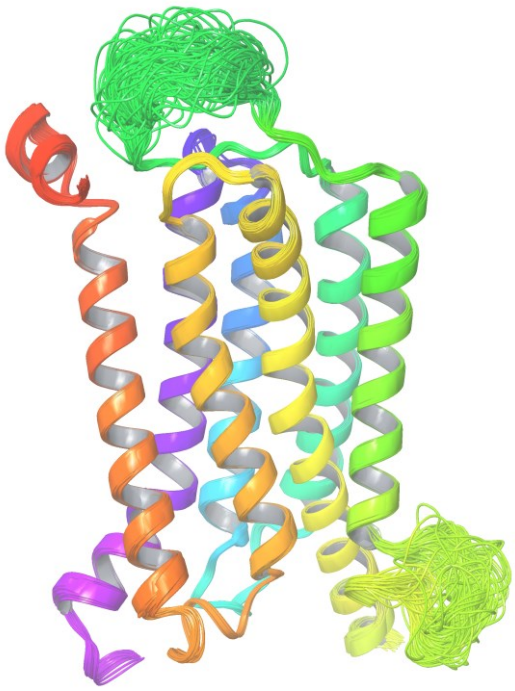

Figure 14: **Superposition of the backbone of one hundred homology models of the 7 TMH of mGlu7 receptor**. The extracellular site of the receptor is located at the top of the figure. The crystal structure of 7 TMH mGlu5 receptor (PDB ID: 4OO9) was used as template.

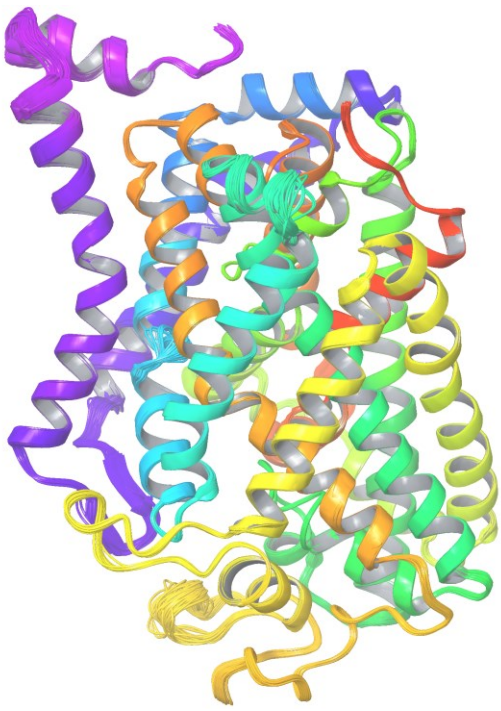

Figure 15: **Superposition of the backbone of one hundred homology models of GAT1.** The extracellular site of the receptor is located at the top of the figure. The crystal structure of dDAT (PDB ID: 4XP4) was used as template.

4.2 Molecular docking

In order to validate the constructed homology models, molecular docking approaches were performed using libraries of known binders and decoys for the different mGlu receptors and GAT1.

4.2.1 Virtual screening scoring values

VSW protocol was performed on constructed grids of the receptor models in maestro (version 2015.3). The retrieved crystal structures of VFT of the mGlu2 and the mGlu7 receptor (PDB ID: 5CNJ, 3MQ4) and 7 TMH of the mGlu5 receptor (PDB ID: 4OO9) were first docked with the IFD protocol in maestro before the VSW protocol. The one hundred constructed homology models of 7 TMH mGlu2 and mGlu7 receptor and GAT1 were docked with VSW protocol first, but the PAM state of mGlu7 receptor homology model and both NAM and PAM state of mGlu2 receptor homology model had to be further improved with IFD protocol. The IFD protocol generated new conformational states of the receptors that were used for docking.

It is desirable that all known binders for a particular receptor can bind and form interactions with the binding site of the receptor model. In order to use the models for predictions of ligand interactions the models should also be able to split between known binders and non-binders/decoys for the receptors, such that the binding site is more reliable when docking the library of toxicants. Ligand sets of both known binders and non-binders/decoys were docked with Glide by the VSW module into receptor grids and scored. The negative docking values equal high scores, so the lower docking score the better score and stronger affinity for the binder to the model.

The receptor models are snapshots of a conformational state of the receptor, which means that the docking scores from VSW are not final and can vary depending on the conformational state of the model. A mean docking score value was therefore calculated for each receptor model, which was used as a threshold value when docking the toxicants.

The following tables (8-13) lists the results from VSW for the receptor and transporter models that were able to dock all known binders and were used in the glide docking with toxicants (Tox21 library). Figure 16-18 shows three binding modes from VSW protocol with NAMs in the allosteric binding pocket of the mGlu2, the mGlu7 and the mGlu5 receptor.

mGlu2 receptor:

The crystal structure of the VFT domain of the mGlu2 receptor (PDB ID: 5CNJ) was used in docking calculations of agonists and antagonists. During ligand recognition and binding, the binding pocket needs to adapt to the structure of the ligand, and therefore the agonist bound conformation must differ from the antagonist bound conformation of a receptor. To account for this, the crystal structure first had to be docked with one agonist and one antagonist with IFD protocol in maestro (version 2015.3). Known agonists and antagonists were then docked into different conformational states of the VFT from the IFD process using the VSW protocol, and scored (table 8).

The more negative docking score, the stronger is the compound predicted to bind to the targets. It was desirable that the ligands with the highest experimental affinity score had the best docking scores in the model, which can be seen in table 8 where there is a good relative correlation between the docking scores and the affinity of the ligands to the receptor.

Table 8: **Docking scores from VSW with 13 agonists and 7 antagonists in the orthosteric binding site of the crystal structure of VFT mGlu2 receptor (PDB ID: 5CNJ).** The table includes the 10 best ranked agonists ligands (of a total of 13 ligands) and the 7 best ranked antagonists from VSW. The compounds with the lowest docking scores are predicted to have highest affinity to the receptor. The calculated mean scoring values are also shown.

mGlu2 receptor orthosteric binding site					
Agonist (chirality)	**Docking score**	**Affinity (pK_i)**	**Antagonist (chirality)**	**Docking score**	**Affinity (pK_i)**
MGS0028	-8.97	9.2	MGS0039	-9.20	8.6-8.7
(S)-4C3HPG	-8.72	4.8	LY341495	-9.16	8.6
DCG-IV (1S,3R)	-7.56	7.0	PCCG-4	-7.78	5.1*
Eglumegad	-7.35	7.8-7.9	(+)-MCPG	-6.75	4.6
LY379268	-7.32	7.9	α-methylserine-O-phosohate (R)	-6.73	5.3
(1S,3R)-ACPD	-6.95	5.0-5.4	α-methylserine-O-phosphate (S)	-6.67	5.3
DCG-IV (2R,2S)	-6.93	7.0	eGlu	-5.22	4.4-4.6
(2R,3R)-APDC	-6.86	5.0			
L-CCG-I	-5.99	6.3			
LY2812223	-5.89	-			
Mean score values	-7.25			-7.36	

* pIC_{50}. - no available affinity value for that particular ligand.

The one hundred constructed homology models of 7 TMH of the mGlu2 receptor were docked with known PAMs and known NAMs using the VSW protocol in maestro (version 2015.3). None of the homology models were able to dock all the known PAMs and NAMs, so we needed to generate new conformational states of the receptor with IFD protocol and re-dock the known PAMs and NAMs with the VSW protocol. The final PAM and the NAM conformational state of 7 TMH of the mGlu2 receptor used in VSW are based on the IFD with the high affinity binders JNJ-40068782 (PAM) and RO4988546 (NAM). All known PAMs were then able to dock into the final PAM conformational state, and all known NAMs could dock into the final NAM conformational state. There were a good relative correlation between the docking scores and the affinity values for the known binders (table 9).

Table 9: **Docking scores from VSW with 31 PAMs and 13 NAMs in the allosteric binding site of the constructed homology model of 7 TMH mGlu2 receptor.** The table includes the 10 best ranked allosteric modulators from VSW. The compounds with the lowest docking scores are predicted to have highest affinity to the receptor. The calculated mean scoring values are also shown.

mGlu2 receptor allosteric binding site

PAM (Chirality)	**Docking score**	**Affinity** (pEC_{50})	**NAM** (Chirality)	**Docking score**	**Affinity** (pIC_{50})
JNJ-40068782	-11.56	7.3	RO5488608	-12.10	7.9-8.7*
Compound 34	-11.43	7.1	Ro4491533	-11.98	7.8
AZD8529	-11.34	6.7	RO4988546	-11.60	-
Compound 14	-11.04	6.8	MNI-136	-11.04	7.3-8.1
Compound 48	-11.03	6.4	Compound 4 (R)	-10.44	6.0
4-MPPTS	-11.02	5.8	Compound 2 (R)	-10.34	6.1
JNJ-40411813	-10.92	6.8	Compound 3 (R)	-9.59	5.8
JNJ-42153605_1	-10.58	7.8	MNI-137	-9.33	7.1-7.9
BINA (R)	-10.40	7.0	MNI-135	-9.27	6.9-8.0
JNJ-40411813	-10.34	6.8	Compound 4 (S)	-8.97	6.0
Mean score values	-10.96			-10.47	

*pK_i. - no available affinity value for that particular ligand.

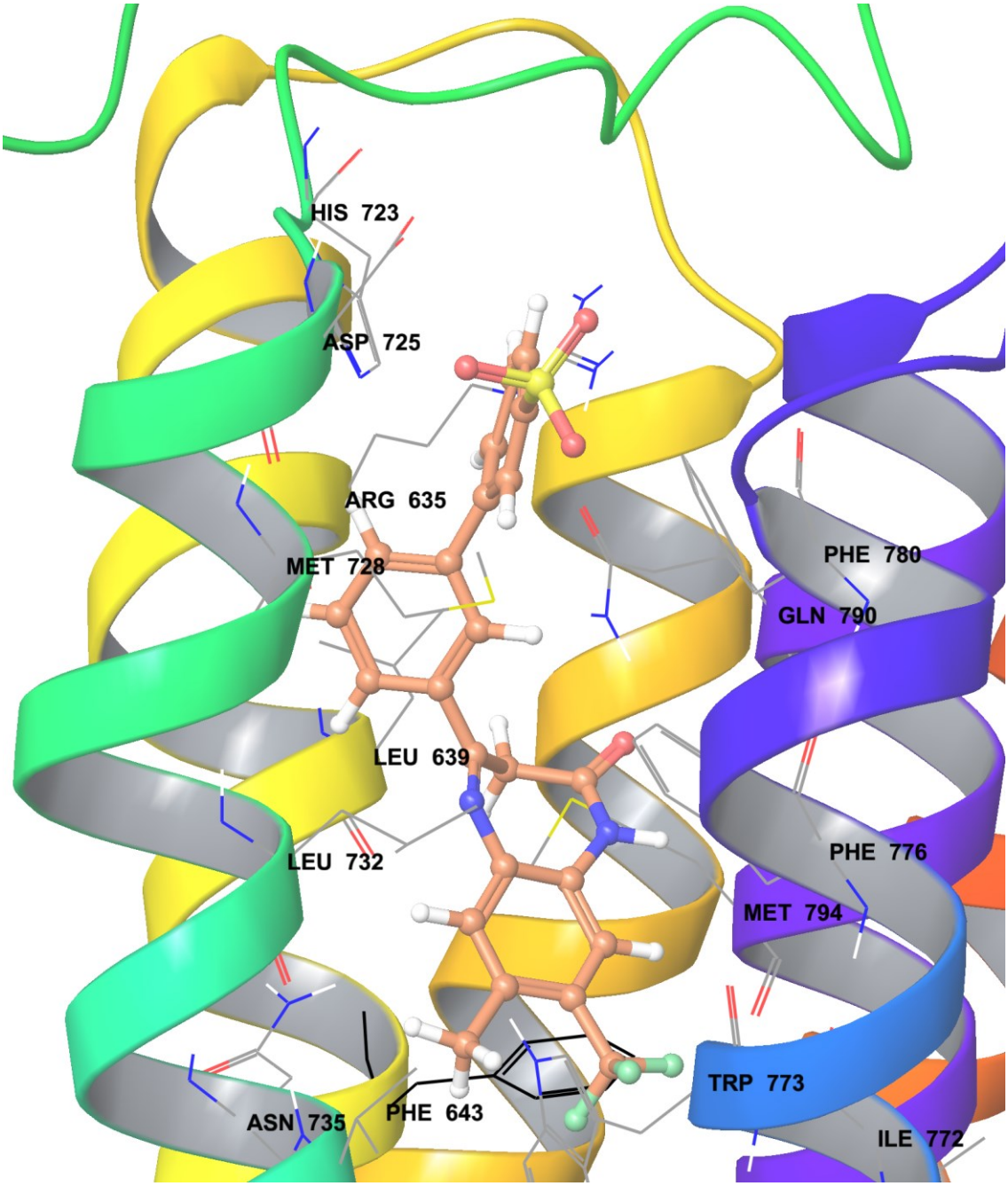

Figure 16: **Binding mode of RO5488608 (NAM) in the allosteric binding pocket of the constructed homology model of the mGlu2 receptor.** The backbone of the 7 TMH are shown in ribbon. The amino acid residues are in a 3 Å sphere radius around the ligand. The residue Phe643$^{3.40}$ is displayed in black.

mGlu7 receptor:

The crystal structure of VFT mGlu7 receptor (PDB ID: 3MQ4) was used for docking to the orthosteric binding site of the mGlu7 receptor. The IFD protocol was first performed in order to incorporate correct agonist/antagonist conformational states of the crystal structure before docking with the VSW protocol. The results from VSW protocol with the final models of mGlu7 receptor agonist/antagonist conformational states are shown in the following table. There was a good relative correlation between the docking scores and the experimental affinity scores.

Table 10: **Docking scores from VSW with 13 agonists and 15 antagonists in the orthosteric binding site in the crystal structure of the VFT of mGlu7 receptor (PDB ID: 3MQ4).** The table includes the 10 best ranked ligands for each conformational state. The compounds with the lowest docking scores are predicted to have highest affinity to the receptor. The calculated mean scoring values are also shown.

mGlu7 orthosteric binding site					
Agonist (Chirality)	**Docking score**	**Affinity (pEC_{50})**	**Antagonist (Chirality)**	**Docking score**	**Affinity (pK_i)**
LSP1-2111 (S)	-6.74	4.3	DCG-IV (R)	-7.07	4.7
LSP4-2022 (R)	-6.56	4.9	DCG-IV (S)	-6.38	4.7
LSP4-2022 (S)	-6.46	4.9	LY341495	-6.23	6.1
PPG (S)	-6.43	3.7*	α-methylserine-O-phosphate (S)	-5.82	4.4
LSP1-2111 (R)	-6.34	4.3	MSOPPE (S)	-5.79	3.6
L-serine-O-phosphate	-6.22	4.5	MAP4	-5.69	3.8
L-AP4	-6.19	3.7*	MPPG (R)	-5.26	3.8
PPG (R)	-6.18	3.7*	α-methylserine-O-phosphate (R)	-5.24	4.4
(1S,3R)-ACPD	-5.96	3.0-3.1*	(+)-MCPG	-5.20	3.2
L-glutamic acid	-5.11	3.1*	MPPG (S)	-5.18	3.8
Mean score values	-6.22			-5.79	

* pK_i

One hundred homology models of the 7 TMH of mGlu7 receptor were docked with known NAM binders with VSW protocol. The ligand set comprised of 5 NAMs. Nineteen out of the 100 homology models were able to dock all the 5 NAMs. The model listed in table 11 was the one with the best BEDROC score and was used for the docking calculations with the toxicants of the Tox21 library. There was a good relative correlation between the docking scores and the affinity scores for each known NAM, where the one with the lowest docking score (most negative value) was predicted to be a ligand that had the best affinity for the receptor. It was not performed VSW protocol on the PAM conformational state of the mGlu7 receptor (conformational state generated by IFD protocol) because there is only one known PAM for this receptor.

Table 11: **Docking scores from VSW with 5 NAMs in the allosteric binding site of the constructed homology model of 7 TMH mGlu7 receptor.** The compounds with the lowest docking scores are predicted to have highest affinity to the receptor. The calculated mean scoring value is also shown.

mGlu7 receptor allosteric binding site		
NAM (chirality)	**Docking score**	**Affinity (pIC_{50})**
ADX71743 (S)	-9.40	7.2
ADX71743 (R)	-9.40	7.2
MDIP	-9.23	7.6
MMPIP	-8.74	6.1-7.6
XAP044	-7.50	5.2
Mean score value	-8.85	

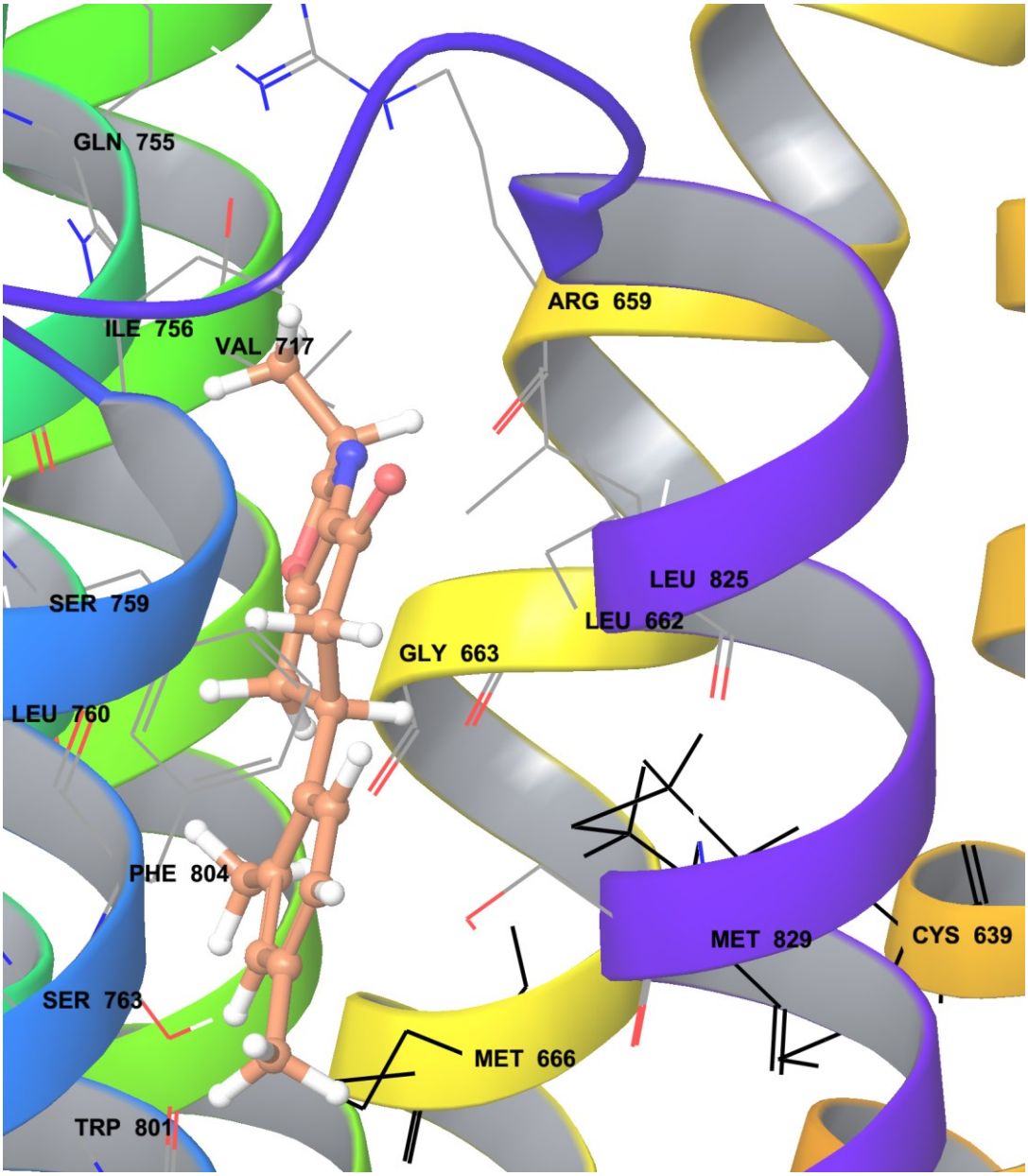

Figure 17: **Binding mode of ADX71743 (S) (NAM) in the allosteric binding pocket of the constructed homology model of the mGlu7 receptor.** The backbone of the 7 TMH are shown in ribbon. The amino acid residues are in a 3 Å sphere radius around the ligand (except for Cys639$^{2.49}$ and Met829$^{7.44}$, which are ~4 Å sphere radius around the ligand). The amino acid residues Cys639$^{2.49}$, Met666$^{3.40}$ and Met829$^{7.44}$ are displayed in black.

mGlu5 receptor:

VSW calculations were performed on the crystal structure of 7 TMH of mGlu5 receptor (PDB ID: 4OO9). IFD protocol was first performed with VU0405386-1 (PAM) and basimglurant (NAM) in order to get PAM and NAM induced conformational states of the binding pocket. The following table lists the results from VSW protocol with known PAMs and NAMs for the mGlu5 receptor.

Table 12: **Docking scores from VSW with 23 PAMs and 58 NAMs to the allosteric binding site of the crystal structure of 7 TMH mGlu5 receptor (PDB ID: 4OO9).** The table includes the 10 best ranked PAMs and NAMs from VSW. The compounds with the lowest docking scores are predicted to have highest affinity to the receptor. The calculated mean scoring values are also shown.

mGlu5 receptor allosteric binding site					
PAM (Chirality)	**Docking score**	**Affinity (pEC_{50})**	**NAM (Chirality)**	**Docking score**	**Affinity (pIC_{50})**
CPPHA	-10.76	6.3*	GRN-529	-11.19	8.6
ADX-47273	-10.75	7.3	Compound 30	-10.83	7.8
NCFP	-10.52	6.0-6.7	Basimglurant	-9.97	-
VU0092273	-10.32	7.5	VU0366058	-9.80	7.0
VU0364289	-10.24	5.8	Compound 41	-9.18	7.9**
VU0424465	-10.24	8.8	Dipraglurant	-9.18	7.7
VU0361747	-10.22	6.9	Compound 23	-9.17	9.1
VU-29	-10.04	8.1	Compound 11a (R)	-9.15	7.4
VU0357121	-9.93	7.5	Compound 29b	-9.01	7.8
VU0403602-4	-9.90	-	Mavoglurant (S)	-8.98	-
Mean score values	-10.29			-9.65	

*pIC_{50}. **pEC_{50}. - no available affinity value for the particular ligand.

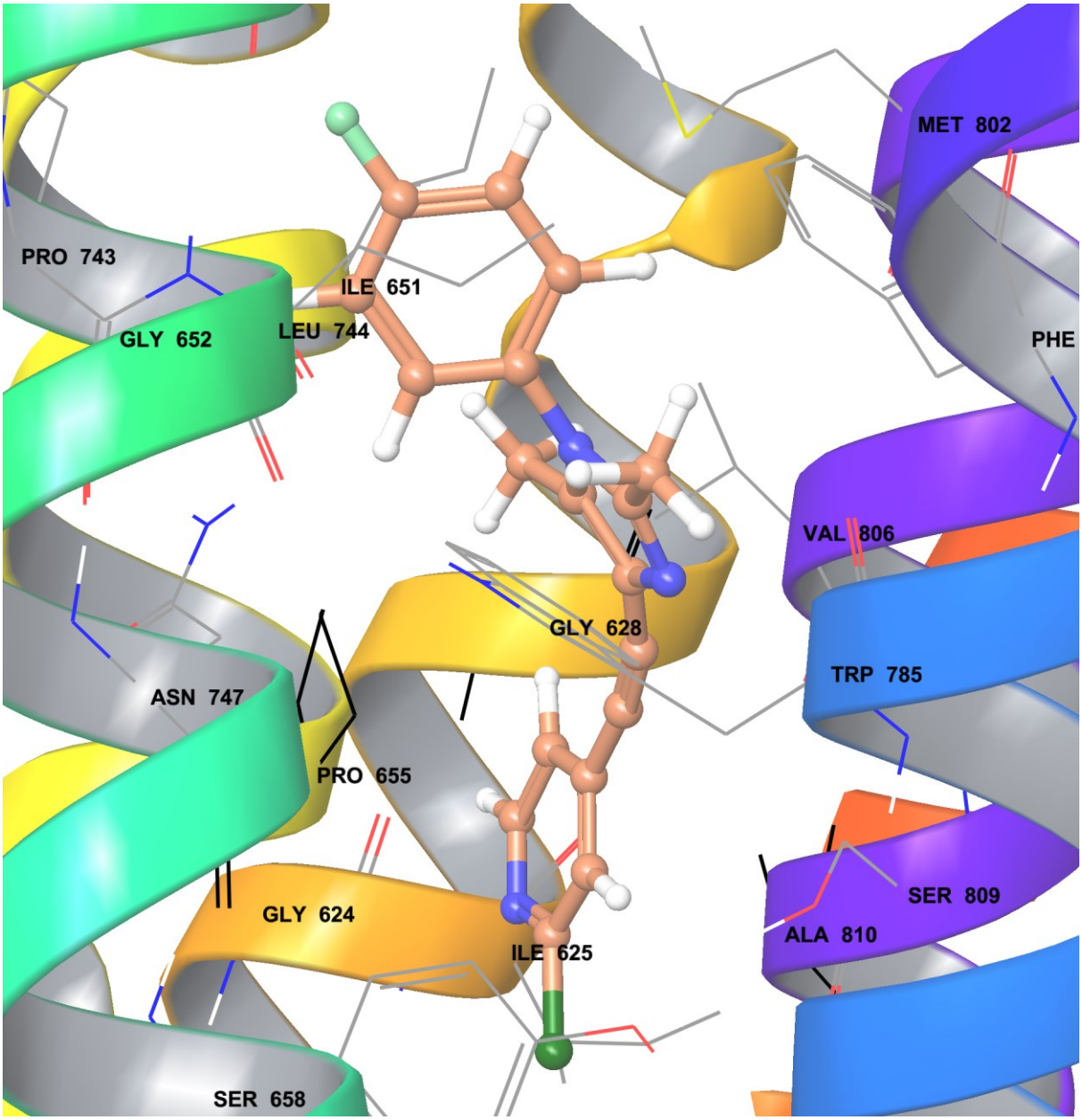

Figure 18: **The binding mode of basimglurant (NAM) in the allosteric binding pocket of the crystal structure of the mGlu5 receptor (PDB ID: 4OO9).** The backbone of the 7 TMH are shown in ribbon. The amino acid residues are in a 3 Å sphere radius around the ligand. The amino acid residues Gly628$^{2.49}$, Pro655$^{3.40}$ and Ala810$^{7.41}$ are displayed in black.

GAT1:

One hundred constructed homology models of GAT1 were docked with 18 known inhibitors with VSW protocol. One of the models was able to dock all the ligands and was used in docking calculations with toxicants. The following table lists the 10 top ranked inhibitors from the VSW protocol with GAT1.

Table 13: **Docking scores from VSW with 18 inhibitors to GAT1.** The table includes the 10 best ranked ligands. The compounds with the lowest docking scores are predicted to have highest affinity to the receptor. The calculated mean score value is also shown.

GAT1 orthosteric binding site		
Inhibitor (Chirality)	**Docking score**	**Affinity (pIC_{50})**
Tiagabine (R)	-8.83	7.2
CI-966 (R)	-8.17	6.6
Tiagabine (S)	-7.92	7.2
SKF89976A (S)	-7.69	6.9
EF-1500 (R)	-7.45	4.9-5.7
EF-1500 (S)	-7.45	4.9-5.7
SKF89976A (R)	-7.45	6.9
LU32-176B (R)	-7.43	5.4
EF-1520 (R)	-7.42	5.1-5.4
EF-1520 (S)	-7.05	3.6-3.9
Mean score value	-7.69	

4.2.2 Induced fit docking scores

By using the IFD protocol the binding pocket for several receptor models were improved. IFD was performed on retrieved crystal structures of VFT of the mGlu2 and the mGlu7 receptor (PDB ID: 5CNJ, 3MQ4) and the 7 TMH domain of the mGlu5 receptor (PDB ID: 4OO9) in order to prepare them for further docking. IFD was also used to improve models with the best BEDROC score, which needed refinements. In the IFD, a known high affinity binder for each selected receptor model was docked and scored and the structure of the ligand and receptor could freely change conformation to adapt to each other (table 14).

Table 14: **Overview of the results from IFD with agonist, antagonists, PAMs and NAMs with each of the receptor models that needed to be improved.** The more negative docking and IFD scores, the stronger was the compound predicted to bind to the receptors.

Receptor	Type of binder	Ligand (Chirality)	Docking score	IFD score	Affinity (pK_i)
mGlu2	Agonist	Eglumegad	-6.91	-854.52	6.9
	Antagonist	LY341495	-8.50	-862.20	8.6
	PAM	JNJ-40068782	-11.40	-340.15	7.3*
	NAM	RO4988546	-10.87	-348.32	-
mGlu7	Agonist	L-serine-O-phosphate	-6.07	-610.74	4.5
	Antagonist	α-methylserine-O-phosphate (R)	-4.14	-610.48	4.4
	PAM	AMN082	-12.60	-438.40	6.5-6.8*
mGlu5	PAM	VU0405386-1	-9.91	-388.78	-
	NAM	Basimglurant	-9.08	-384.33	-

* pEC_{50}. - no available affinity value for the particular ligand.

The selection of the binders for IFD was based on their affinity to their receptors and their structural topology. If the purpose of the improvement was to make the binding pocket bigger, so all the known binders for the receptor binding site could dock and interact with the binding site, a large compound was selected.

The crystal structure of the VFT of mGlu2 receptor (PDB ID: 5CNJ) is in complex with an agonist (LY2812223), which makes the VFT in a closed conformational state, and the purpose with the IFD was to "open up" the conformation. This had to be taken into account when selecting an antagonist for the IFD protocol. The antagonist could not be too large because it would not be able to fit into the closed conformation. In addition, the ligand had to have high affinity to the receptor. The high affinity antagonists LY341495 were therefore selected.

None of the 100 constructed homology models of the 7 TMH of mGlu2 receptor were able to dock all the known NAMs and PAMs. The known allosteric modulators for the mGlu2 receptor are relatively large molecules, and it was necessary to utilize IFD in order to fit the large JNJ-40068782 (PAM) and RO4988546 (NAM) inside the binding pocket.

The crystal structure of the VFT of mGlu7 receptor (PDB ID: 3MQ4) is in complex with the antagonist LY-341495. (LY-341495 and LY341495 are two different compounds; LY-341495 is an antagonist for the mGlu7 receptor, and LY341495 is an antagonist for the mGlu2 receptor). The VFT is in an open conformational state, which makes the binding pocket large compared to an agonist state. It was therefore necessary to select a relative small agonist (L-serine-O-phosphate) in order to get the VFT in a more closed state.

By using the IFD protocol and incorporate flexibility into the receptor and the ligand, it was possible to optimize the binding pocket such that all ligand could be docked by using VSW to these IFD optimized receptor models. This was also the case for the PAM state of the constructed homology models of mGlu7 receptor. The mGlu7 receptor has so far only one known PAM, the agonist PAM AMN082. AMN082 was first docked with Glide (VSW protocol) to one hundred constructed homology models of the 7 TMH of mGlu7 receptor, where none of the models could fully fit the ligand into the binding pocket. It was then performed IFD protocol with AMN082 to improve the binding pocket, which resulted in output poses where the ligand were fully docked inside the binding pocket. The best ranked output pose from IFD were selected as the best binding mode. This was clearly an improvement from the previous VSW docking.

4.2.3 Evaluation of the models, BEDROC scores

To evaluate the models, BEDROC was performed on the models to determine if they could differentiate between the actives and the decoys. The models with the best BEDROC scores were used for the docking of the Tox21 library.

Table 15 shows the BEDROC scores for the final models that were used in glide docking with toxicants. The α=20 weights the first 8 % of the screening results and ranges from 0 to 1, with 1 being the ideal score. The models represented in table 15 were the ones that were the best in distinguishing between the actives and the decoys, and were considered as the most reliable models.

Table 15: **Overview of the BEDROC score for the final models that were used in glide docking with the Tox21 library.**

Receptor/ Transporter	**Conformation State**	**BEDROC score (α=20)**
mGlu2	Agonist	0.394
	Antagonist	0.454
	PAM	0.168
	NAM	0.175
mGlu7	Agonist	0.163
	Antagonist	0.157
	PAM	(-)
	NAM	0.522
mGlu5	PAM	0.436
	NAM	0.375
GAT1	Inhibitor	0.625

(–) indicates lack of BEDROC score for the PAM state of the mGlu7 receptor since only one PAM is known.

Enrichment plots for each model was also generated, that illustrated the performance of the models (figure 19-23). The Y-axis represents the "sensitivity" and defines the true positive results. The blue dots in the plot represent the ligands that are docked. The X-axis represents "specificity" that defines how many incorrect positive results that occurs among the negative results. The black diagonal line represents random results.

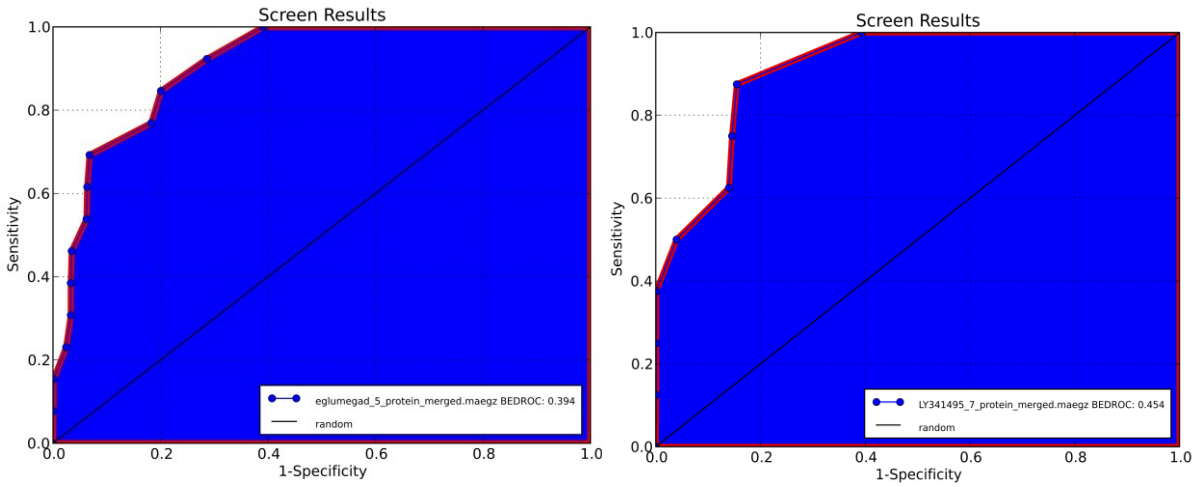

Figure 19: **Enrichment plots of agonist (left) and antagonist (right) states of the mGlu2 receptor**.

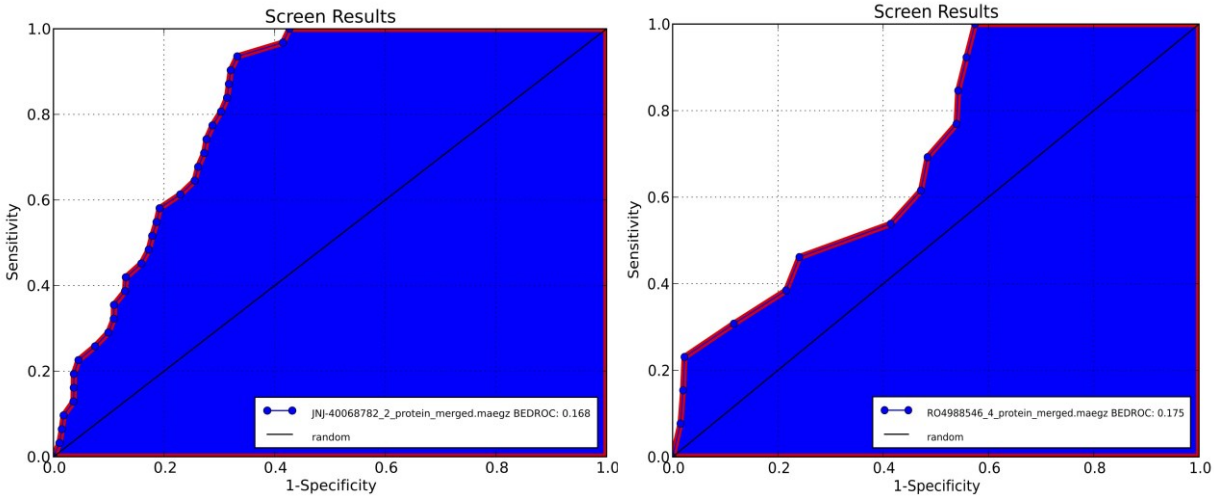

Figure 20: **Enrichment plots of PAM (left) and NAM (right) states of the mGlu2 receptor**.

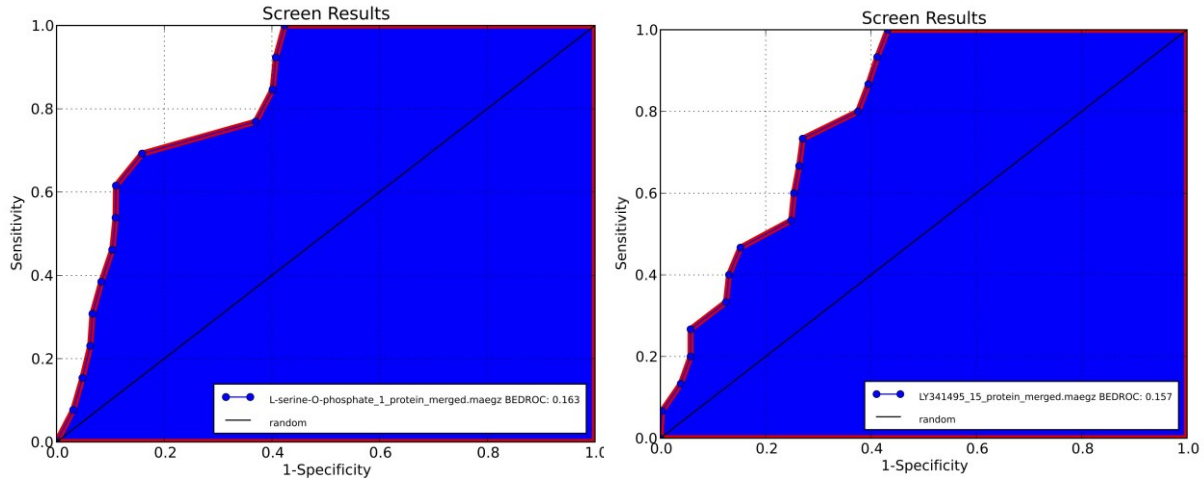

Figure 21: **Enrichment plots of agonist (left) and antagonist (right) states of the mGlu7 receptor**.

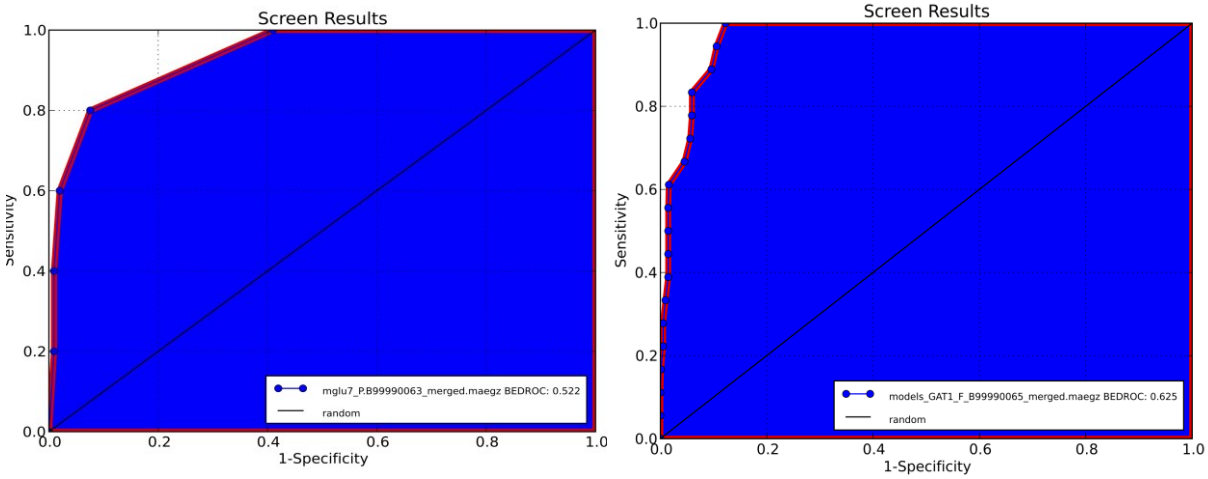

Figure 22: **Enrichment plots of a NAM state of the mGlu7 receptor (left) and an inhibitor state of the GAT1 (right).**

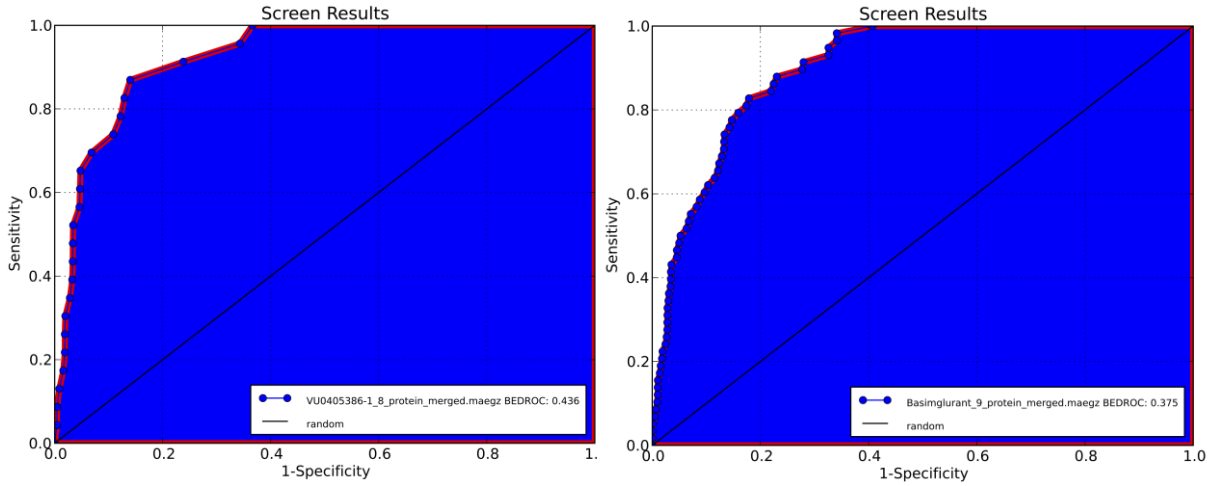

Figure 23: **Enrichment plots of PAM (left) and NAM (right) states of the mGlu5 receptor.**

It was not possible to perform BEDROC approach in order to validate the PAM conformational state of the mGlu7 receptor model, since only one PAM for the mGlu7 receptor has been published (agonist PAM, AMN082). It was therefore necessary to compare the best binding mode from the IFD protocol with former IFD calculations of AMN082 to mGlu7 receptors, done by Feng et al. (27) to see if the IFD result were realistic. The binding site of mGlu7 receptor has a large overall fraction of hydrophobic residues that can form hydrophobic interactions with the ligand (27). Our docking showed that a benzene ring in AMN082 and the amino acid Trp801$^{6.50}$ formed a π-π interaction and that Phe808$^{6.57}$ formed a π-cation bond to the protonated amine group in AMN082 (figure 24). According to the results from Feng et al. the amino acid residue Ile 756$^{5.40}$ can contribute to the selectivity of the receptor and be important in the binding of AMN082. In our model, Ile 756$^{5.40}$ was located ~2,1 Å from one of the benzene rings of AMN082, which could indicate a hydrophobic interaction between the receptor and the ligand. It was therefore concluded that the result from IFD protocol with AMN082 were realistic and the model were used for docking prediction of the toxicants.

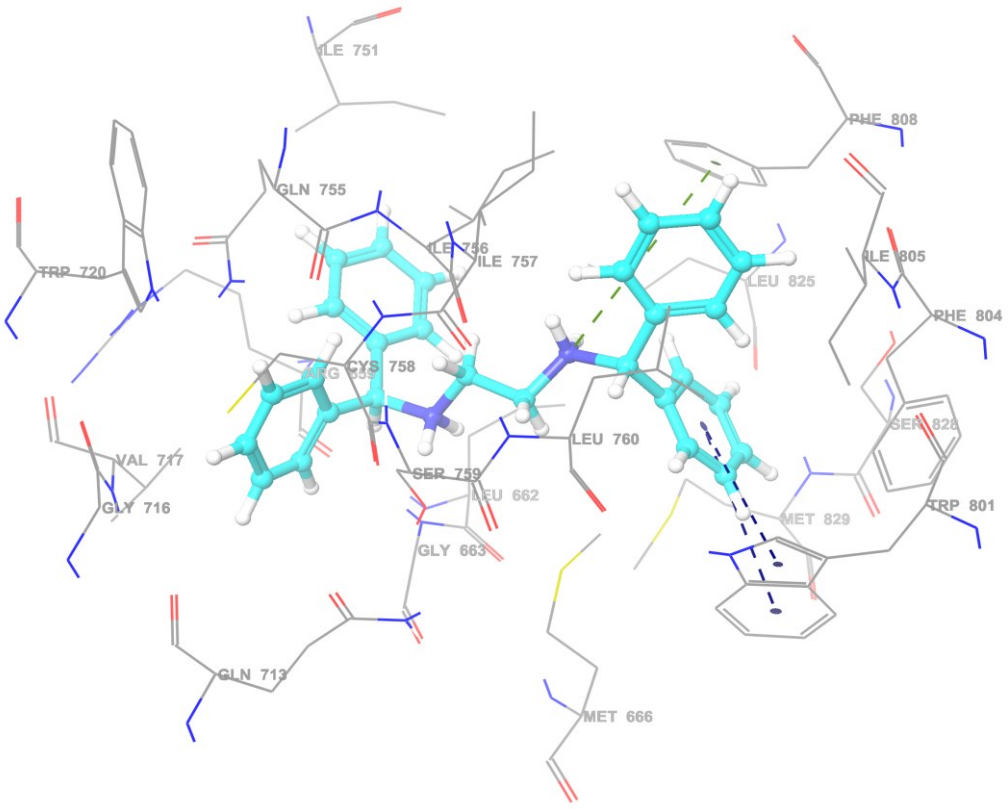

Figure 24: **The binding mode of the agonist PAM AMN082 in the allosteric binding site of mGlu7 receptor.** The dotted dark blue line represents π-π interactions and the green line represents π-cation interactions between the ligand and the residues. The amino acid residues are in a 3 Å sphere radius around the ligand.

4.2.4 Screening scores of exogenous toxicants

In order to predict if toxicants could bind to the receptor models, a ligand set of 8194 different toxic compounds, that increased to 9757 compounds after preparation with LigPrep in maestro (version 2015.3) where they were separated according to their chirality and conformations, were docked with Glide and scored in each receptor and transporter model.

During docking into orthosteric and allosteric binding sites of the mGlu receptor models, several conformational states of the receptors were considered. For docking into the orthosteric site both agonist and antagonist induced conformations from the IFD were used, and for docking into the allosteric site, both PAM and NAM induced conformations were used. This enabled investigations of both active and inactive receptor conformations in the binding of the toxicants. For the GAT1 model the orthosteric binding site was investigated for the binding of the toxicants. The average docking scores from VSW were used to estimate mean score values for each receptor and the transporter model. The mean score values were used as threshold values in order to predict which toxicants that interacted most strongly with the mGlu receptors and GAT1 (lower docking scores than threshold value for known binders)

The scoring values from the docking calculation with toxicants predicted several of them to dock stronger than the known binders to the receptor models. This applied especially for the antagonist conformational state of the mGlu7 receptor, where 475 toxicants had better scoring values than the threshold value from the known antagonist binders. Table A1-A6 in appendix A gives an overview of the 10 top ranked toxicants for each target that had a better docking score than the calculated threshold values. Table 16 includes the toxicants that were further investigated and discussed in this thesis. This included toxicants with the best docking scores in combination with the highest CNS MPO value.

The following figures (25-35) illustrate the binding modes of the selected toxicants and known binders for each conformational state of the models. The labeled amino acids are mainly the ones that anticipated in the binding of the toxicants and the binders.

Table 16: **Scoring values of toxicants docked to different conformation states of the models.** The more negative docking score the higher the compounds are predicted to bind to the receptor. The calculated threshold values from VSW protocol for each model are also included in the table.

Model	Conformational state	Toxicant (chirality)	Docking score	Threshold value from VSW of known binders
mGlu2	Agonist	1,4-cyclohexane dicarboxylic acid	-8.66	-7.25
	Antagonist	Thalidomide (S)	-8.59	-7.36
	PAM	Oxyphenbutazone	-12.11	-10.96
	NAM	Fluspirilene	-14.34	-10.47
mGlu7	Agonist	Goserelin	-9.74	-6.22
	Antagonist	Argipressin	-9.47	-5.79
	PAM	5-{4'-[(2-butyl- 3H-imidazo[4,5b]pyridine -3-yl)methyl] biphenyl-2-yl}tetrazol-1-ide	-11.39	-12.60
	NAM	Xenalipin	-10.04	-8.85
mGlu5	PAM	Taprostene	-12.78	-10.29
	NAM	Droperidol	-10.89	-9.65
GAT1	Inhibitor	Liarozole (R)	-9.68	-7.69

mGlu2 receptor:

A total of 8378 toxicants were able to dock to the agonist state of the crystal structure of mGlu2 receptor (PDB ID: 5CNJ), where 35 of them had a docking score better than the threshold score. 9404 toxicants were docked to the antagonist state of mGlu2 receptor, where 95 of them had a better scoring value than the threshold value. The constructed homology model of 7 TMH mGlu2 receptor in PAM conformational state were able to dock 8324 toxicants in the allosteric binding site, where 53 compounds had a better score than the calculated threshold value. The NAM conformational state docked a total of 8887 toxicants, where 332 had a scoring value better than the threshold value.

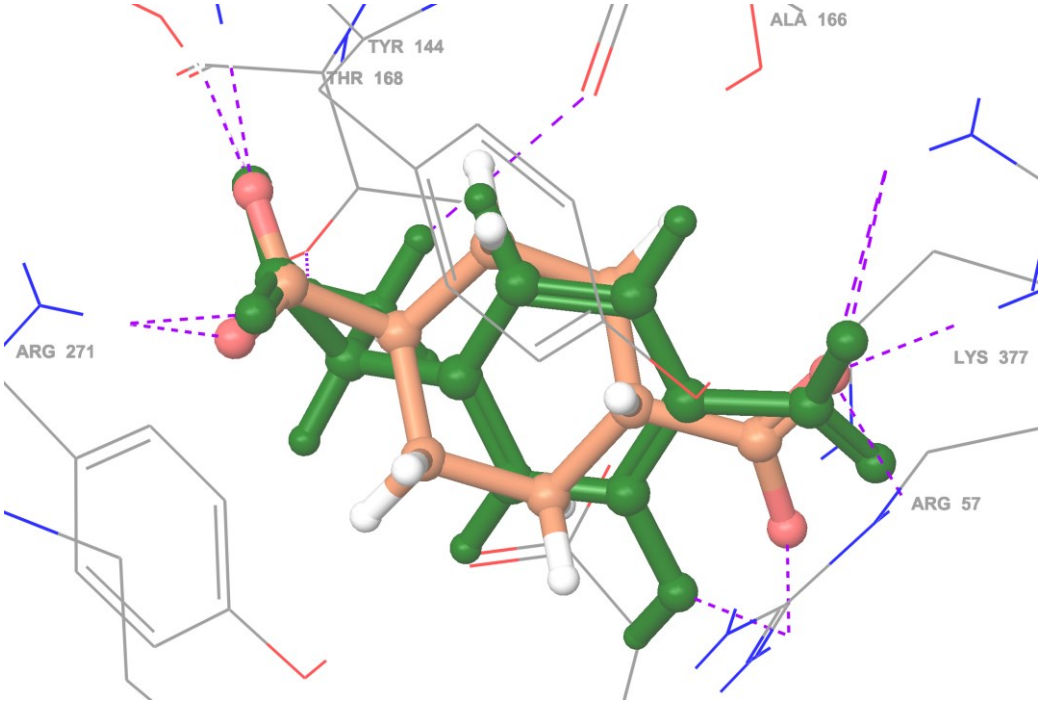

Figure 25: **The binding mode of the toxicant 1,4-cyclohexanedicarboxylic acid (shown in orange carbons) in the orthosteric binding site of mGlu2 receptor agonist conformational state superimposed with the agonist (S)-4C3HPG (shown in dark green).** The dotted purple line represents H-bonds and the amino acid residues are in a 3 Å sphere radius around the ligands.

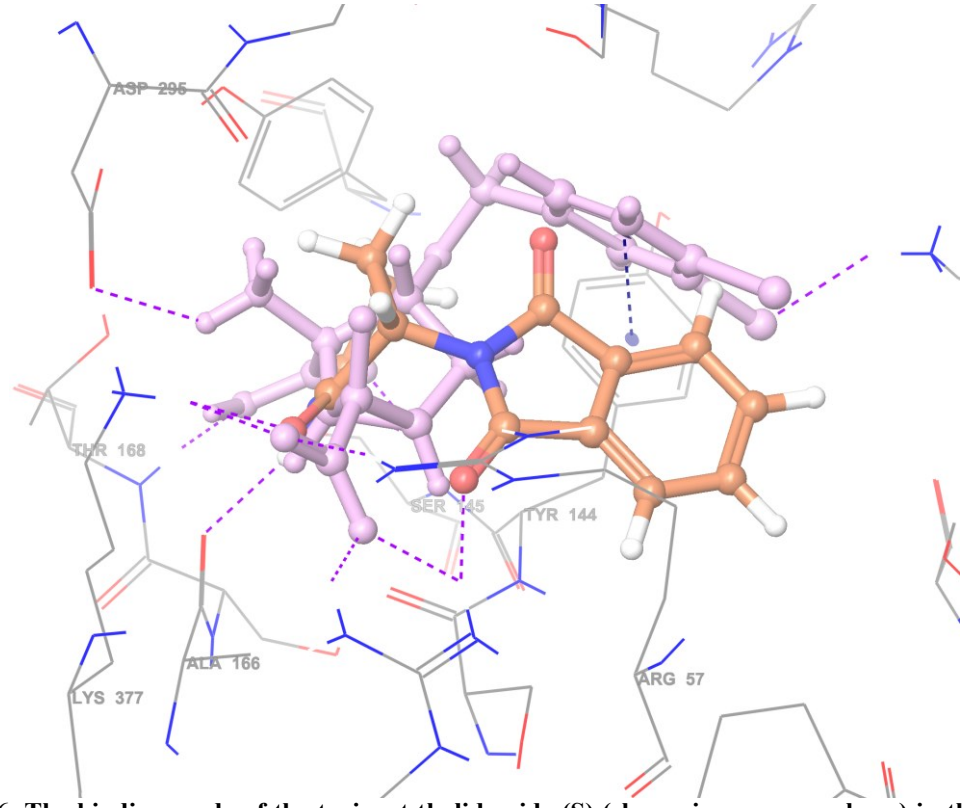

Figure 26: **The binding mode of the toxicant thalidomide (S) (shown in orange carbons) in the orthosteric binding site of mGlu2 receptor in an antagonist conformational state, superimposed with the antagonist MGS0039 (shown in light pink color).** The dotted purple lines represent H-bonds and the dark blue line represents π-π interactions. The amino acid residues are in a 3 Å sphere radius around the ligands.

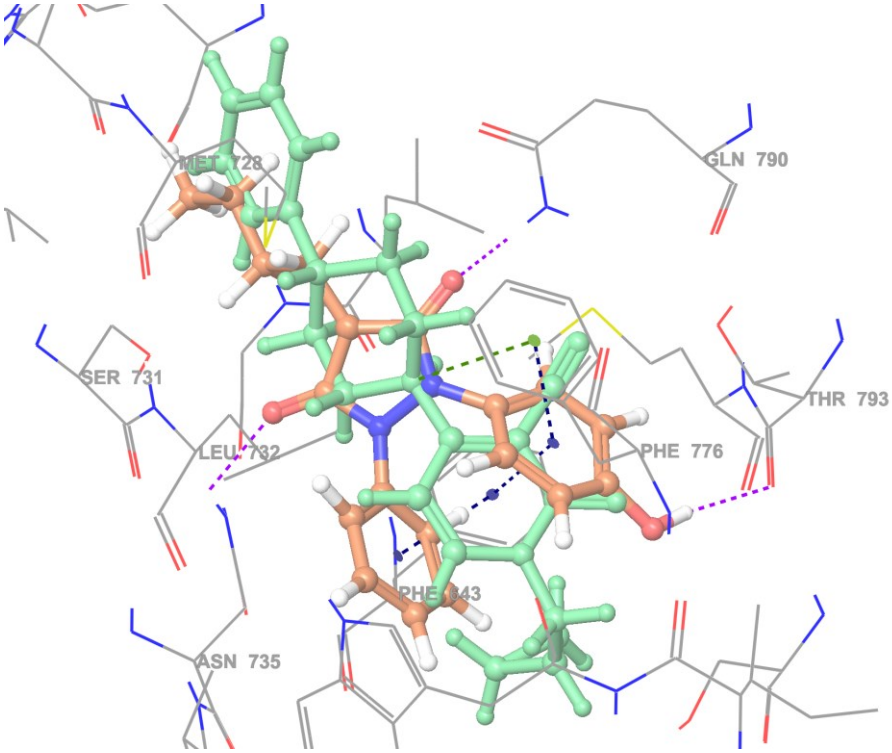

Figure 27: **The binding mode of the toxicant oxyphenbutazone (orange carbons) in the allosteric binding site in the mGlu2 receptor PAM conformational state superimposed with the PAM JNJ-40068782 (light green).** The dotted purple lines represent H-bonds, π-π interactions are shown in dark blue and the green dotted line represent π-cation interations. The amino acid residues are in a 3 Å sphere radius around the ligands.

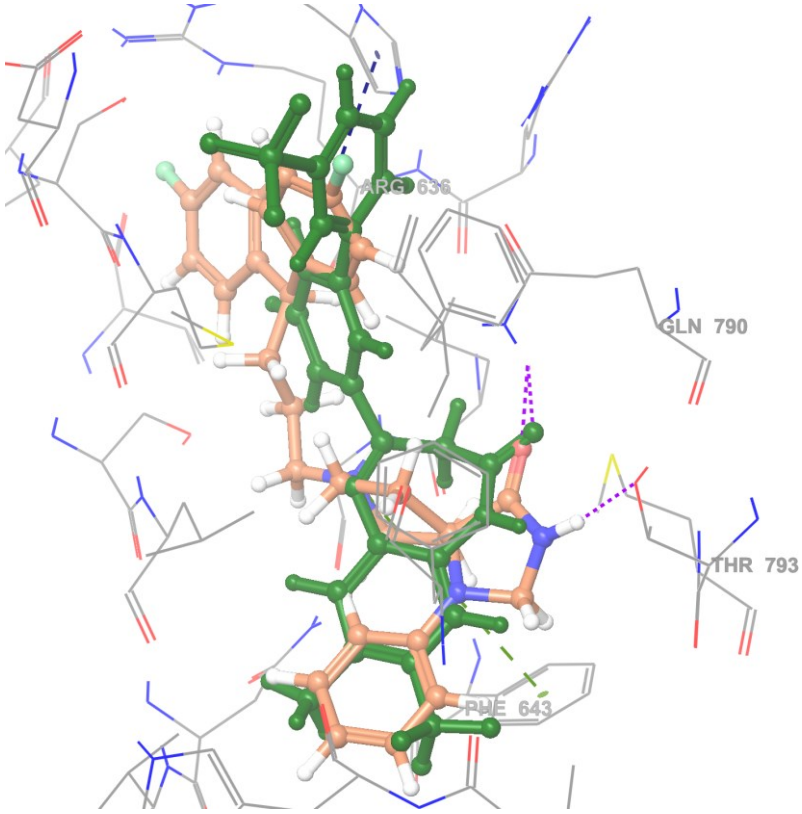

Figure 28: **The binding mode of the toxicant fluspirilene (orange carbons) in the allosteric binding site in the mGlu2 receptor NAM conformational state superimposed with the NAM RO5488608 (dark green).** The purple dotted lines represent H-bonds, π-π interactions are shown in dark blue, π-cation interactions are shown in green. The amino acid residues are in a 3 Å sphere radius around the ligands.

mGlu7 receptor:

A total of 9685 toxicants were docked to the orthosteric binding site of the agonist conformational state of the crystal structure of VFT mGlu7 receptor (PDB ID: 3MQ4), where 220 had a docking score better than the calculated threshold value. 9647 toxicants were docked into the antagonist conformational state, and 475 had a scoring value over the threshold value.

Since it exists only one known PAM for the mGlu7 receptor, it was impossible to calculate a mean score value from VSW. Therefore, the docking score from the IFD protocol was used as a threshold value. A total of 8586 toxicants were able to dock to the allosteric binding site of mGlu7 receptor PAM state, but none had a scoring value better than the threshold value. For the NAM conformational state, 7354 toxicants were docked to the allosteric binding site and out of these 158 compounds had better scoring value than the threshold value.

mGlu5 receptor:

A total of 8319 toxicants were able to dock into the allosteric binding site of PAM state of the crystal structure of mGlu5 receptor (PDB ID: 4OO9) and 23 of these had a better docking score than the threshold value. Out of 8338 toxicants docked to the NAM conformational state, 83 had a better scoring value than the threshold value.

GAT1:

The constructed homology model of GAT1 were able to dock a total of 9518 toxicants in the orthosteric binding pocket and 276 compounds with a scoring value better than the calculated threshold value.

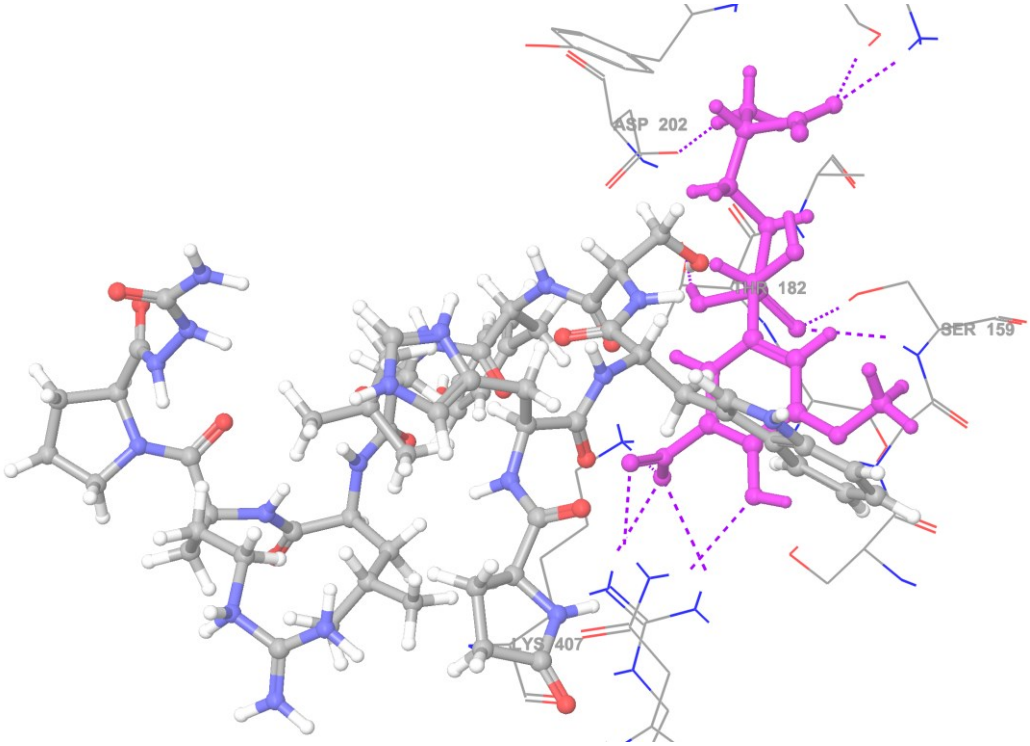

Figure 29: **The binding mode of the toxicant goserelin (shown in gray carbons) in the orthosteric binding site of the mGlu7 receptor antagonist conformational state superimposed with the known agonist LSP1-2111 (S) (shown in pink).** The dotted purple lines represent H-bonds between the agonist and the amino acid residues. The amino acid residues are in a 3 Å sphere radius around the ligands.

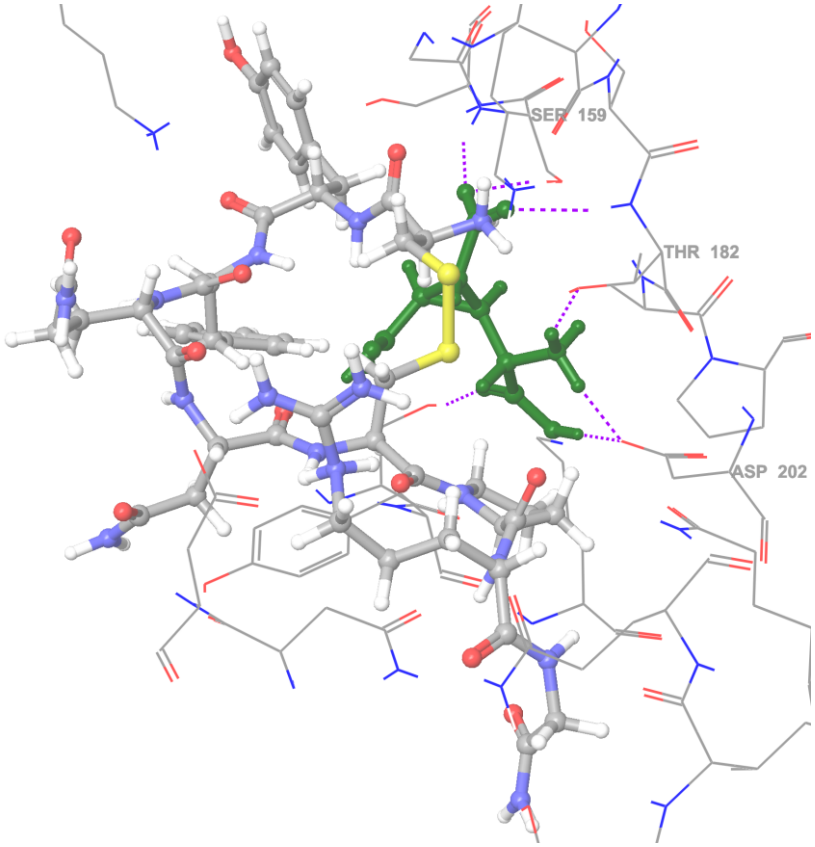

Figure 30: **The binding mode of the toxicant argipressin (gray carbons) in the orthosteric binding site of the mGlu7 receptor antagonist conformational state superimposed with the antagonist DCG-IV (R) (shown in dark green).** The dotted purple lines represent H-bonds between the antagonist and the amino acid residues. The amino acid residues are in a 3 Å sphere radius around the ligands.

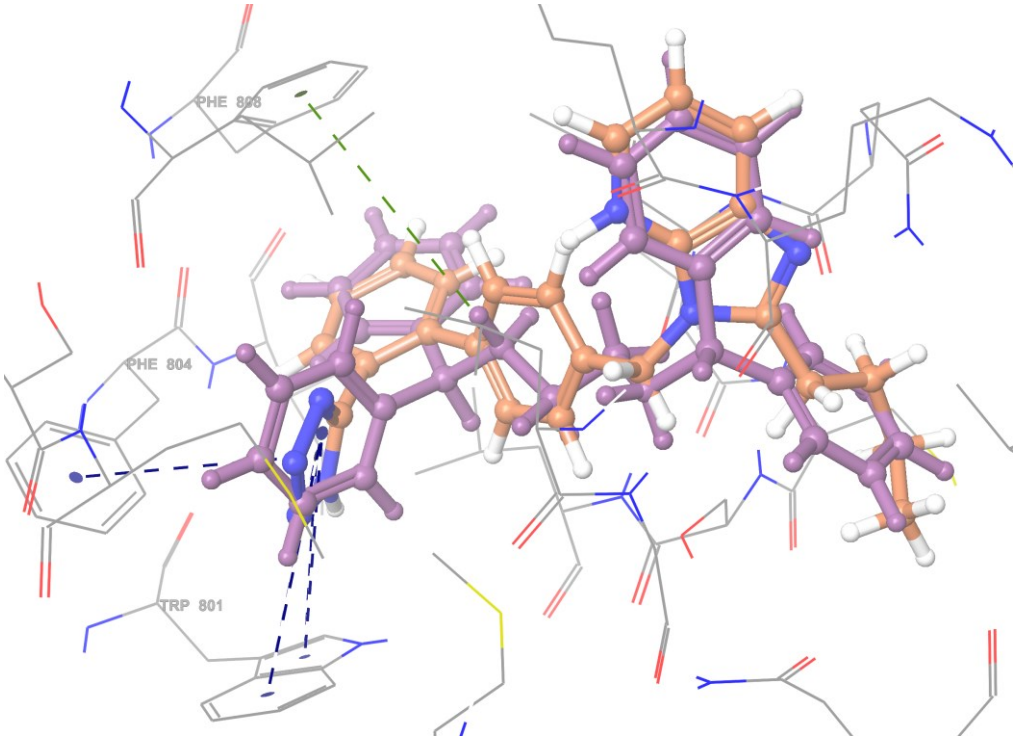

Figure 31: **The binding mode of toxicant 5-{4'-[(2-butyl-3H-imidazo[4,5-b]pyridin-3-yl)methyl]biphenyl-2-yl}tetrazol-1-ide (shown in orange carbons) in the allosteric binding site of the mGlu7 receptor NAM conformational state superimposed with the agonist PAM AMN082 (shown in light purple).** π-π interactions are shown in dark blue dotted lines and π-cation interactions are shown in dotted green line. The amino acid residues are in a 3 Å sphere radius around the ligands.

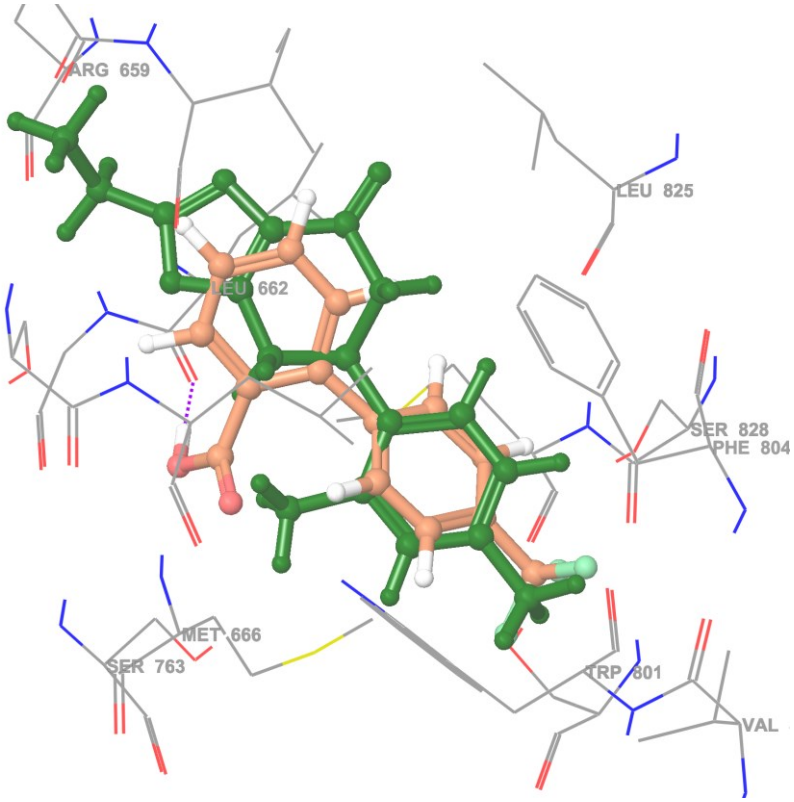

Figure 32: **The binding mode of toxicant xenalipin (shown in orange carbons) in the mGlu7 model NAM conformational state superimposed with the NAM ADX71743 (S) (shown in dark green).** H-bond between the carboxyl group in xenalipin and the backbone of Leu662$^{5.46}$, is shown in purple color. The amino acid residues are in a 3 Å sphere radius around the ligands.

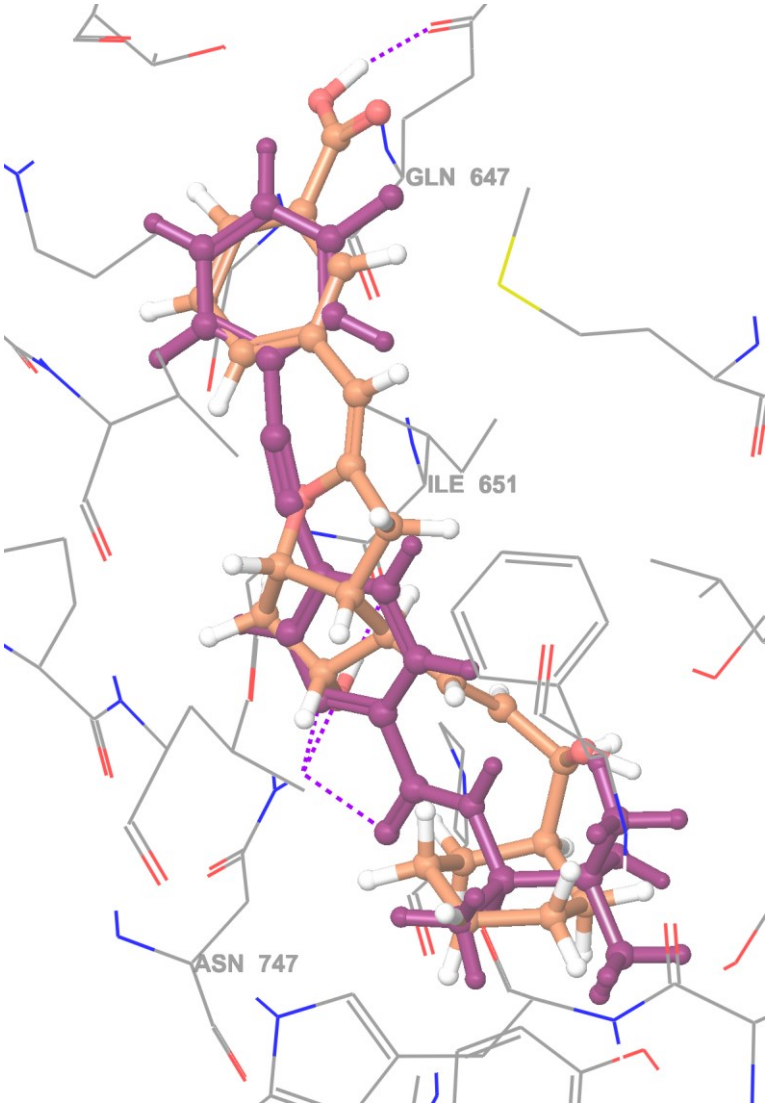

Figure 33: **The binding mode of toxicant taprostene (shown in orange carbons) in the allosteric binding site of the mGlu5 receptor PAM conformational state superimposed with the PAM VU0425565 (shown in dark purple).** The fluoro substituent on the acetylated phenyl ring on VU0425565 is not indicated, but it is situated against Gln647$^{3.32}$ in a meta-position relative to the acetylene area. The dotted purple lines represent H-bonds. The amino acid residues are in a 3 Å sphere radius around the ligands.

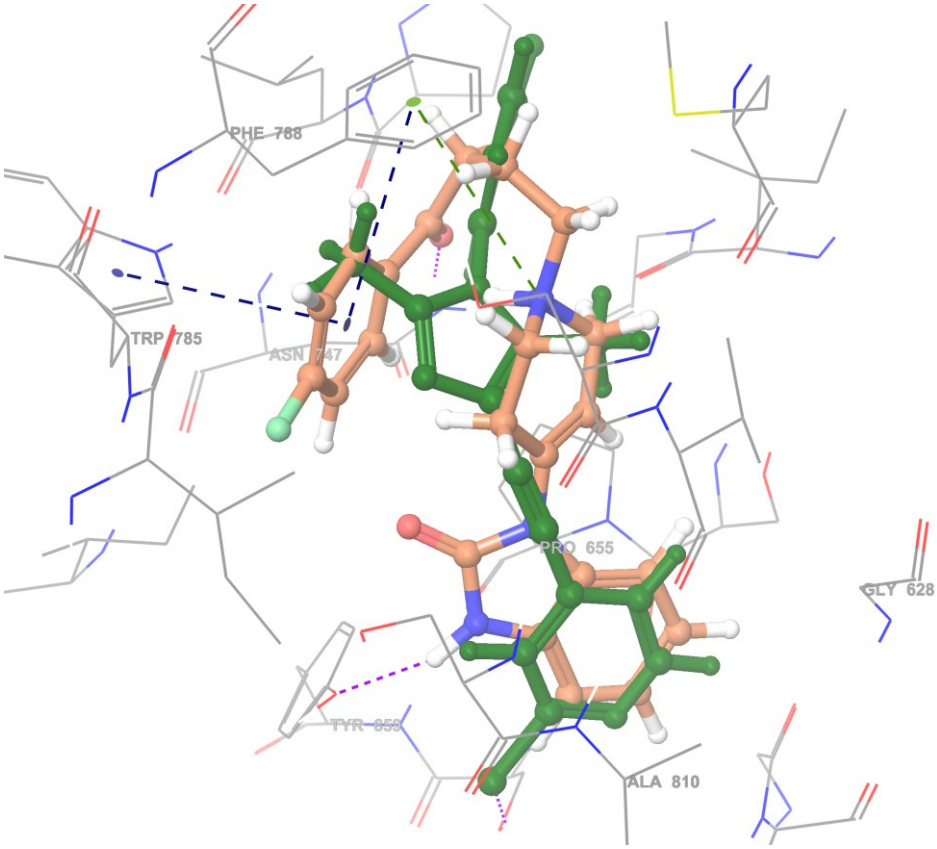

Figure 34: **The binding mode of the toxicant droperidol (orange carbons) in the allosteric binding site in the mGlu5 receptor NAM conformational state superimposed with the NAM basimglurant (dark green).** The dotted purple line represents H-bonds, π-π interactions are shown in dark blue dotted lines and π-cation interactions are shown in a dotted green line. The amino acid residues are in a 3 Å sphere radius around the ligands.

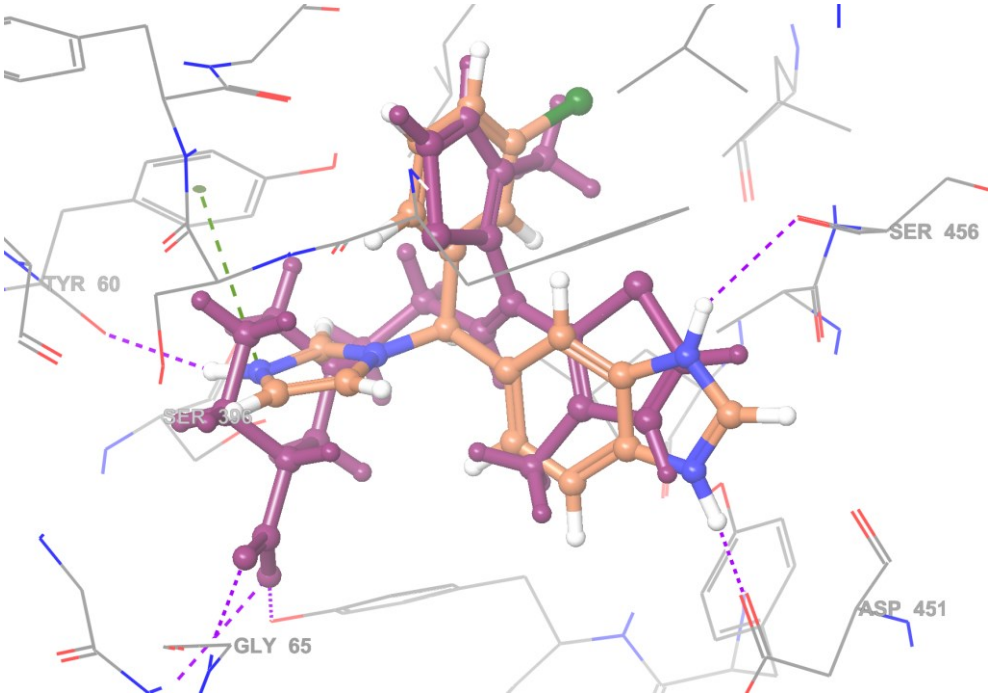

Figure 35: **The binding mode of the toxicant liarozole (R) (shown in orange carbons) in the GAT1 model superimposed with GAT1 inhibitor tiagabine (R) (shown in dark purple).** The purple dotted lines represents H-bonds and π-cation interaction are shown in a dotted green line. The amino acid residues are in a 3 Å sphere radius around the ligands.

4.3 CNS MPO predictions

CNS-MPO was used to predict BBB penetration for the toxic compounds retrieved from the Tox21 database (spring 2012). From a total of 9757 toxic compounds, 6803 compounds had a CNS-MPO score ≥ 4, which indicates that these compounds have physicochemical properties similar to CNS drugs and that they probably are able to pass the BBB. In addition, 388 of the toxic compounds had the maximum score of 6.

5. DISCUSSION

The results show that many toxicants of the Tox21 virtual library may interact with mGlu receptors and the GAT1. This included toxic compounds that varied in size and in physicochemical properties. Many of the toxicants had also better docking scores than several of the known binders, including high affinity binders.

5.1 Alignments

Visual inspection of the multiple sequence alignment between the mGlu receptors showed high amino acid conservation, especially in the 7 TMH and the ECD regions (figure 11). In addition, mGlu1 and mGlu5 receptor had a longer intracellular C-terminal tail than the other mGlu receptors. This similarity between mGlu1 and mGlu5 receptor may reflect that they belong to the same subgroup of mGlu receptors.

Available literature indicates that the TM2, TM3, TM5, TM6, TM7 and ECL2 are the main contributors to the binding of allosteric modulators in mGlu receptors (23–25). Interestingly, it was observed that there was high conservation in these regions, especially in TM6. These observations is in agreement with the observations by Topiol et al. (33), that also suggested that it is greater sequence conservation in the 7 TMH than in the ECD VFT regions.

The loop regions were the least conserved regions in the alignment, which differed both in type of amino acid residues and length of the loops. There are more challenges in loop modeling, because of the differences between the GPCRs and the less conservation among the amino acid residues in these regions. The differences of the conservation in the sequences could also be seen in the structure of the constructed homology models of mGlu2 and mGlu7 receptors. The superposition of the 100 homology models of mGlu2 and mGlu7 receptors showed that the backbone of the helices were quite similar, which could reflect the high conservation in the 7 TMH (figure 13-14). The loop regions were slightly different among the 100 homology models and were the most inaccurate parts of the models, due to the lack of conservation and structural flexibility. Since the allosteric binding pocket were the main interest in this thesis, loop region was not focused on regarding accurate loop modeling.

5.2 Evaluation of the models

A good relative correlation was observed between the docking (Glide) scores from the VSW protocol and the binding affinity for several of the known binders to the mGlu receptors and GAT1. If a model is reliable, a ligand with high affinity for the receptor should get a good docking score and be ranked on the top of the list. This could indicate that the models give a good prediction for compounds that bind to the native mGlu receptors and GAT1.

The ideal template for homology modeling should be in an appropriate conformational state. If the purpose is to construct an agonist binding state of a receptor, it is desirable to use a template that is bound to an agonist, and to an antagonist if the goal is an antagonist induced conformation of the receptor. For modeling of the inhibitor conformational state of GAT1, this was not a problem since the template dDAT (PDB ID: 4XP4) were bound to an inhibitor. For the modeling of 7 TMH mGlu2 and mGlu7 receptor, available 7 TMH template structures were in complexes with NAMs only, which made the modeling of the PAM conformational state more challenging. Different templates, including active/inactive states, will result in different homology models. It is reasonable to believe that the homology modeling would have been easier and some of the models may have had higher quality if templates with the correct type of compound were available for all the targets.

In the validation of the models, it was also important with visual inspection of the binding pockets. The allosteric binding sites of the mGlu receptor in the present study were similar in shape and in size, except for a small unique sub-pocket in the allosteric binding site of the mGlu5 receptor, which was situated between the TM2, TM3 and TM7. This small sub-pocket exists for all the mGlu receptors but it is only in the mGlu5 receptor that it is possible for ligands to enter this sub-pocket due to the size of the amino acid residues. The mGlu5 receptor possesses smaller amino acid residues in this part of the binding site, including Gly628$^{2.49}$, Pro655$^{3.40}$ and Ala810$^{7.41}$ (figure 18) (10). The mGlu2 receptor and the mGlu7 receptor have larger amino acid residues in this area of the binding site, which block ligands to enter. This includes the residue Phe643$^{3.40}$ and Val823$^{7.41}$ in the mGlu2 receptor and Cys639$^{2.49}$, Met666$^{3.40}$ and Met829$^{7.44}$ in the mGlu7 receptor (figure 16 and 17) (10). By comparing binding modes from VSW of the constructed homology models of the 7 TMH of mGlu2 and mGlu7 receptor to crystal structure of the 7 TMH of mGlu5 receptor it was clear that this was the case. The high affinity mGlu5 receptor NAM basimglurant did bind much

deeper into the allosteric binding site of mGlu5 receptor and the acetylene aromatic area of the ligand was able to enter the sub-pocket (figure 18). The amino acid residue Phe643$^{3.40}$ in the allosteric binding pocket of mGlu2 receptor blocks the RO5488608 (NAM) from entering the sub-pocket (figure 16). The NAM ADX71743 is blocked by the residues Cys639$^{2.49}$, Met666$^{3.40}$ and Met829$^{7.44}$ and is not able to reach the corresponding sub-pocket in mGlu7 receptor (figure 17). Another observation was that the ligands for mGlu2 and mGlu7 receptor are bound much higher in the binding pocket, further against the extracellular side of the receptor compared to the binders for mGlu5 receptor. This observations corresponds to the results from Harpsøe et al. (10), which indicates that there are residues in the binding pocket of the models that are in correct conformation concerning this sub pocket.

The BEDROC results showed that there were some variations between the scoring of the models ranging from 0.157 for the mGlu7 receptor antagonist conformational state to 0.625 for the GAT1 model (table 15). A bad BEDROC score can indicate that a model is not able to differentiate between binders and non-binders/decoys. However, a bad BEDROC value does not necessary mean that the model is not accurate. Decoys for each known binders were downloaded from DUD.E. The decoys are theoretical compounds with similar Mw and physiochemical properties as the binders, but most probably do not bind to the receptors. Each model that has been used in this thesis has relative few known binders, and many of them have different topology, some are very small molecules and some much larger molecules for the same receptor. It was decided to construct models that were able to fit all binders for a receptor, which resulted in that many of the models had conformations with a big and open binding pocket, also capable of binding decoy molecules. A bad BEDROC score may come from the open binding pockets of some of the models that can easier adopt to the structure of some of the decoys in front of larger known binders. This could probably have been avoided if the binding pocket had been in a more closed state, but then again the larger known binders could not be able to fit into the binding pocket. Even though some BEDROC scores were not optimal, it did not directly mean that the models had low quality, but that the size of the binding pockets were open and the size of the known binders for one receptor varied. In addition, BEDROC as a statistic method is not optimal for receptor models with few known binders. Ideally each receptor should have at least 50 known binders for the method to be optimal. An alternative approach could be to upload the constructed homology models to Structural Analysis and Verification Server (SAVES, http://services.mbi.ucla.edu/SAVES/) or

Model Quality Assessment Server (ModFOLD, http://www.reading.ac.uk/bioinf/ModFOLD/) in order to validate the protein structures.

Since the native receptors can be in different conformational states, there are possibilities that the final models in the present study are not optimal for some of the ligands. It may have been better to dock toxicants with several conformation states of one target, in order to include different variations in the binding pockets. One approach could be to use IFD protocol for the receptor model with all the known binders, and select the best output poses from each docking and use them in glide docking with toxicants. This would result in different conformations of the binding pocket and it could increase the likelihood of getting a representative model in the best conformational state for each ligand. However, the main goal was to predict if the compounds of the Tox21 library could bind or not, and the docking of known binders and decoys clearly indicates that.

5.3 Glide docking with exogenous toxicants

By investigating the binding mode of the selected toxicants, and compare them to the docking studies of known compounds, it was possible to predict if the binding of the toxicants were likely to occur (table 16). If the binding poses of a known binder and a toxicant have much in common, it increases the probability for the toxicant to actually bind to the receptor. Together with the scoring value that gives the most important contribution to the prediction.

The Tox21 ligand set (spring 2012) comprised of several CNS drugs in addition to environmental toxicants. Many CNS drugs were able to bind to the models with high affinity and get better docking scores than many of the environmental toxicants. This may be due to that CNS drugs are designed and optimized to reach and bind with high affinity to different CNS receptors and transporters. Even though some of the ligands from the Tox21 dataset are known CNS drugs, they are referred as toxic compounds throughout this thesis.

It is important to have in mind, that the receptor models are only snapshots of the native receptor structure and some of the toxicants that did not bind or had a worse docking score than the calculated mean score from VSW protocol, may bind to another conformations of the receptor. There may be a possibility that other conformation state of the receptor models

would result in both higher docking score and the binding of some of the low scored toxicants.

5.3.1 mGlu2 receptor

The highest ranked toxicant for the agonist state of mGlu2 receptor was deferoxamine, which is a quite large molecule. That such a large molecule may bind to the orthosteric binding site is quite surprising, as the known agonists for the mGlu2 receptor are in general small molecules. The third on the list was 1,4-cyclohexanedicarboxylic acid, which is a relatively small molecule. Its binding mode was compared with the binding mode of the mGlu2 receptor known agonist (S)-4C3HPG since they were quite similar in shape and structure (figure 25). The molecules were orientated in the same region in the binding site, and 1,4-cyclohexanedicarboxylic acid formed interaction with the same residues as for (S)-4C3HPG (although the agonist did form H-bonds with some more residues that are not mentioned in this thesis). Both compounds formed H-bonds with Arg57, Arg61, Ser145 (backbone) and Arg271. They also formed a salt bridge to Lys377, which is not shown in the figure 25. In addition, 1,4-cyclohexanedicarboxylic acid also formed a salt bridge to Arg61. Its docking value was better than the calculated mean score, which could indicate that 1,4-cyclohexanedicarboxylic acid has the potential to bind stronger than some known agonists.

Antagonists in general are much larger molecules than most agonist compounds for a receptor. This could also be observed for the binding of toxicants for the antagonist conformation state for the mGlu2 receptor. Larger toxicants were able to fit into the binding pocket of the antagonist state rather than to the agonist state, which also could reflect the fact that the VFT is in a more open state when bound to an antagonist. Thalidomide (S) was the fourth ranked toxicants that bound to the antagonist state of mGlu2 receptor, and is the toxic enantiomer that gives serious adverse effects for unborn children. Showed in figure 26 is the binding pose of thalidomide (S) and the antagonist MGS0039. The molecules are placed in the same region in the orthosteric binding site. Thalidomide (S) had a better docking score than the calculated mean score, but the high affinity antagonist MGS0039 had the overall best docking score. This could indicate that thalidomide (S) can compete with several of the known antagonists for the orthosteric binding site of the mGlu2 receptor.

It is important to note that environmental toxicants can affect humans in different ways. If a pregnant woman is exposed to some toxicants, it could harm the unborn child in many ways. This happened with the scandal in Germany in the late 50s where the toxic enantiomer (S) of thalidomide were administrated to pregnant women, which resulted in several fetal death and many children that were born with malfunctioned limbs. This negative effect of the drug was fortunately discovered, but it may be that there are more toxic compounds that can affect unborn children but are not identified yet.

The 10 best ranked toxicants for both the PAM and the NAM conformational state of mGlu2 receptor had better docking score than the calculated mean score value from VSW. Oxyphenbutazone and fluspirilene had the best docking scores and were able to form interactions with the PAM and the NAM conformational states of mGlu2 receptor. It was also observed that many of the same amino acid residues were involved in the binding of toxicants both in the PAM and NAM conformational states. This is in agreement with Lundstrom et al. (20) that suggested that PAMs and NAMs have overlapping binding sites in the mGlu2 receptor.

Comparing oxyphenbutazone binding mode with the binding mode of JNJ-40068782 (PAM) showed that the ligands were occupying the same region in the receptor binding pocket, despite their structural dissimilarities (figure 27). They both interacted with the amino acid residue Phe776$^{6.53}$, but JNJ-40068782 formed π-cation interactions with its protonated amino group and oxyphenbutazone formed π-π interactions with one of its benzene rings. Oxyphenbutazone also formed H-bond with the backbone of Thr793$^{7.31}$, H-bond with Asn735$^{5.47}$ and Gln790$^{7.29}$ and π-π interactions with Phe643$^{3.40}$.

Figure 28 shows the binding mode of fluspirilene superimposed with the binding mode of the high affinity mGlu2 receptor binder RO5488608. They occupied the same region in the binding pocket and both compounds formed H-bond with the amino acid residue Gln790$^{7.29}$. Fluspirilene also formed π-cation interactions with Phe643$^{3.40}$ and π-π interactions with Arg636$^{3.33}$, which according to Lundstrom et al. (20) are both residues of importance for the binding of NAMs in mGlu2 receptors. In addition, both RO5499608 and fluspirilene formed favorable contact with Phe780$^{6.57}$, which also plays a role in the binding of allosteric modulators to mGlu2 receptors (20).

Fluspirilene did also bind to the allosteric binding site of the mGlu7 receptor. This was not so surprising considering the high conservation in the allosteric binding pocket between the mGlu receptors. Table 5 (section 3.4.2) gives an example of the conservation between corresponding amino acid residues in the 7 TMH, especially between the mGlu2 receptor and the mGlu7 receptor.

5.3.2 mGlu7 receptor

In general, known agonists for the mGlu7 receptor are larger molecules than the known antagonists. This is interesting, since most often receptor antagonists are bigger molecules than receptor agonists. The toxicants that were able to dock to the agonist and the antagonist conformation state of mGlu7 receptor were in general large molecules with poor BBB penetration properties. These results may be due to the fact that the models had poor BEDROC score (agonist: 0.163, antagonist: 0.157).

As observed in figure 29 and 30 the size and structure of the agonist LSP1-2111 (S), the antagonist DCG-IV and the toxicants goserelin and argipressin are quite different. The docking indicated that these toxicants were not able to make any interactions with the orthosteric binding site (both agonist and antagonist state) and docked in a region different from that of the known orthosteric binders. Goserelin could not be fully docked into the binding site, and large parts of the molecule were on the outside of the binding pocket (figure 29).

Fluspirilene, which was top ranked for the mGlu2 receptor, was also able to dock into the mGlu7 receptor and was predicted as the third best binder of the docked toxicants. 5-{4'-[(2-butyl-3H-imidazo[4,5-b]pyridin-3-yl)methyl]biphenyl-2-yl}tetrazol-1-ide, was the second on the list and was able to dock into the allosteric binding site of mGlu7 receptor in the PAM conformational state (figure 31). AMN082 (agonist PAM) is a symmetrical molecule with two benzene rings on each side. 5-{4'-[(2-butyl-3H-imidazo[4,5-b]pyridin-3-yl)methyl]biphenyl-2-yl}tetrazol-1-ide on the other hand, is not a symmetrical molecule, but it seems to have the ability to be orientated in the same region as AMN082. The compounds did not form the same interactions in the receptor but both molecules had good contact with Ile756$^{5.40}$, which according to Feng et al. (27) might contribute to receptor selectivity. A

tetrazole ring on the toxicant was able to form π-π interactions with Phe804$^{6.53}$ and Trp801$^{6.50}$. Feng et al. (27) also proposed that Phe804$^{6.53}$ could contribute to enhancing the binding affinity of the AMN082, which may be an important amino acid in the binding of ligands to the allosteric binding site. None of the toxicants that bound to the PAM conformation state of mGlu7 receptor had a better docking score than the threshold value. The threshold value was -12.60, which only represents the docking score of the high affinity agonist PAM binder AMN082. It may be the case that it exists more mGlu7 receptor PAMs with less affinity than AMN082. 5-{4'-[(2-butyl-3H-imidazo[4,5-b]pyridin-3-yl)methyl]biphenyl-2-yl}tetrazol-1-ide got a relative high docking score of -11.39 and it would have been interesting to have more PAMs to compare with.

The exogenous compound xenalipin got the highest docking score of the toxic compounds for the NAM state of the mGlu7 receptor (figure 32). According to Harpsøe et al. (10) Ile756$^{5.40}$, Gln775$^{5.39}$ and Val800$^{6.49}$ are important determinants for selective NAM binding to the mGlu7 receptor. Val800$^{6.49}$ is placed deep in the binding pocket, and makes good contact with the methyl group of ADX71743 (S) and the fluorocarbon moiety of xenalipin. These groups also have good contact with Ile756$^{5.40}$. In addition, the hydroxycarbon group in xenalipin forms H-bond with Leu662$^{3.36}$. Compared to the known NAM binder ADX71743 (S), xenalipin can be considered as a shorter molecule without a long chain, which is present in the NAM and points up against the extracellular side. The lack of this long chain results in that xenalipin does not form good interactions with Gln755$^{5.39}$, because this residue is too far away from the ligand. Since we do not know which amino acids that are essential for binding and activation, it is not clear if xenalipin can make the “right” contacts for being a NAM, but it is clear that there is some similarities with the binding mode of ADX71743 (S).

5.3.3 mGlu5 receptor

The mGlu5 receptor allosteric binding site goes more deeply into the receptor due to its sub-pocket, compared with the mGlu2 and mGlu7 receptor. It was observed that the toxicants that bound to the mGlu5 receptor were longer in size than those interacting with mGlu2 and mGlu7 and were able to dock deeply into the allosteric binding pocket.

According to Dore´ et al. (23), by changing the methyl substituent on the phenyl ring in the acetylene area on mavoglurant to a fluoro substituent, switches the molecule from a NAM to a

PAM. This was observed for several of the mGlu5 receptor PAMs, including the high affinity VU0424465 (PAM) where the phenyl ring included a fluoro substituent. Figure 33 shows VU0424465 superimposed with the top ranked docked toxicant taprostene in the allosteric binding pocket. These compounds have quite similar topology and taprostene were able to dock in the same region as the PAM. Unfortunately, VU0424465 was orientated so it could not reach the sub pocket in the allosteric binding site. It is reasonable to believe that the benzene ring in the acetylene area in VU0424465 could be docked into the sub-pocket of the receptor, but instead it points towards the extracellular side of the receptor. This was in fact the case for all the PAMs having such benzene ring. The reason for this is not clear, it may be correct, but it can be because some of the amino residues are not in an optimal conformation.

Droperidol, which is a potent antidopaminergic drug that also has some antagonist activity at histamine and serotonin receptors, was the fourth compound on the list that bound to the NAM state of the mGlu5 receptor. It had a docking score of -10.89 that was better than the calculated mean score. As seen in figure 34 droperidol has the ability to bind deeply into the allosteric binding site, similarly to the NAM basimglurant. Basimglurant was able to form H-bonds with Tyr659$^{3.44}$. For the upper part of droperidol, as seen in figure 34, the molecule is rotated so that the benzene ring is in a parallel position relative to its own cyclohexane. It is assumed that a molecule always wants to be in an orientation that gives it as low internal energy as possible. The present orientation for droperidol will probably give the molecule a high internal energy. However, the benzene ring was able to form π-π interactions with Phe788$^{6.53}$ and Trp785$^{6.50}$. In addition, Phe788$^{6.53}$ also formed π-cation interactions with the protonated amino group on droperidol.

According to Harpsøe et al. (10) and Dore´ et al. (23) a stable water network is present in the bottom of the allosteric binding pocket in the mGlu5 receptor, which can create H-bonds and lower the activation energy in the receptor. These water molecules create a H-bond network with the amino acid residues Tyr659$^{3.44}$, Thr781$^{6.46}$ and the backbone of Ser809$^{7.39}$ in the bottom of the allosteric binding pocket (10,23). It was observed that many of the toxicants with a long topology were able to create H-bonds with these amino acid residues, this applied especially for the toxicants that docked into the PAM conformational state. It would have been interesting to add water molecule in order to see if they would have affected the binding mode and the docking score.

5.3.4 GAT1

Liarozole (R) was the fourth ranked toxicant that was able to dock into the GAT1. It had a docking score above the calculated mean score, which may indicate that this toxicant can be a strong binder for the transporter. Figure 35 illustrates the binding mode of both the toxicant and the high affinity inhibitor tiagabine (R) in the GAT1 binding pocket. According to the binding modes, they are both occupying the same region of the binding pocket, and they seem to have corresponding functional groups that theoretically can form the same type of hydrophobic interactions with amino acid residues. However, there are some small differences. Tiagabine (R) was able to form H-bonds with the backbone of Leu64 and Gly65 and H-bond with Tyr140. Liarozole (R) on the other hand, could form H-bonds with the backbone of Tyr60 and Ser456, H-bond with Asp451 and π-cation interaction with Tyr60.

5.4 CNS MPO predictions

CNS MPO values can predict CNS drug-like properties for the toxic compounds in order to investigate if the compounds have physicochemical properties to penetrate the BBB and enter the CNS. Several of the toxicants that were able to dock into the receptor and transporter models had a CNS MPO scoring value ≥ 4, which is considered as the threshold for putative BBB penetration. The CNS MPO results selected out those toxicants with the CNS drug like properties, which was taken for further analysis. The toxicants that were investigated and discussed in this thesis were the ones with the best docking scores in combination with the highest CNS MPO value.

Most of the toxic compounds that were analyzed had a CNS MPO scoring value ≥ 4, but there were some with a CNS MPO value below 4. This included the toxic compounds that docked into the VFT of mGlu7 receptor. None of the top 10 ranked toxicants for the VFT mGlu7 receptor, both agonist and antagonist conformational state, had a CNS MPO value ≥ 4. This could reflect the fact that their binding pockets were very open and that large compounds were able to bind, and the two top docked toxicants to mGlu7 receptor goserelin (agonist conformational state) and argipressing (antagonist conformational state) had a CNS MPO value of 2.0. This value may appear due to their large structure and high Mw, and may indicate that they are not able to cross the BBB.

It is also important not to rely entirely on this calculated value. The toxicant fluspirilene was the top ranked ligand for the NAM conformation state of mGlu2 receptor. This toxicant had a calculated CNS MPO value of 1.86, which would reflect that the ligand would not be able to penetrate the BBB. In fact, this is a typical antipsychotic drug used in the treatment of schizophrenia.

The CNS MPO value may give an indication about which compounds that may cross the BBB by passive transport. It is not taken into account that some toxic compounds may be able to enter the CNS through active transport. However, the CNS MPO values give a good prediction for sorting out compounds with CNS drug-like physicochemical properties, but it has some flaws where some compounds that do cross the BBB, get values below 4.

5.5 Future Directions

The present study predicts several compounds of the Tox21 database as putative binders to the tested mGlu receptors and GAT1. The toxic library contained many CNS drugs, which were able to dock with high affinity to the receptor and transporter models. It would perhaps be advantageous to sort out CNS drugs prior to docking, in order to only investigate the environmental toxicants. However, it is very important to recognize the impact CNS drugs could have on these receptors and GAT1, where unexplained adverse effects could in fact be a result of drugs acting on some of these mGlu receptors and GAT1.

The GABA-B receptor plays an important role in the CNS and has close structural similarities with the mGlu receptors. The receptor is widely distributed within the CNS and disruption of the receptor could interfere with several physiological processes in humans. Due to structural and functional similarities between mGlu receptors and GABA-B receptor it would have been interesting to dock the Tox21 library into the GABA-B receptor to see if some toxicants could bind to this receptor.

The limited knowledge about how toxic compounds can affect the humans and if they play a role in the development of several CNS diseases makes this field of study very important for the public health and treatment of several diseases. The studies in this thesis are theoretical approaches where 3D protein structures and ligands are treated rigid or semi-rigid, which do

not fully represent the true native proteins and their environments. In order to optimize the theoretical docking processes it could have been interesting to include some environmental factors such as water. In addition, the toxic compounds also need to be tested *in vitro* before any clear conclusion about their binding affinity and putative CNS toxicity can be made. Studies in investigating the potential effects that the pollutants have on humans on individual and population levels would also be necessary.

6. CONCLUSION

The docking calculations of toxicants in constructed homology models and X-ray structures of mGlu2, mGlu5 and mGlu7 receptors and GAT1 revealed that several toxicants with different topology have the ability to bind to the receptors and the GAT1. There was observed a correlation between the type of binding pocket and the kind of toxicants that could bind and interact. Many toxicants had better docking scores than known binders, and could compete with endogenous and exogenous compounds that target these receptors and GAT1. The Tox21 library also included several CNS drugs, which were able to bind with high affinity to many of the models. By using CNS MPO values it was possible to sort out and focus mainly on substances that seemed to have physiochemical properties that enable them to reach the CNS.

Further studies should include *in vitro* affinity investigations of the toxicants for the receptors and the GAT1, in addition to the testing of type of putative CNS toxicity they may give. If the toxic compounds can outcompete the binding of glutamate, GABA or CNS drugs it can result in adverse effects in humans, possibly give rise to increased side effects and reduce the effectiveness of CNS drugs.

REFERENCES

1. Genc S, Zadeoglulari Z, Fuss SH, Genc K, Genc S, Zadeoglulari Z, et al. The Adverse Effects of Air Pollution on the Nervous System. J Toxicol J Toxicol. 2012 Feb 19;2012, 2012:e782462.

2. Genuis SJ, Kelln KL, Genuis SJ, Kelln KL. Toxicant Exposure and Bioaccumulation: A Common and Potentially Reversible Cause of Cognitive Dysfunction and Dementia. Behav Neurol Behav Neurol. 2015 Feb 4;2015, 2015:e620143.

3. Marrs TC, Maynard RL. Neurotranmission systems as targets for toxicants: a review. Cell Biol Toxicol. 2013 Dec;29(6):381–96.

4. Manivannan Y, Manivannan B, Beach TG, Halden RU. Role of Environmental Contaminants in the Etiology of Alzheimer's Disease: A Review. Curr Alzheimer Res. 2015 Feb;12(2):116–46.

5. US EPA O. Toxicology Testing in the 21st Century (Tox21) [Internet]. [cited 2016 Apr 2]. Available from: https://www.epa.gov/chemical-research/toxicology-testing-21st-century-tox21

6. Pajouhesh H, Lenz GR. Medicinal Chemical Properties of Successful Central Nervous System Drugs. NeuroRx. 2005 Oct;2(4):541–53.

7. Wager TT, Hou X, Verhoest PR, Villalobos A. Moving beyond rules: the development of a central nervous system multiparameter optimization (CNS MPO) approach to enable alignment of druglike properties. ACS Chem Neurosci. 2010 Jun 16;1(6):435–49.

8. Hassel B, Dingledine R. Chapter 17 - Glutamate and Glutamate Receptors A2 - Price, Scott T. BradyGeorge J. SiegelR. Wayne AlbersDonald L. In: Basic Neurochemistry (Eighth Edition) [Internet]. New York: Academic Press; 2012 [cited 2016 Mar 11]. p. 342–66. Available from: http://www.sciencedirect.com/science/article/pii/B9780123749475000171

9. Zhou R, Chen F, Feng X, Zhou L, Li Y, Chen L. Perinatal exposure to low-dose of bisphenol A causes anxiety-like alteration in adrenal axis regulation and behaviors of rat offspring: A potential role for metabotropic glutamate 2/3 receptors. J Psychiatr Res. 2015 May;64:121–9.

10. Harpsøe K, Isberg V, Tehan BG, Weiss D, Arsova A, Marshall FH, et al. Selective Negative Allosteric Modulation Of Metabotropic Glutamate Receptors – A Structural Perspective of Ligands and Mutants. Sci Rep. 2015 Sep 11;5:13869.

11. Pittenger C, Bloch MH, Williams K. Glutamate Abnormalities in Obsessive Compulsive Disorder: Neurobiology, Pathophysiology and Treatment. Pharmacol Ther. 2011 Dec;132(3):314–32.

12. Olsen RW, Li G-D. Chapter 18 - GABA A2 - Price, Scott T. BradyGeorge J. SiegelR. Wayne AlbersDonald L. In: Basic Neurochemistry (Eighth Edition) [Internet]. New

York: Academic Press; 2012 [cited 2016 Mar 11]. p. 367–76. Available from: http://www.sciencedirect.com/science/article/pii/B9780123749475000183

13. Geng Y, Bush M, Mosyak L, Wang F, Fan QR. Structural mechanism of ligand activation in human GABAB receptor. Nature. 2013 Dec 12;504(7479):254–9.

14. Lee S-M, Booe JM, Pioszak AA. Structural insights into ligand recognition and selectivity for classes A, B, and C GPCRs. Eur J Pharmacol. 2015 Sep 15;763, Part B:196–205.

15. Katritch V, Cherezov V, Stevens RC. Structure-Function of the G Protein–Coupled Receptor Superfamily. Annu Rev Pharmacol Toxicol. 2013;53(1):531–56.

16. Chung KY. Structural Aspects of GPCR-G Protein Coupling. Toxicol Res. 2013 Sep;29(3):149–55.

17. Conn PJ, Lindsley CW, Meiler J, Niswender CM. Opportunities and challenges in the discovery of allosteric modulators of GPCRs for treating CNS disorders. Nat Rev Drug Discov. 2014 Sep;13(9):692–708.

18. Rang H., Dale M. Rang & Dales Pharmacology. 7th ed. Edinburgh: Churchill Livingstone Elsevier; 2012. 777 p.

19. Pin J-P, Galvez T, Prézeau L. Evolution, structure, and activation mechanism of family 3/C G-protein-coupled receptors. Pharmacol Ther. 2003 Jun;98(3):325–54.

20. Lundström L, Bissantz C, Beck J, Wettstein J, Woltering T, Wichmann J, et al. Structural determinants of allosteric antagonism at metabotropic glutamate receptor 2: mechanistic studies with new potent negative allosteric modulators: Structural determinants of NAMs at mGlu 2. Br J Pharmacol. 2011 Sep 2;164(2b):521–37.

21. Strasser A, Wittmann H-J. Sequence Alignment and Homology Modelling. In: Modelling of GPCRs [Internet]. Dordrecht: Springer Netherlands; 2013 [cited 2016 Mar 30]. p. 13–28. Available from: http://link.springer.com/chapter/10.1007/978-94-007-4596-4_3

22. Wierońska JM, Zorn SH, Doller D, Pilc A. Metabotropic glutamate receptors as targets for new antipsychotic drugs: Historical perspective and critical comparative assessment. Pharmacol Ther. 2016 Jan;157:10–27.

23. Doré AS, Okrasa K, Patel JC, Serrano-Vega M, Bennett K, Cooke RM, et al. Structure of class C GPCR metabotropic glutamate receptor 5 transmembrane domain. Nature. 2014 Jul 31;511(7511):557–62.

24. Wu H, Wang C, Gregory KJ, Han GW, Cho HP, Xia Y, et al. Structure of a Class C GPCR Metabotropic Glutamate Receptor 1 Bound to an Allosteric Modulator. Science. 2014 Apr 4;344(6179):58–64.

25. Gentry PR, Sexton PM, Christopoulos A. Novel Allosteric Modulators of G Protein-coupled Receptors. J Biol Chem. 2015 Aug 7;290(32):19478–88.

26. Flor PJ, Acher FC. Orthosteric versus allosteric GPCR activation: The great challenge of group-III mGluRs. Biochem Pharmacol. 2012 Aug 15;84(4):414–24.

27. Feng Z, Ma S, Hu G, Xie X-Q. Allosteric Binding Site and Activation Mechanism of Class C G-Protein Coupled Receptors: Metabotropic Glutamate Receptor Family. AAPS J. 2015 May;17(3):737–53.

28. Chun L, Zhang W, Liu J. Structure and ligand recognition of class C GPCRs. Acta Pharmacol Sin. 2012 Mar;33(3):312–23.

29. Xu T, Zhang L, Wang X, Wei D. A novel protocol of energy optimisation for predicted protein structures built by homology modelling. Mol Simul. 2010 Nov 1;36(13):1104–9.

30. Cooke RM, Brown AJH, Marshall FH, Mason JS. Structures of G protein-coupled receptors reveal new opportunities for drug discovery. Drug Discov Today. 2015 Nov;20(11):1355–64.

31. Scimemi A. Structure, function, and plasticity of GABA transporters. Front Cell Neurosci [Internet]. 2014 Jun 17 [cited 2016 Apr 4];8. Available from: http://www.ncbi.nlm.nih.gov/pmc/articles/PMC4060055/

32. Gabrielsen M, Ravna AW, Kristiansen K, Sylte I. Substrate binding and translocation of the serotonin transporter studied by docking and molecular dynamics simulations. J Mol Model. 2012 Mar;18(3):1073–85.

33. Topiol S, Sabio M. 7TM X-ray structures for class C GPCRs as new drug-discovery tools. 1. mGluR5. Bioorg Med Chem Lett. 2016 Jan 15;26(2):484–94.

34. Christopher JA, Aves SJ, Bennett KA, Doré AS, Errey JC, Jazayeri A, et al. Fragment and Structure-Based Drug Discovery for a Class C GPCR: Discovery of the mGlu5 Negative Allosteric Modulator HTL14242 (3-Chloro-5-[6-(5-fluoropyridin-2-yl)pyrimidin-4-yl]benzonitrile). J Med Chem. 2015 Aug 27;58(16):6653–64.

35. Lemke TL, Williams DA. Foye's Principles of Medicinal Chemistry. 6th ed. Philadelphia: Wolters Kluwer/Lippincott Williams & Wilkins; 2008. 1377 p.

36. Höltje H-D. Molecular modeling : basic principles and applications. 3rd, rev. and expanded ed. Weinheim: Wiley-VCH; 2008. 310 p.

37. Schmidt T, Bergner A, Schwede T. Modelling three-dimensional protein structures for applications in drug design. Drug Discov Today. 2014 Jul;19(7):890–7.

38. Ravna A, Sylte I. Homology Modeling of Transporter Proteins (Carriers and Ion Channels). In: Orry AJW, Abagyan R, editors. Homology Modeling [Internet]. Humana Press; 2012 [cited 2016 Mar 11]. p. 281–99. (Methods in Molecular Biology). Available from: http://dx.doi.org/10.1007/978-1-61779-588-6_12

39. Venclovas Č. Methods for Sequence–Structure Alignment. In: Orry AJW, Abagyan R, editors. Homology Modeling [Internet]. Humana Press; 2012 [cited 2016 Mar 11]. p. 55–82. (Methods in Molecular Biology). Available from: http://dx.doi.org/10.1007/978-1-61779-588-6_3

40. Bordner A. Force Fields for Homology Modeling. In: Orry AJW, Abagyan R, editors. Homology Modeling [Internet]. Humana Press; 2012 [cited 2016 Mar 11]. p. 83–106. (Methods in Molecular Biology). Available from: http://dx.doi.org/10.1007/978-1-61779-588-6_4

41. Costanzi S. Homology Modeling of Class A G Protein-Coupled Receptors. In: Orry AJW, Abagyan R, editors. Homology Modeling [Internet]. Humana Press; 2012 [cited 2016 Mar 11]. p. 259–79. (Methods in Molecular Biology). Available from: http://dx.doi.org/10.1007/978-1-61779-588-6_11

42. Kołaczkowski M, Bucki A, Feder M, Pawłowski M. Ligand-optimized homology models of D_1 and D_2 dopamine receptors: application for virtual screening. J Chem Inf Model. 2013 Mar 25;53(3):638–48.

43. Katritch V, Rueda M, Abagyan R. Ligand-Guided Receptor Optimization. In: Orry AJW, Abagyan R, editors. Homology Modeling [Internet]. Humana Press; 2012 [cited 2016 Mar 11]. p. 189–205. (Methods in Molecular Biology). Available from: http://dx.doi.org/10.1007/978-1-61779-588-6_8

44. Leach AR, Shoichet BK, Peishoff CE. Prediction of Protein−Ligand Interactions. Docking and Scoring: Successes and Gaps. J Med Chem. 2006 Oct 1;49(20):5851–5.

45. Totrov M, Abagyan R. Flexible ligand docking to multiple receptor conformations: a practical alternative. Curr Opin Struct Biol. 2008 Apr;18(2):178–84.

46. Huang S-Y, Grinter SZ, Zou X. Scoring functions and their evaluation methods for protein–ligand docking: recent advances and future directions. Phys Chem Chem Phys. 2010;12(40):12899.

47. About MODELLER [Internet]. [cited 2016 Jan 4]. Available from: http://www.salilab.org/modeller/

48. RCBS PDB. About the PDB Archive and the RCSB PDB [Internet]. [cited 2016 Mar 21]. Available from: http://www.rcsb.org/pdb/static.do?p=general_information/about_pdb/index.html

49. Southan C, Sharman JL, Benson HE, Faccenda E, Pawson AJ, Alexander SPH, et al. The IUPHAR/BPS Guide to PHARMACOLOGY in 2016: towards curated quantitative interactions between 1300 protein targets and 6000 ligands. Nucleic Acids Res. 2016 Jan 4;44(D1):D1054–68.

APPENDIX

A. Docking scores of toxicants docked to the mGlu receptor and GAT1 models.

Table A1: **Scoring values of toxicants docked to agonist and antagonist conformational state of the crystal structure of mGlu2 receptor (PDB ID: 5CNJ).** The more negative docking score the higher the compounds are predicted to bind to the receptor. 1,4-cyclohexanedicarboxylic acid are listed twice because of axial and equatorial positions of the functional groups.

mGlu2 receptor orthosteric binding site			
Agonist		**Antagonist**	
Toxicant	**Docking score**	**Toxicant**	**Docking score**
Deferoxamine	-8.76	Imidazolidinyl urea	-8.74
Uric acid	-8.73	2,4-Diaminohypoxanthine	-8.73
1,4-cyclohexane dicarboxylic acid	-8.66	4-Aminofolic acid	-8.60
1,4-cyclohexane dicarboxylic acid	-8.27	Thalidomide (S)	-8.59
Tipranavir	-8.00	FD&C Green no. 1	-8.55
Imidazolidinyl urea	-7.94	2-Amino-1-phenol-4-sulfonic acid	-8.54
6-Propyl-2-thiouracil	-7.91	Folic acid	-8.32
3-Nitrobenzamide	-7.87	1,4-cyclohexane dicarboxylic acid	-8.30
Taltirelin	-7.77	Raltitrexed	-8.24
5-Amino-3-sulfosalicylic acid	-7.66	Thymopentin	-8.20

Table A2: **Scoring values of toxicants docked to PAM and NAM conformational state of the constructed homology model of the 7 TMH of mGlu2 receptor.** The more negative docking score the stronger the compounds are predicted to bind to the receptor. Fluspirilene are listed twice because of axial and equatorial positions of the functional groups.

mGlu 2 receptor allosteric binding site			
PAM		**NAM**	
Toxicant	**Docking score**	**Toxicant**	**Docking score**
Oxyphenbutazone	-12.11	Fluspirilene	-14.34
Carbocyanine	-11.90	Penfluridol	-13.82
Fluridone	-11.83	Itriglumide	-13.44
Imatinib	-11.78	N-[1-{2-[(2R)-2-(3,4-dichlorophenyl)-5-oxo-4-phenylmorpholin-2-yl]ethyl}-4-(3-fluorophenyl)piperidin-4-yl]acetamide butanedioate	-13.27
6-Hydroxy-2-naphthyl disulfide	-11.75	(2-{[4-(4-chloro-2,5-dimethoxyphenyl)-5-(2-cyclohexylethyl)-1,3-thiazol-2-yl]carbamoyl}-5,7-dimethyl-1H-indol-1-yl)acetic acid trifluoroacetate	-13.25
Metolazone	-11.75	Spiperone	-13.02
5-fluoro-1-(3-fluorobenzyl)-N-(1H-indol-5-yl)-1H-indole-2-carboxamide	-11.70	Rutin	-12.98
Feprazone	-11.64	Cromolyn	-12.96
Flufenpyr-ethyl	-11.64	Fluspirilene	-12.91
Taprostene	-11.58	Pimozide	-12.85

Table A3: **Scoring values of toxicants docked to agonist and antagonist conformational state of the crystal structure of VFT of mGlu7 receptor (PDB ID: 3MQ4).** The 10 best ranked toxicants are shown in this table. The more negative docking score the stronger the compounds are predicted to bind to the receptor.

mGlu7 orthosteric binding site			
Agonist		**Antagonist**	
Toxicant	**Docking score**	**Toxicant**	**Docking score**
Goserelin	-9.74	Argipressin	-10.28
Argipressin	-9.47	Desmopressin	-10.11
Terlipressin	-9.34	Triptorelin pamoate	-10.04
Saralasin	-9.14	Pentagastrin	-9.23
Peplomycin	-8.92	Gonadorelin	-9.17
Polymycin B	-8.68	Suramin	-9.03
Peplomycin	-8.56	Colistin a	-8.91
Polymycin B	-8.56	Bleomycin	-8.91
Bimosiamose	-8.53	Mecobalamin	-8.79
Vancomycin	-8.31	Deslorelin	-8.79

Table A4: **Results from glide docking with toxicants to NAM and PAM conformational state for the constructed homology model of 7 TMH of mGlu7 receptor**. The 10 best ranked toxicants are shown in this table. The more negative docking score the higher the compounds are predicted to bind to the receptor.

mGlu7 receptor allosteric binding site			
PAM		**NAM**	
Toxicant	**Docking score**	**Toxicant**	**Docking score**
Devazepide	-11.74	Xenalipin	-10.04
5-{4'-[(2-butyl-3H-imidazo[4,5-b]pyridin-3-yl)methyl]biphenyl-2-yl}tetrazol-1-ide	-11.39	2-Ethylanthracene-9,10-dione	-10.02
Fluspirilene	-11.32	9-Anthracenemethanol	-10.00
Bifonazole	-10.99	1-Amino-2-methylanthraquinone	-9.93
Bisoxatin	-10.94	2,7-Acetyl aminofluorene	-9.86
Losartan	-10.94	2-Hydroxy anthraquinone	-9.83
Halofantrine	-10.72	Oxcarbazepine	-9.82
Fluorescein 5(6)-isothiocyanate	-10.71	2-Acetylaminofluorene	-9.78
Fendiline	-10.70	2-Methylanthraquinone	-9.78
Phenolphthalin	-10.69	Tenylidone	-9.78

Table A5: **Results from Glide docking with toxicants to PAM and NAM conformational state for the crystal structure of 7 TMH mGlu5 receptor (PDB ID: 4OO9)**. The 10 best ranked toxicants are shown. The more negative docking score the higher the compounds are predicted to bind to the receptor.

Mglu5 receptor allosteric binding site			
PAM		**NAM**	
Toxicant	**Docking score**	**Toxicant**	**Docking score**
Taprostene	-12.78	Bucindolol	-11.64
{4-[3 (aminomethyl)phenyl] piperidin-1-yl}{5-[(2fluoro phenyl) ethynyl]furan-2-yl} methanone	-11.87	Fluprostenol	-11.26
Fluprostenol	-11.79	Doxazosin	-11.22
L-Cichoric acid	-11.39	Droperidol	-10.89
4-(3-{[4-(2-methyl-1H-imidazol -1-yl)phenyl] sulfanyl}phenyl) tetrahydro-2H-pyran-4-carbox amide methanesulfonate	-11.21	2,4-Diaminohypoxanthine	-10.74
Praziquantel	-11.02	3-({(3R,4R)-6-[(5-fluoro-1,3-benzothiazol-2-yl) methoxy]-4-hydroxy-3,4-dihydro-2H-chromen-3-yl}methyl) benzoic acid	-10.62
6-Hydroxy-2-naphthyl disulfide	-11.01	Talniflumate	-10.56
Ketanserin	-10.87	Trazodone	-10.47
[2-({[2-(4-tert-Butyl-1,3-thiazol -2-yl)-1-benzofuran-5-yl]oxy} methyl)phenyl]acetic acid	-10.84	Prazosin	-10.38
Famprofazone	-10.72	Doxazosin	-10.33

Table A6: **Scoring values of toxicants docked to the constructed homology model of GAT1.** The 10 best ranked toxicants are shown in this table. The more negative docking score the higher the compounds are predicted to bind to the receptor.

GAT1 orthosteric binding site	
Toxicant (chirality)	**Docking score**
Efonidipine	-10.01
Ioversol (S)	-9.85
Chlorhexidine	-9.71
Azelnidipine	-9.68
Liarozole (R)	-9.68
Fluorescein	-9.56
Manidipine dihydrochloride	-9.45
Ioversol (R)	-9.44
Relcovaptan	-9.37
Liarozole (S)	-9.35